

Ab Initio Studies of Excited States and  
Reactions of Organic Molecules

Thesis by  
Lawrence Brook Harding

In Partial Fulfillment of the Requirements  
for the Degree of  
Doctor of Philosophy

California Institute of Technology  
Pasadena, California

1979

(Submitted August 31, 1978)

## ACKNOWLEDGEMENTS

First, I thank Bill Goddard whose enthusiasm for chemistry and skepticism of almost everything has been the basis of an exciting and educational collaboration.

I would also like to express my appreciation to all past and present members of the Goddard research group for many stimulating discussions, advice, assistance and comic relief. In this regard I am particularly pleased to acknowledge Bill Wadt, Tim Suratt and Tony Rappé.

I also thank Frances Houle, Jack Beauchamp and Peter Dervan for repeated attempts to keep me in touch with the realities of an experimental science. I hope they were at least partly successful.

I think it is also appropriate to acknowledge my fourth grade teacher, Miss Marshall, for introducing me to electrons, nuclei, atoms and molecules. Little did she realize what she was starting.

Finally, I thank Carolyn to whom I am greatly indebted for her constant encouragement, warmth and understanding.



## ABSTRACT

Part A: Extensive ab initio calculations (double zeta plus polarization function basis with correlated wavefunctions) on the addition of  $^1\text{O}_2$  to ethylene are combined with standard thermochemical methods of estimating substituent effects to predict the energetics of the addition of  $^1\text{O}_2$  to substituted olefins. The results include estimates for peroxy biradical, open 1,4-zwitterion, and perepoxide intermediates. It is concluded that only the first two play a role in this reaction. Detailed comparisons of the theoretical predictions with experimental results are also reported. It is shown that many aspects of the stereospecificity and regioselectivity can be understood assuming a biradical intermediate or transition state.

Part B: Generalized valence bond (GVB) and configuration interaction (CI) calculations using an extensive basis [double zeta plus polarization functions (DZd)] have been carried out on peroxymethylene ( $\text{H}_2\text{COO}$ , often referred to as carbonyl oxide or as the Criegee intermediate), dioxirane, and dioxymethylene ( $\text{OCH}_2\text{O}$ ). The ab initio thermochemical results are combined with existing thermochemical data to analyze possible modes of ozonolysis. The predicted heat of formation of peroxymethylene is 29.1 kcal, indicating that the dissociation of the primary ozonide to form peroxymethylene biradical and formaldehyde is 9 kcal endothermic. The ring state, dioxirane, is predicted to be 36 kcal below peroxymethylene with dioxymethylene lying 15 kcal above the ring state. Gas phase experimental results are shown to be consistent with the predicted thermochemistry. In addition, solution phase results on the stereospecificity of ozonolysis are shown to be consistent with a biradical intermediate.

Part C: Large basis set configuration interaction, bending potential curves for three states ( $^3B_1$ ,  $^1A_1$ , and  $^1B_1$ ) of neutral  $CH_2$  and one state ( $^2B_1$ ) of  $CH_2^-$  are reported. Vibronic calculations using these potential curves are found to lead to excellent agreement with the observed  $^1B_1 - ^1A_1$  spectrum. Similar calculations on the  $^3B_1 - ^2B_1$  and  $^1A_1 - ^2B_1$  photoelectron spectra indicate the presence of hot bands in the observed negative ion spectrum. Reassignment of the observed spectrum based on these calculations leads to the prediction of a  $^1A_1 - ^3B_1$  splitting of  $0.38 \pm 0.05$  eV.

Part D: The ground and valence excited states of ketene ( $H_2CCO$ ) were studied using ab initio generalized valence bond (GVB) and configuration interaction (GVB-CI) wavefunctions. The character and properties of the states are analyzed in terms of the GVB wavefunctions. The calculated vertical excitation energies (in eV) are 3.62 ( $^3(n \rightarrow \bar{\pi}^*)$  or  $^3A_2$ ), 3.69 ( $^1(n \rightarrow \bar{\pi}^*)$  or  $^1A_2$ ), 5.39 ( $^3(\pi \rightarrow \pi^*)$  or  $1^3A_1$ ), and 7.37 ( $^3(\bar{\pi} \rightarrow \bar{\pi}^*)$  or  $2^3A_1$ ). (Here  $\bar{\pi}$  indicates a  $\pi$ -like orbital in the plane of the molecule.) These results are in excellent agreement with the observed electron impact excitation energies, 3.8 ( $^1A_2$ ) and 5.35 eV ( $^3A_1$ ). Note in particular the small separation (0.07 eV) of the  $^3A_2$  and  $^1A_2$  states (0.5 eV for  $H_2CO$ ) and the 2-eV separation in the  $\pi\pi^*$  triplet states in the two planes. The calculated ground state dipole moment, 1.62 D, is in fair agreement with the experimental value of 1.41 D. The calculated dipole moments of

the  $^3A_2$ ,  $^1A_2$ ,  $1^3A_1$ , and  $2^3A_1$  excited states are 2.76, 3.43, 2.43, and 0.27 D, respectively.

Part E: Ab initio configuration interaction (GVB-CI) methods are used to study the excited Rydberg states of formaldehyde formed by exciting out of either the  $n$  or  $\pi$  orbital into the various 3s, 3p, and 3d-like Rydberg orbitals. The resulting excitation energies are in good agreement (within  $\sim 0.1$  eV) with the available experimental results. Calculated oscillator strengths are in fair agreement with experiment. Two states  $^1(\pi \rightarrow \pi^*)$  and  $^1(\pi \rightarrow 3s)$  are calculated to lie between 10.7 and 10.8 eV, corresponding closely to a broad unassigned peak in the electron impact spectrum (10.5-11.0 eV). We have assigned other peaks in the electron impact spectrum at 11.4-12.0 eV and 12.5-12.8 eV as resulting from  $(\pi \rightarrow 3p)$  and  $(\pi \rightarrow 3d)$  transitions, respectively.

## TABLE OF CONTENTS

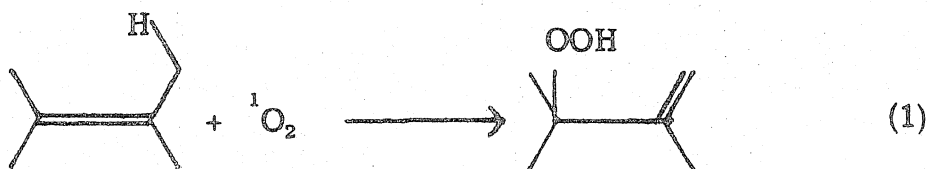
	<u>Page</u>
<u>Part A.</u> The Mechanism of the Ene Reaction of Singlet Oxygen with Olefins.....	1
I. Introduction.....	2
II. Summary of Previous Results.....	5
III. Energetic Estimates.....	13
IV. Results.....	19
V. Discussion.....	25
VI. Summary.....	45
VII. Appendix.....	47
VIII. References.....	56
<u>Part B.</u> The Mechanisms of Gas Phase and Liquid Phase Ozonolysis.....	63
I. Introduction.....	64
II. Calculational Details.....	68
III. Results.....	72
IV. Discussion.....	79
V. Conclusion.....	91
VI. References.....	96
<u>Part C.</u> Methylene: Ab Initio Vibronic Analysis and Reinterpretation of the Spectroscopic and Negative Ion Photoelectron Experiments.....	108
I. Results.....	109
II. References.....	111
<u>Part D.</u> The Generalized Valence Bond Description of the Low-Lying States of Ketene.....	113
I. Introduction.....	114
II. Calculational Details.....	117

	<u>Page</u>
III. The GVB Orbitals.....	120
IV. Discussion.....	122
V. Comparisons with Formaldehyde and Ethylene.....	127
VI. Summary.....	129
VII. References.....	135
<u>Part E.</u> Ab Initio Theoretical Studies of the Rydberg States of Formaldehyde.....	143
I. Introduction.....	144
II. Computational Details.....	145
III. Results.....	149
IV. Discussion.....	153
V. References.....	165

PART A: THE MECHANISM OF THE ENE REACTION  
OF SINGLET OXYGEN WITH OLEFINS

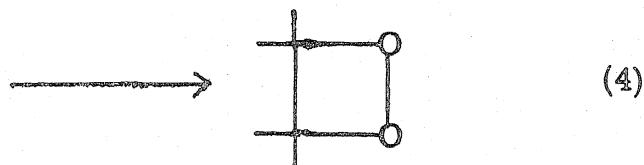
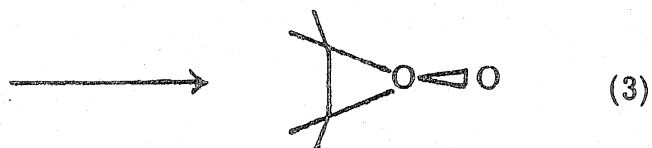
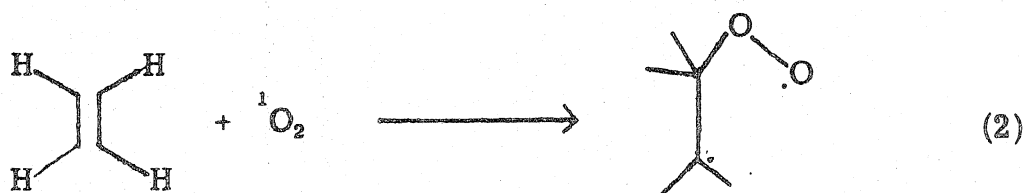
# I. Introduction

The ene reaction of singlet-oxygen with olefins,



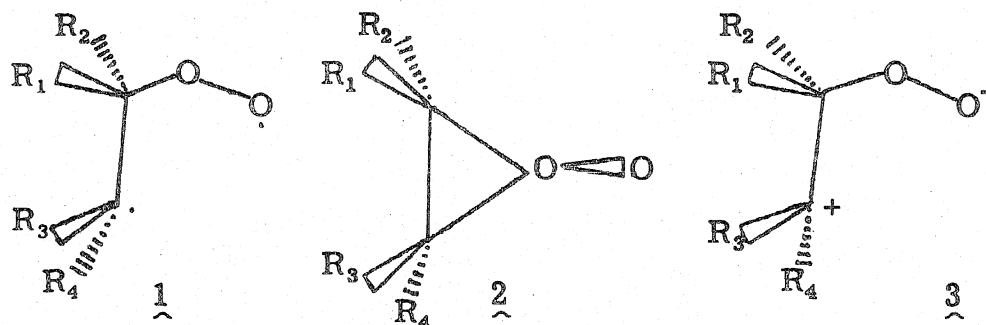
is of synthetic,<sup>2</sup> environmental,<sup>3,4</sup> and biochemical<sup>5-8</sup> significance. As such, it has been the focus of intensive experimental and theoretical studies extending over the last 20 years. The mechanism of this reaction has become an increasingly controversial question with numerous conflicting results and interpretations appearing in the literature (*vide infra*).

We have carried out extensive *ab initio* studies (large basis set, generalized valence bond, and configuration interaction wavefunctions) on key intermediates in proposed  ${}^1\text{O}_2$ -olefin reaction mechanisms.<sup>9</sup> Analogous theoretical calculations on



the bond energies of simple molecules [e.g., D(Me-Me), D(Me-OH), D(HO-OH)] were shown to lead to an accuracy of  $\pm 5\%$  (0-4 kcal). However, the level of calculation necessary for this accuracy is such that it is currently impractical for applications to a large number of substituted olefins.

In this paper we report an extrapolation of our theoretical work to reactions of  $^1\text{O}_2$  with substituted olefins. To do this, we combine the ab initio results with thermochemical estimates of substituent effects in a manner similar to that developed by Benson.<sup>10</sup> Using this procedure, the key energetic quantities for such possible intermediates as 1, 2, and 3 are estimated. These energetics lead



to a number of intriguing interpretations and predictions for both gas phase and solution phase  $^1\text{O}_2$ -olefin chemistry.

From this analysis, we conclude that the gas phase mechanism involves a biradical 1 with (at most) a small barrier for decomposition to reactants and (at most) a small barrier to hydrogen abstraction forming the ene product. Depending upon the substituents, the gas phase biradical, 1, will incorporate varying degrees of



zwitterionic character. Furthermore, in a sufficiently polar solvent, the zwitterionic character can dominate.

The organization of this paper is as follows. Section II contains a summary of the key experimental and theoretical results. In Section III, we present a description of the procedure used for the thermochemical estimates together with derivations of the necessary parameters. In Section IV we use these theoretical methods to examine the addition of  $^1\text{O}_2$  to alkyl and methoxy substituted olefins and in Section V we compare these results to the relevant experimental studies.

## II. Summary of Previous Results

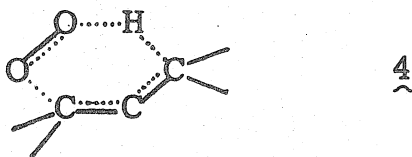
### A. Experimental Studies

In this section we briefly summarize some of the important experimental results on the  $^1\text{O}_2$ -olefin ene reaction.

Early work by Foote,<sup>11</sup> Schenck,<sup>12</sup> and Nickon<sup>13</sup> showed that the double bond in the product hydroperoxide is invariably shifted to a position adjacent to the original double bond, as shown in (1). These results eliminated mechanisms such as (5), involving an initial hydrogen abstraction, to form an allyl radical, followed by



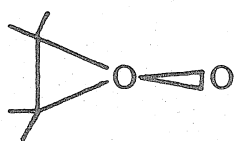
radical recombination. Thus, Nickon, et al.<sup>13</sup> concluded that the mechanism must be of a cyclic nature 4. They noted however that



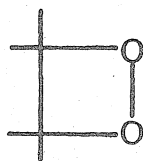
these results do not yield any information concerning the timing of the formation of C-O and O-H bonds, and therefore could not exclude a nonconcerted mechanism involving any of several intermediates.

Later, Litt and Nickon<sup>14</sup> analyzed the rates and product distributions of several photooxidations in terms of six possible

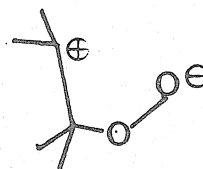
intermediates, 5-10.



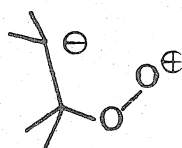
5



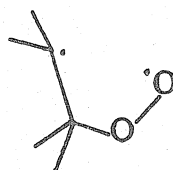
6



7

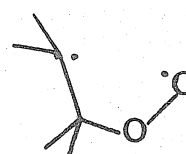


8



singlet

9



triplet

10

The perepoxide 5 was first proposed as an intermediate by Sharp.<sup>15</sup> Nickon, however, argued against the intermediacy of pereperoxides citing as evidence the product distributions from photooxidation of trimethylethylene.<sup>14</sup> Studies on the photooxidation of norbornene showed a lack of the carbonyl products expected from a dioxetane intermediate, 6, and no evidence of carbonium-ion like rearrangements. Thus, Nickon<sup>14</sup> concluded that neither 6 nor 7 are likely intermediates. In addition, the higher reactivity of tri and tetra alkyl substituted olefins relative to mono and di substituted olefins was cited as evidence against the intermediacy of 8. Foote<sup>16</sup> has also concluded that the zwitterionic intermediates, 5, 7, and 8, are not plausible due to the lack of a correlation between the reaction rates and solvent polarity.

Nickon<sup>14</sup> and later Foote<sup>16</sup> and Kearns<sup>17</sup> have considered and ruled out the possibility of diradical intermediates. Nickon

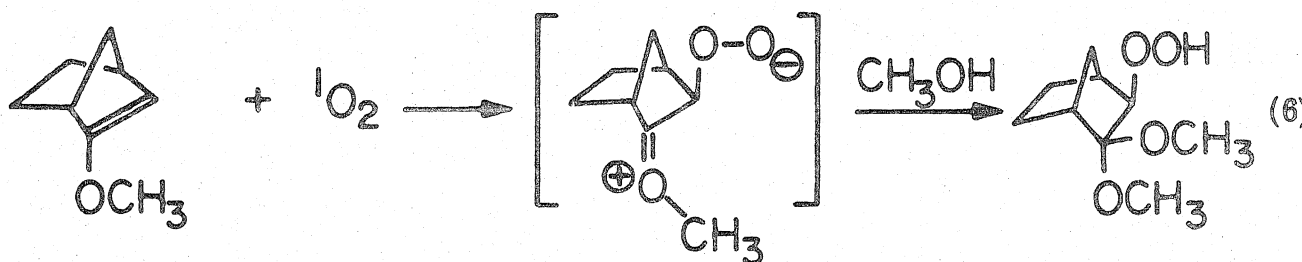
cited the lack of a detectable cis-trans isomerization of starting olefin as evidence against reversible formation of biradicals. Nickon also presented a detailed thermochemical and kinetic argument against irreversible diradical formation.

Foote<sup>16a</sup> and others<sup>17</sup> have cited the lack of Markovnikov and other substituent directing effects as evidence against a biradical intermediate. Foote<sup>16b</sup> has also interpreted the unusually low reactivity of 1-methylcyclohexene toward  $^1\text{O}_2$  as evidence for participation of the C-H bond in the transition state. He concludes, however, that the degree of C-H bond breaking in the transition state is small.

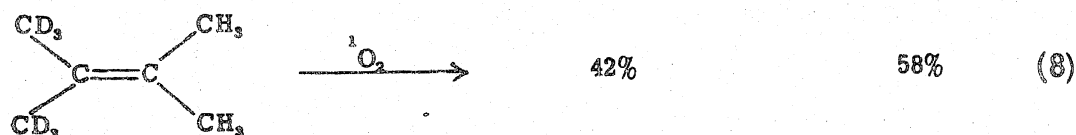
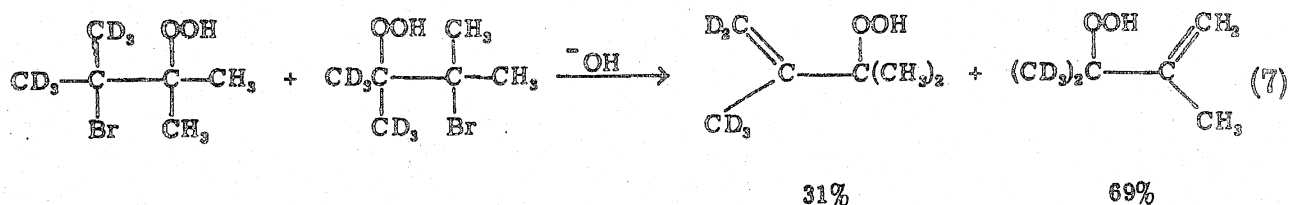
Jefford<sup>18-20</sup> has recently reported an analysis of the reaction of  $^1\text{O}_2$  with a series of substituted norbornenes and methylenenorbornanes, the objective being to probe the nature of the transition state for hydroperoxidation. By comparing exo-endo rate constants of compounds with varying degrees of steric impedance, Jefford<sup>18</sup> concluded that  $^1\text{O}_2$  does not simultaneously form C-O bonds with both ends of the double bond. Consequently, Jefford considers the intermediacy of a perepoxide as unlikely. He further noted that the steric evidence is most consistent with a one step process in which significant dipolar character is developed in the early stages. Jefford also cites the small intermolecular deuterium isotope effects ( $K_{\text{H}}/K_{\text{D}} = 1.14$ )<sup>18b</sup> as evidence against significant participation of the C-H bond in the transition state and the dependence of product composition<sup>21,22</sup> on solvent as evidence for

a dipolar transition state. The latter conflicts with the observations of Foote<sup>12</sup> and others<sup>13</sup> who have cited the lack of a solvent polarity dependence as evidence against a strongly dipolar transition state.

In their most recent work, Jefford et al.<sup>20</sup> cite the isolation of products incorporating methanol (solvent) as evidence for a zwitterionic intermediate (either a perepoxide or an open 1,4-zwitterion) in the addition of  $^1\text{O}_2$  to 2-methoxynorborn-2-ene (6).



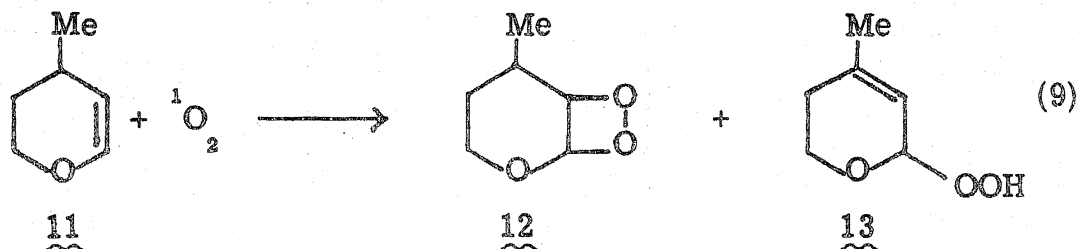
Kopecky<sup>23,24</sup> has recently reported the results of a novel approach to the question of perepoxide intermediates. In these experiments, a perepoxide is generated by treatment of a  $\beta$ -halohydroperoxide with base and the resulting product distribution, (7), is shown to be different from the photooxidation results (8).



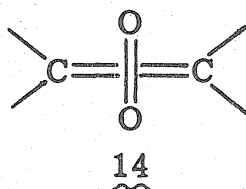
Thus, it was concluded that the perepoxide is not an intermediate in the latter process.

Several experimental studies have been interpreted to support the intermediacy of perepoxides. Recent experiments by McCapra<sup>25</sup> are in apparent conflict with the earlier work of both Nickon<sup>14</sup> and Jefford.<sup>18</sup> In reactions of camphenylidene-adamantane and adamantylidene-camphene with  ${}^1\text{O}_2$ , McCapra reports the isolation of products resulting from carbonium ion rearrangements. These results are interpreted to support the intermediacy of a perepoxide, or zwitterionic species.

Further evidence comes from an extensive study, by Bartlett *et al.*<sup>26</sup> of tritium isotope effects on the reaction of  ${}^1\text{O}_2$  with methyl dihydropyrans, 11. In this work, the primary and secondary isotope



effects are used to probe the interactions between various centers in the transition state(s) leading to both dioxetane, 12, and allylic hydroperoxide, 13, products. They conclude that the transition state leading to ene product, 13, is not a simple six centered cyclic structure, 4, and that the observed isotope effects are more consistent with the criss-cross transition state 14 of a classic  $2_s + 2_a$



concerted cycloaddition. They further note that this probably leads to a perepoxide intermediate.

#### B. Theoretical Studies

In addition to the above experimental studies, a few theoretical efforts directed at elucidating the  $^1\text{O}_2$ -olefin reaction mechanisms have been reported. In 1971, Kearns<sup>17</sup> analyzed the various proposed modes of addition using orbital correlation diagrams. He concluded the preferred mode leads to formation of a perepoxide, 5.

Fukui<sup>27</sup> has reported the results of semiempirical calculations, CNDO/2-CI, on these reactions from which he concluded that addition to form perepoxides is the favored mode. He notes, however, that the calculations indicate the perepoxide is not a true minimum on the reaction path and, therefore, terms the perepoxide a quasi-intermediate. In addition, Fukui<sup>28</sup> has reported a HOMO-LUMO analysis (assuming a perepoxide-like transition state and incorporating intermolecular

nonbonded attractions) which rationalizes the observed direction of addition of  $^1\text{O}_2$  to unsymmetrical olefins.

Paquette<sup>29</sup> has noted a strong correlation between the reactivity of an olefin toward  $^1\text{O}_2$  and the ionization potential of the olefin the most reactive olefins being those with the lowest ionization potential. This trend was also rationalized using a HOMO-LUMO analysis with a perepoxide-like transition state. We note, however, that the assumption of a perepoxide is not crucial to this analysis.

The most extensive theoretical study published to date is that of Dewar and Thiel.<sup>30</sup> Using the semiempirical MINDO/3 method on the reaction of  $^1\text{O}_2$  with ethylene and with several substituted olefins, Dewar concluded that in most cases this reaction proceeds through a discrete perepoxide intermediate. The only exceptions found were certain electron rich olefins with were predicted to form the open zwitterionic intermediate, 7, upon adding  $^1\text{O}_2$ . In the addition of  $^1\text{O}_2$  to propene, the MINDO/3 calculations predict that addition to form the perepoxide is 16 kcal exothermic with a barrier to addition of 11 kcal. Subsequent rearrangement to propene-hydroperoxide is predicted to proceed with a barrier of 21 kcal.

Ab initio calculations (GVB-CI) by Harding and Goddard<sup>9</sup> are in disagreement with both the CNDO and the MINDO results. The GVB-CI calculations place the perepoxide, 5, 17 kcal endothermic from ethylene plus  $^1\text{O}_2$ , well above the observed gas phase activation energies for allylic hydroperoxidation (2-10 kcal).<sup>31</sup> The ab initio



calculations also indicate the biradical species, 9, to be 8 kcal below the perepoxide (or 9 kcal above the reactants). According to the ab initio GVB-CI results then, the biradical is an energetically permissible intermediate while the perepoxide is not. Finally, Harding and Goddard<sup>32</sup> have shown that certain unusual aspects of the stereochemistry of <sup>1</sup>O<sub>2</sub> hydroperoxidation can be understood on this basis of a biradical mechanism and that the observed stereochemistry is not consistent with the perepoxide mechanism as suggested by Fukui.<sup>28</sup>

### III. Energetic Estimates

As indicated in the introduction, the approach here is to combine the results of extensive ab initio theoretical studies on the addition of  $^1\text{O}_2$  to ethylene with standard thermochemical methods of estimating substituent effects to predict the energetics for reactions involving unsubstituted olefins. In order to avoid ambiguities, we present here a detailed discussion of the methods and parameters used in this work.

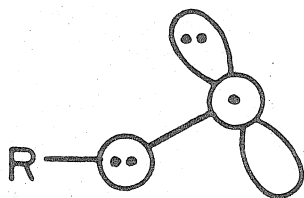
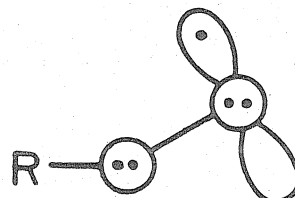
#### A. Group Additivity Parameters

The method of group additivities (GA) has been developed and extensively tested by Benson and coworkers.<sup>10</sup> Benson has shown that for most compounds the GA method leads to  $\Delta H_f^\circ$  estimates with an accuracy of  $\pm 1$  kcal/mole. Similar estimates for free radicals give heats of formation with a comparable accuracy. In the present work, we use the parameters of reference 10a, augmented (vide infra) with parameters from the ab initio calculations (for perepoxides) and from experiment (for radical centers).

The perepoxide parameters are derived using the calculated (GVB-CI) heat of formation of the parent perepoxide (51.6 kcal).<sup>9</sup> This gives an O-O bond energy of 40.6 kcal (relative to  $\text{O}(^1\text{D})$  and ethylene oxide) for the parent perepoxide which is assumed to be unchanged by substitution on the carbons. Thus, the heat of formation of a substituted perepoxide is obtained by adding 64.2 kcal to the estimated  $\Delta H_f^\circ$  of the corresponding epoxide. No corrections for

nonbonded repulsions are made although these are expected to favor placing the terminal oxygen on the least hindered side of the olefin.

The group additivity parameters for peroxy radicals are derived assuming,  $D_0(\text{ROO-H}) = D_0(\text{HOO-H}) = 89.7$  kcal, for all saturated groups, R. In terms of group functions this can be expressed as,  $G[\text{C}(\text{O}_2\cdot)(\text{X})(\text{Y})(\text{Z})] = G[\text{C}(\text{O})(\text{X})(\text{Y})(\text{Z})] + 16.8$ . It is important at this point to note that there are two low-lying states of peroxy radicals (see Section V B), a  $\pi^3$  ground state, 15, and a  $\pi^4$  excited state, 16.

1516

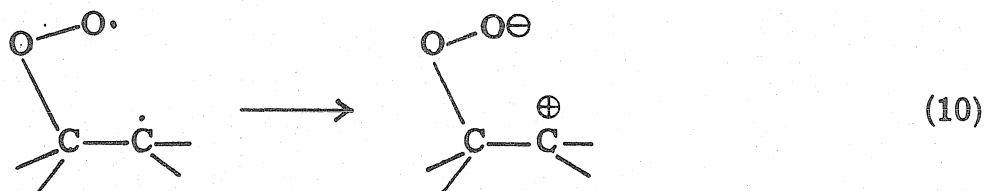
The above estimates apply to the  $\pi^3$  ground state. Ab initio calculations<sup>33</sup> and experiments<sup>34</sup> on  $\text{HO}_2$  indicate the  $\pi^4$  state is 20 kcal higher. For the processes addressed in this paper then, the  $\pi^4$  state of the peroxy radical should not play an important role.

Finally, group functions for carbon centered radicals are summarized in Table I. These are based on C-H bond energies (also listed in Table I) derived from the radical heats of formation

of reference 10a. In these derivations, the value of  $G[C(C\cdot)(X)(Y)(Z)]$  is assigned to be equal to  $G[C(C)(X)(Y)(Z)]$ . Thus, the parameters in Table I together with the peroxy radical group functions are sufficient to estimate the heats of formation of the relevant biradicals.

### B. Zwitterion Estimates

The 1,4-zwitterion,  $\underline{7}$ , is an important proposed intermediate of  $^1O_2$ -olefin reactions. In order to estimate the energy of this species, we consider the process starting with the biradical, ionizing the carbon radical electron and attaching the electron to the oxygen radical center, (10). The energy for this



process is then approximated with equation (11),

$$\Delta E(\text{kcal}) = \text{IP}(\text{C}\cdot) - \text{EA}(\text{O}\cdot) - 332.1/R \quad (11)$$

where,

$\Delta E$  is the zwitterion-biradical energy separation (kcal/mole)

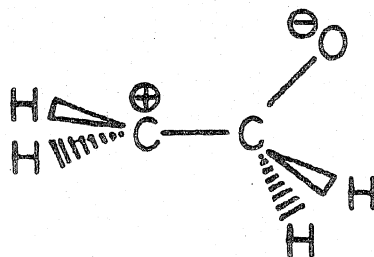
$IP(C\cdot)$  is the estimated ionization potential (kcal/mole) of the carbon centered radical (see Table II)

$EA(O\cdot)$  is the estimated electron affinity (kcal/mole) of the oxygen centered radical (18.5 kcal)<sup>35</sup>

$R$  is the distance ( $\text{\AA}$ ) between the two radical centers (2.65  $\text{\AA}$ ).

The resulting zwitterion-biradical energy separations are given in Table II.

To test the validity of this relationship, we carried out a model calculation on the energy of a 1,3-zwitterion 17 relative to the



17

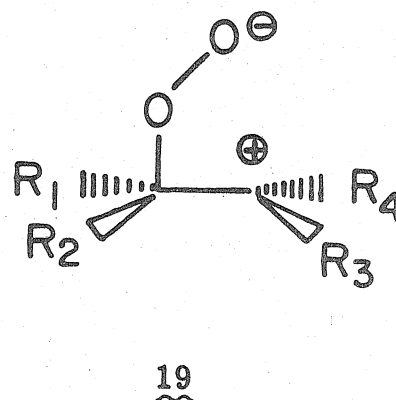
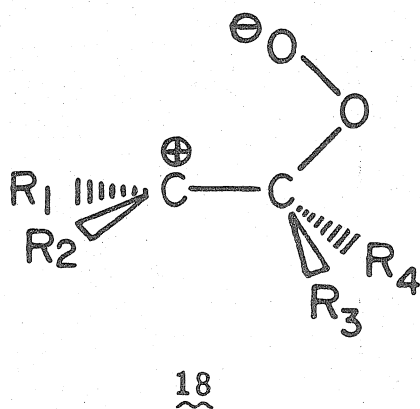
corresponding biradical. In this calculation (Appendix A) the ionization potential, electron affinity and biradical-zwitterion separation are all calculated with the same quality GVB wavefunction.<sup>37, 38</sup> The results are as follows,

$$\text{IP}(\text{C}\cdot) = 208.2 \text{ kcal}$$

$$\text{EA}(\text{O}\cdot) = 1.9 \text{ kcal}$$

$$332.1/R = 139.5 \text{ kcal}$$

and, therefore, using (11), we obtain an excitation energy of  $\Delta E = 66.8 \text{ kcal}$  for the zwitterion state relative to the biradical state. For comparison, the calculated GVB excitation energy is  $61.8 \text{ kcal}$  indicating an error, in the estimate, of  $5 \text{ kcal}$ . Thus, the estimated zwitterion energies are considerably less accurate than the biradical estimates, however, the error is sufficiently small that the predicted trends should be reliable. In particular, predictions concerning the preferred direction of addition to unsymmetrical olefins are expected to be quite accurate. The key assumption in this is that the relative energies of two zwitterions, for example, 18 and 19, are dominated by the



stability of the carbonium ion fragment.

Estimates of this kind indicate that the +CCOO<sup>-</sup> zwitterions, 7, are much more stable (~ 100 kcal) than -CCOO<sup>+</sup> zwitterions, 8. Therefore, the latter is not a likely intermediate and will not be considered further.

#### IV. Results

##### A. Alkyl Substituted Olefins

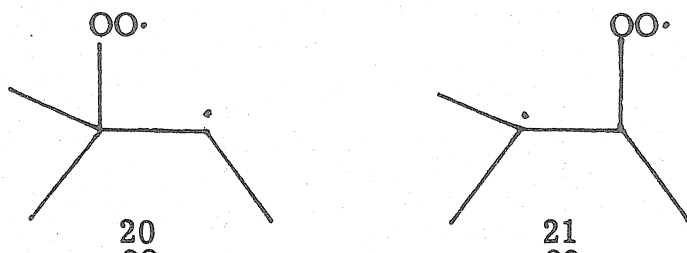
The results of the energetic estimates on the addition of  $^1\text{O}_2$  to alkyl-substituted olefins are shown in Table III. Of the three proposed intermediates considered (5, 7, and 9) the one of lowest energy is the peroxy biradical. In fact, the peroxy biradical is the only intermediate having a sufficiently low energy to be consistent with the observed activation energies (also shown in Table III). The perepoxides are on the average  $\sim 10$  kcal above the observed activation energy while the open zwitterions are too high by 15-50 kcals.

Comparing the energies necessary to form the peroxy biradical to the observed activation energies, it is found that within the uncertainty of the estimates ( $\pm 2$  kcal) the two are equal. Thus, if the biradical is an intermediate, there must be very low barriers ( $\sim 0.5$  kcal) both to the initial addition forming the biradical and to the subsequent hydrogen abstraction. Such a low barrier is consistent with the form of the wavefunctions; there are no orbital phase restrictions or nonbonded interactions which would lead to large barriers. Indeed, the H-abstraction process is analogous to bimolecular radical disproportionation reactions, processes which are known to proceed with near zero activation energies.<sup>10</sup>

An important result in Table III is the predicted direction of  $^1\text{O}_2$  attack on unsymmetrically substituted olefins. Taking as an example trimethylethylene, the estimates predict that addition of  $^1\text{O}_2$  to the disubstituted end of the double bond, 20, is 0.6 kcal



lower energy than addition at the monosubstituted end, 21. This is



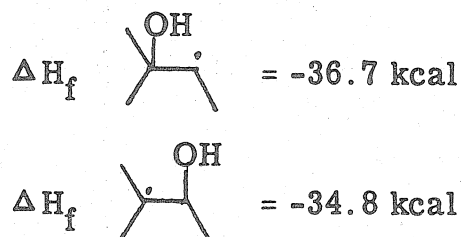
counter to the intuition of many chemists. It is generally assumed that addition of a radical to a double bond leads to the most highly substituted radical center. For the case of radical HX addition, this is the explanation of the well known Markovnikov directing effect. For this reason, and because the energy difference between 20 and 21 is smaller than the expected error limits of these estimates, it is important to consider carefully whether or not the predicted ordering is correct.

In fact, we believe the predicted ordering is correct and note the following experimental results in support of this prediction. Starting with the experimentally determined heats of formation of the two analogous alcohols,<sup>39</sup>

$$\Delta H_f \left( \text{CH}_3\text{C}(\text{OH})(\text{CH}_3)\text{CH}_2\text{CH}_3 \right) = -79.07 \pm 0.35 \text{ kcal}$$

$$\Delta H_f \left( \text{CH}_3\text{C}(\text{OH})(\text{CH}_3)\text{CH}(\text{CH}_3)_2 \right) = -75.35 \pm 0.36 \text{ kcal}$$

and assuming (see Table I) a secondary C-H bond energy of 94.5 kcal and a tertiary C-H bond energy of 92.7 kcal leads to,



Again, the less substituted radical is predicted to be more stable (by 1.9 kcal in this instance)! This estimate made use of standard C-H bond energies to secondary and tertiary carbons. In order to reverse the predicted radical ordering, it would be necessary to assume that the tertiary C-H bond is ~3.5 kcal weaker than the secondary C-H bond. This is approximately twice the accepted difference (1.8 kcal)<sup>10</sup> and, hence, it is concluded that the predicted radical order is correct.

Note that the preferred direction of addition of <sup>1</sup>O<sub>2</sub> to form a zwitterion is the opposite of that to form a biradical. These estimates clearly show that if a zwitterion is involved in the product determining step, addition of <sup>1</sup>O<sub>2</sub> should invariably occur at the least substituted carbon.

The thermochemical estimates for additions to six-membered cyclic olefins exhibit an interesting trend. For both cyclohexene and methyl cyclohexene the observed activation energies are significantly above the energy necessary to form the biradical. This could indicate an additional conformational barrier to either the initial addition or to H-abstraction. This effect is most pronounced for cyclohexene where the H-abstraction must be endocyclic.

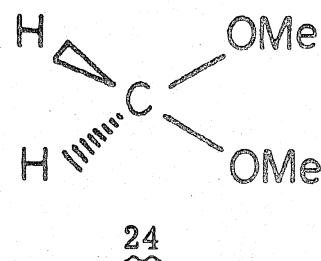
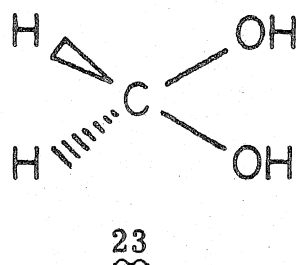
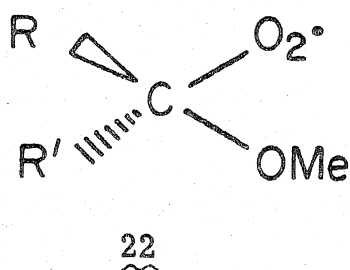
A detailed comparison of these predictions to experimental results is made in Section VC.

#### B. Methoxy Substituted Olefins

The results for the addition of <sup>1</sup>O<sub>2</sub> to methoxy-olefins are shown in Table IV. Although not shown, estimates of the perepoxide

energetics give results comparable to those found for alkyl olefins (i. e., the perepoxides are typically  $\sim 10$  kcal above the biradical).

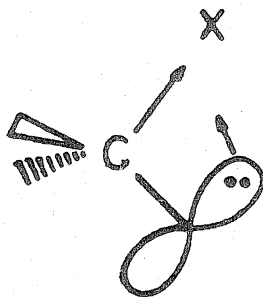
Before discussing these results in more detail, it is necessary to consider an important factor governing the conformation of these olefin- $O_2$  adducts. Addition of  $^1O_2$  to the carbon alpha to the methoxy group leads to structure 22. This structure is



analogous to methanediol (23) and dimethoxymethane (24) in that all possess an O-C-O linkage. It is now well established<sup>40</sup> that the preferred OCOR dihedral angle in such compounds is  $\sim 90^\circ$ . That such geometries are preferred is often referred to as the anomeric effect.

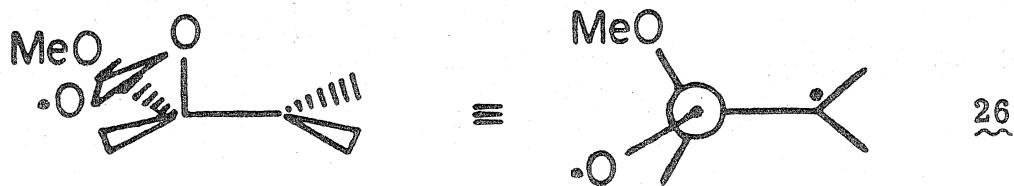
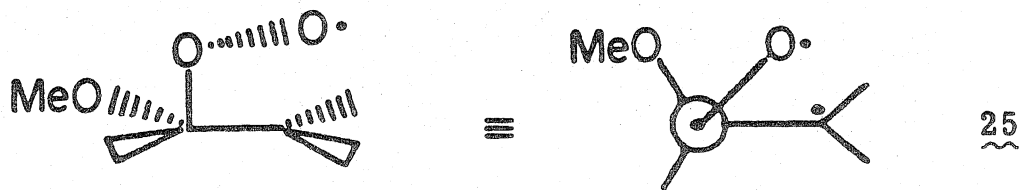
The origin of this effect can be described as follows;<sup>32, 41-44</sup> the CO  $\sigma$  bonds, being highly polarized toward the oxygen, can effectively stabilize an adjacent lone pair lying in the same plane.

In effect, the oxygen lone pair delocalizes into the region of the adjacent polar sigma bond as shown below,



The result is an increased stability (2-6 kcal, see Appendix B) of conformations in which the oxygen lone pair is in the same plane as the adjacent ionic bond.

In considering the addition of  $^1\text{O}_2$  to a methoxy olefin then, the anomeric effect dictates a preference for conformations in which the O-O bond is gauche to the methoxy, C-O bond, as shown in 25 and 26 (the left drawing is a side view, the right a top view).



In conformation 26, the oxygen radical center is not adjacent to an abstractable hydrogen and, therefore, this conformation can not go directly to product. As the barrier to dissociation to olefin +  $^1\text{O}_2$  is small ( $\sim 0.5$  kcal) compared to rotational barriers ( $\sim 3$  kcal),<sup>10</sup> if conformation 26 is formed, it will simply dissociate.

In conformation 25 the oxygen radical center is adjacent to the substituent cis with respect to the MeO group. Since the barriers to product formation ( $\sim 0.5$  kcal) are small relative to the rotational barriers, conformation 25, if formed, will lead to a product hydroperoxide resulting from hydrogen abstraction cis to the MeO group.

In summary, assuming a biradical mechanism and considering the implications of the anomeric effect, leads to a clear prediction for a directing influence of an alkoxy group (or other highly electronegative substituent). The conclusion is that product formation will be biased toward attack of the  $^1\text{O}_2$  on the  $\alpha$  carbon (adjacent to the alkoxy group) and, furthermore, toward abstraction of an hydrogen from the  $\beta$  substituent cis with respect to the alkoxy group. Similar conformational effects are expected for dimethoxy substituted olefins,<sup>45</sup> fluoro olefins,<sup>45</sup> and amino olefins.<sup>45, 46</sup> However, the parameters necessary to predict whether  $\alpha$  or  $\beta$  addition is preferred are not available for these olefins.

These predictions are compared to experimental results in Section VD.

## V. Discussion

### A. Electronic Structure of $^1\text{O}_2$

Before discussing the character of the  $\text{O}_2$ -olefin adducts, it is important to review the character of the states of  $\text{O}_2$ , particularly the  $^1\Delta_g$  state. Letting  $\pi_{g+}$  and  $\pi_{g-}$  indicate (antibonding)  $\pi_g$  orbitals with angular momentum +1 and -1 with respect to the molecular axis, the simple MO descriptions of the low-lying states of  $\text{O}_2$  are,

$$\begin{aligned}
 ^3\Sigma_g^- : \mathcal{A}\{\pi_{g+}(1)\pi_{g-}(2)\alpha(1)\alpha(2)\} &= [\pi_{g+}(1)\pi_{g-}(2) - \pi_{g-}(1)\pi_{g+}(2)]\alpha(1)\alpha(2) \\
 ^1\Delta_{g+} : \mathcal{A}\{\pi_{g+}(1)\pi_{g+}(2)\alpha(1)\beta(2)\} &= \pi_{g+}(1)\pi_{g+}(2)[\alpha(1)\beta(2) - \beta(1)\alpha(2)] \quad (12) \\
 ^1\Delta_{g-} : \mathcal{A}\{\pi_{g-}(1)\pi_{g-}(2)\alpha(1)\beta(2)\} &= \pi_{g-}(1)\pi_{g-}(2)[\alpha(1)\beta(2) - \beta(1)\alpha(2)] \\
 ^1\Sigma_{g+} : \mathcal{A}\{\pi_{g+}(1)\pi_{g-}(2)[\alpha(1)\beta(2) - \beta(1)\alpha(2)]\} &= \\
 &[\pi_{g+}(1)\pi_{g-}(2) + \pi_{g-}(1)\pi_{g+}(2)][\alpha(1)\beta(2) - \beta(1)\alpha(2)]
 \end{aligned}$$

where  $\mathcal{A}$  is the antisymmetrizer, the numbers in parentheses refer to electrons,

the seven doubly-occupied orbitals common to all states ( $1\sigma_g$ ,  $1\sigma_u$ ,  $2\sigma_g$ ,  $2\sigma_u$ ,  $3\sigma_g$ ,  $1\pi_{u+}$  and  $1\pi_{u-}$ ) have been deleted and normalization of the total wavefunction has been neglected.

The dependence of the orbitals  $\pi_{g+}$  and  $\pi_{g-}$  upon the rotation angle,  $\phi$ , about the molecular axis is given by,

$$\pi_{g+}(\rho, \phi, z) = f(\rho, z)e^{+i\phi}$$

$$\pi_{g-}(\rho, \phi, z) = f(\rho, z)e^{-i\phi}$$

where  $z$  is the distance along the axis and  $\rho$  is the distance perpendicular to the axis. An alternative choice of orbitals is to use  $\cos \phi$  and  $\sin \phi$  as the angular terms,

$$\pi_{gx}(\rho, \phi, z) = f(\rho, z) \cos \phi$$

$$\pi_{gy}(\rho, \phi, z) = f(\rho, z) \sin \phi.$$

In terms of these orbitals, we can construct four wavefunctions,

$$\begin{aligned} {}^3\Sigma_g^- &: \mathcal{A}\{\pi_{gx}\pi_{gy}\alpha\alpha\} = (\pi_{gx}\pi_{gy} - \pi_{gy}\pi_{gx})\alpha\alpha \\ {}^1\Delta_{ga} &: \mathcal{A}\{\pi_{gx}\pi_{gy}(\alpha\beta - \beta\alpha)\} = (\pi_{gx}\pi_{gy} + \pi_{gy}\pi_{gx})(\alpha\beta - \beta\alpha) \\ {}^1\Delta_{gs} &: \mathcal{A}\{(\pi_{gx}\pi_{gx} - \pi_{gy}\pi_{gy})\alpha\beta\} = (\pi_{gx}\pi_{gx} - \pi_{gy}\pi_{gy})(\alpha\beta - \beta\alpha) \\ {}^1\Sigma_g^+ &: \mathcal{A}\{(\pi_{gx}\pi_{gx} + \pi_{gy}\pi_{gy})\alpha\beta\} = (\pi_{gx}\pi_{gx} + \pi_{gy}\pi_{gy})(\alpha\beta - \beta\alpha) \end{aligned} \tag{13}$$

where the electron numbers have been dropped and the subscripts  $s$  and  $a$  indicate wavefunctions that are symmetric and antisymmetric (respectively) with respect to the  $xz$  plane.

Substitution of the expression,

$$\pi_{g\pm} = \frac{1}{\sqrt{2}} (\pi_{gx} \pm i\pi_{gy})$$

into the  $^3\Sigma_g^-$  and  $^1\Sigma_g^+$  wavefunctions of (12) leads directly to (13).

The same substitution into the  $^1\Delta_g$  states leads to, (14).

$$\begin{aligned} ^1\Delta_{g+} &= \frac{1}{\sqrt{2}} (^1\Delta_{gs} + i^1\Delta_{ga}) \\ ^1\Delta_{g-} &= \frac{1}{\sqrt{2}} (^1\Delta_{gs} - i^1\Delta_{ga}) \end{aligned} \tag{14}$$

Since the two components of the  $^1\Delta_g$  state are degenerate, either form ( $^1\Delta_{g+}$  and  $^1\Delta_{g-}$  or  $^1\Delta_{gs}$  and  $^1\Delta_{ga}$ ) is valid for the free unperturbed molecule.

Suppose now that the molecule is perturbed by the presence of another atom, for example in the xz plane. The introduction of the third, center splits the degeneracy of the  $^1\Delta_g$  components and the choice of component wavefunctions is no longer arbitrary. In this case, the perturbed system still possesses a plane of symmetry (the xz plane) and, therefore, the eigenfunctions of this system must also be eigenfunctions of reflexion through the xz plane. With this constraint, the only choice of component wavefunctions is  $^1\Delta_{gs}$  and  $^1\Delta_{ga}$ , (13).

The  $^1\Delta_{ga}$  and  $^3\Sigma_g^-$  wavefunctions of (13) contain a singly-occupied  $\pi_{gx}$  orbital and a singly-occupied  $\pi_{gy}$  orbital (appropriately antisymmetrized). These wavefunctions both describe 1,2 biradicals, the difference being only in the spin pairing. Since these orbitals have zero overlap, the energy separation is twice the  $K_{xy}$  exchange integral with the triplet lower.

In order to analyze the character of the  $^1\Delta_{gs}$  wavefunction, we first rotate the coordinate system  $45^\circ$  about the z axis and express the



$^1\Delta_{gs}$  wavefunction in terms of the new coordinates,  $\bar{x}$  and  $\bar{y}$ . Thus,

$$x = (\bar{x} + \bar{y}) / \sqrt{2}$$

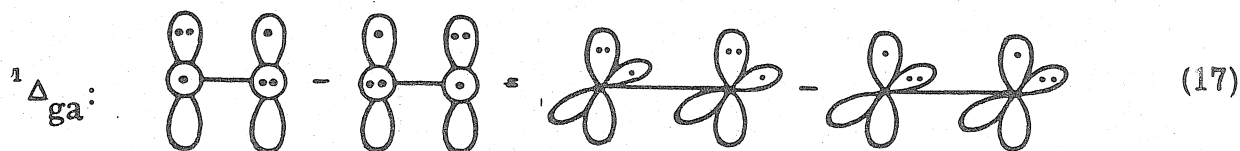
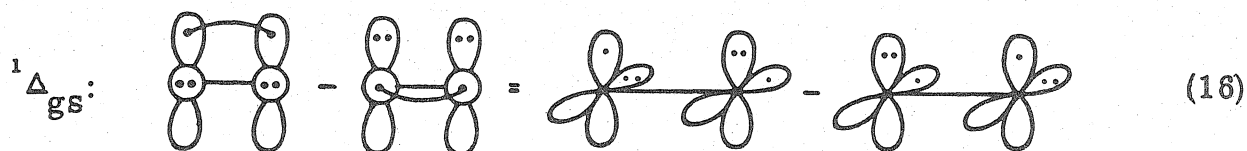
$$y = (\bar{y} - \bar{x}) / \sqrt{2}$$

and in these coordinates, the  $^1\Delta_{gs}$  wavefunction becomes (15).

$$^1\Delta_{gs} = A \{ \pi_{g\bar{x}} \pi_{g\bar{y}} (\alpha\beta - \beta\alpha) \} = (\pi_{g\bar{x}} \pi_{g\bar{y}} + \pi_{g\bar{y}} \pi_{g\bar{x}}) (\alpha\beta - \beta\alpha) \quad (15)$$

Comparing the  $^1\Delta_{ga}$  wavefunction (13) and the  $^1\Delta_{gs}$  wavefunction (15), it is clear that the  $^1\Delta_{gs}$  is simply a  $45^\circ$  rotation of the  $^1\Delta_{ga}$  and, therefore, both are singlet-1,2-biradicals.

In a valence bond wavefunction, the  $^1\Delta_{gs}$  and  $^1\Delta_{ga}$  states may be written schematically as follows,

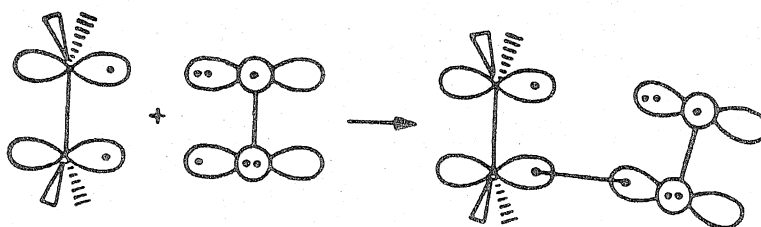


where, in the left drawing a circle represents a p orbital perpendicular to the plane and the right drawing is a 3-D perspective representation of the same wavefunction in the rotated coordinate system. In (16) and (17) the biradical character of the two wavefunctions is readily apparent.<sup>47</sup>

This biradical character of the  $^1\Delta_g$  state invalidates the orbital correlation analysis<sup>17</sup> that led to the prediction of perepoxide intermediates. Implicit in the correlation analysis is the assumption of a reactant electronic structure involving only doubly-occupied orbitals (analogous to one of the two resonance structures in the  $^1\Delta_g$  wavefunction. The analysis presented here shows that such wavefunctions are not correct representations of the reactant  $O_2(^1\Delta_g)$ . Similarly, the orbital phase continuity analysis<sup>49</sup> of Yamaguchi et al.<sup>50</sup> does not apply since the overlap of the relevant reactant orbitals is zero, and therefore, the relative phase is indeterminant.

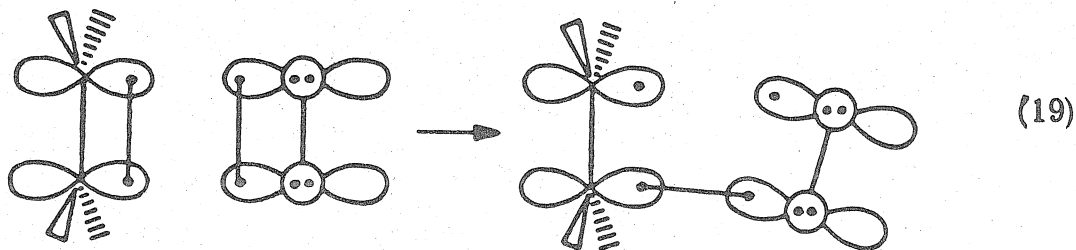
#### B. Electronic Structure of the $^1O_2$ -olefin Adduct.

Coupling one of the singly-occupied orbitals of the  $^1\Delta_{ga}$  state, (17), with a  $p\pi$  orbital of an olefin, leads to the  $\pi^3$  state of the peroxy biradical, (18).



In this olefin-oxygen adduct, the oxygen orbital directed toward the carbon radical center is doubly-occupied. Consequently (18) is prevented from closing directly to the 2+2 cycloaddition product, dioxetane. In order to ring close, it is necessary to orient (18) in such a way as to develop overlap between the two radical orbitals, leading to an additional barrier ( $\sim 12$  kcal for ethylene plus  $^1\text{O}_2$ ) to dioxetane formation.

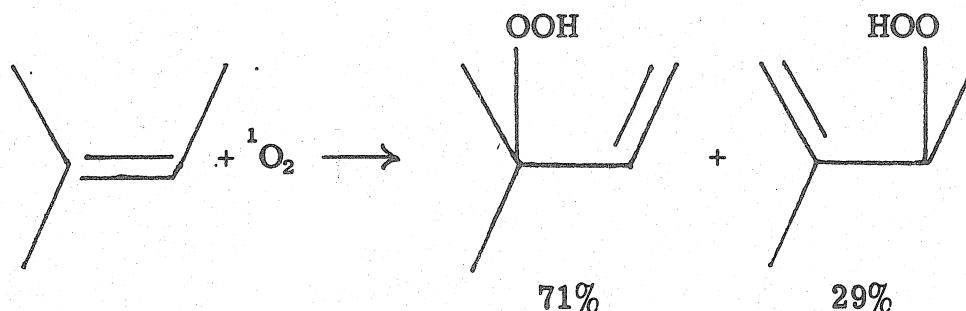
Addition of the  $^1\Delta_g$  state of  $\text{O}_2$  to an olefin leads to the  $\pi^4$  state of the peroxy biradical, (19).



The orbital phase continuity arguments of Yamaguchi<sup>50</sup> do apply to this state and indicate that the concerted  $2_s+2_s$  cycloaddition (without a diradical intermediate) is a forbidden process. However, as noted earlier, the  $\pi^4$  state of peroxy radicals lies 0.88 eV (20 kcal) above the  $\pi^3$  state (due to repulsions between the four  $\pi$  electrons) and therefore, this state is not expected to play a role in  $^1\text{O}_2$ -olefin ene reactions (where  $E_a = 2-10$  kcal).

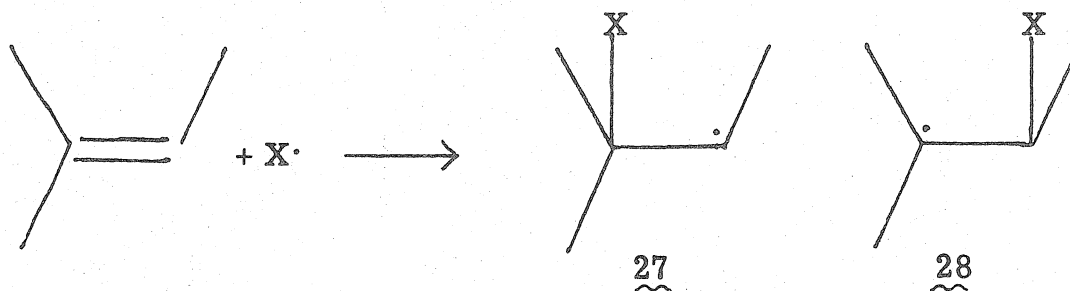
### C. Biradical Intermediates: Experiment

An important and often misinterpreted experiment bearing on the question of biradical intermediates was the determination of the product ratio resulting from the addition of  $^1\text{O}_2$  to trimethyl-ethylene. In the gas phase, the results are as follows,<sup>51</sup>



These and similar solution phase results, showing a lack of Markovnikov directing effects, have been interpreted as evidence against a biradical intermediate.<sup>16,17</sup> The argument is that there are two possible biradical intermediates, 20 and 21. Of these two, the one involving the tertiary radical center 21 is assumed to be more stable. Then, assuming the relative energies of the biradicals to be product determining, leads to a predicted product distribution dominated by the secondary hydroperoxide while experiment shows the tertiary hydroperoxide is the major product. The key assumption in this analysis is that  $\Delta H_f(\text{21}) < \Delta H_f(\text{20})$ . In fact, as discussed in Section IVA, our energetic estimates indicate that this assumption is incorrect, the secondary biradical is more stable than the tertiary. In order to make clear the origin of the Markovnikov effect and why it does not apply here, consider the more general addition of a

radical  $X\cdot$  to trimethylethylene. Again, there are two possible



radicals, a tertiary radical, 28, and a secondary radical, 27. In order to compare the energies of these two radicals, we must use a common reference point, for example the heat of formation of the reactants. The relative radical energies are then given by the C-X bond energies,<sup>52</sup> one involving a tertiary carbon and the second to a secondary carbon. For many radicals (for example  $X = \text{Br}\cdot, \text{I}\cdot, \text{R}_3\text{Si}\cdot, \text{R}_3\text{C}\cdot, \text{H}\cdot, \text{RS}\cdot$ , etc.), the bond energy to a secondary carbon is larger than that to a tertiary carbon. Thus, for these radicals the most stable adduct is the tertiary radical (in agreement with the Markovnikov effect). However, for highly electronegative radicals ( $X\cdot = \text{Cl}\cdot, \text{F}\cdot$  or  $\text{RO}\cdot$ ) the bond to a tertiary carbon is stronger than that to a secondary carbon.<sup>53</sup> The conclusion, then, is that normal Markovnikov directing effects are not expected in the addition of  $^1\text{O}_2$  to unsymmetrical olefins whether or not a biradical is involved at the product determining step. Furthermore, the results of gas phase  $^1\text{O}_2$  additions are consistent with a biradical or biradical-like species being product determining.

The possibility of a biradical intermediate in  $^1\text{O}_2$  hydroperoxidations was first seriously considered by Nickon. Litt and Nickon<sup>14</sup> concluded that a biradical intermediate is not consistent with the experimental evidence. Their reasoning can be summarized as follows:

(i) The observed lack of cis-trans isomerization of olefin indicates that a biradical is not formed reversibly.

(ii) A kinetic analysis of the reaction leads to the conclusion that irreversible biradical formation requires a rate constant for H- abstraction greater than Eyring's transition state frequency.

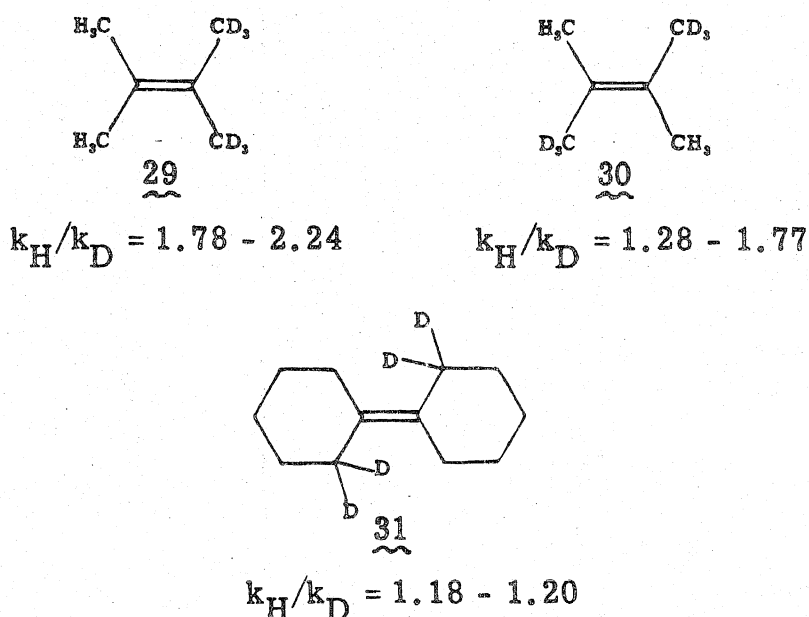
(iii) Primary deuterium isotope effects of 1.2 to 2.1 indicate participation of the C-H bond in the transition state.

Observation (i) indicates that, if the biradical is formed (either reversibly or irreversibly), barriers to product formation must be small relative to bond rotational barriers. As noted in the previous section, the H-abstraction step is analogous to a bimolecular radical disproportionation and on this basis is expected to proceed with near zero activation energy. Therefore, the lack of isomerization (and related work showing no effect of free radical inhibitors) is not inconsistent with a biradical or biradical-like intermediate.

The kinetic analysis, (ii), involved unreasonable assumptions. Of particular importance is the use of a triplet  $\pi \rightarrow \pi^*$  vertical excitation energy to obtain a 1,2-biradical energy (the adiabatic energy is more appropriate). This assumption led to a predicted  $\Delta H$  for addition forming a biradical of +25 kcal (compared

to +6 kcal in the present work). As 25 kcal is well above the observed activation energies, it is not surprising that a kinetic analysis based on this  $\Delta H$  would lead to implausible results.

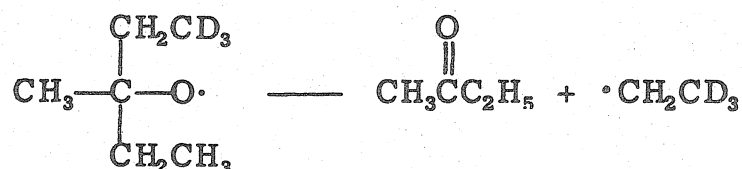
The primary deuterium isotope effects cited by Nickon,<sup>14</sup> (iii), are inconclusive. The observed rate ratios are approximately the size expected for secondary  $\beta$  deuterium isotope effects. For example, the intramolecular isotope effects reported by Nickon<sup>54</sup> are as follows,



where no correction for the number of deuteriums has been made (no correction need be made if any only if these are primary isotope effects). The dependence of the observed isotope effects on the number of deuteriums, however, is evidence that these are secondary isotope effects. Assuming then that these are secondary isotope effects and correcting to a per deuterium basis ( $k_H/k_D = \sqrt[n]{k_{Hn}/k_{Dn}}$ ) leads to  $k_H/k_D$ 's of 1.10-1.16, 1.09-1.21 and 1.09-1.10 respectively. The nearly constant values for these ratios supports the interpretation of these as secondary isotope effects.

More recent work by Kopecky et al.<sup>23</sup> on 29 and 30 led to somewhat smaller total isotope effects, 1.31-1.65 and 1.21-1.46 respectively.

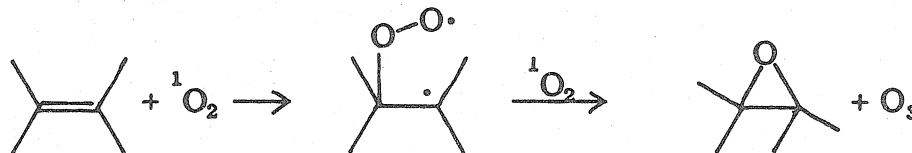
Converting again to per deuterium ratio leads to 1.05-1.09 and 1.09-1.13. For comparison, the secondary  $\beta$  deuterium isotope effect for the formation of ethyl radical from decomposition of methylethylethyl 2,2,2-d<sub>3</sub>-carbonyloxy radical,



is reported to be 1.08<sup>55</sup> (again on a per deuterium basis). Thus the observed isotope effects are consistent with normal  $\beta$  secondary isotope effects implying no C-H bond cleavage in forming the transition state. The slightly higher isotope effect for 30 might be due to a small, product-determining, primary isotope effect subsequent to the rate determining step.

Kopecky's results<sup>23</sup> and related work by Bartlett<sup>26</sup> indicate the magnitude of these isotope effects to be dependent on the solvent. For example Bartlett<sup>26</sup> reports kinetic isotope effects ( $k_{\text{H}}/k_{\text{D}}$ ) of 1.1 in acetonitrile and 1.2 in benzene. Apparently then the nature of the transition state is dependent on the solvent (see Section V E).

Finally, there is some evidence indicating the presence of a true intermediate in a few <sup>1</sup>O<sub>2</sub> hydroperoxidations. Of particular interest is the formation of epoxides under certain conditions.<sup>18, 56</sup> One possible source of the epoxides is from the trapping of a peroxy biradical by <sup>1</sup>O<sub>2</sub>. The latter step is ~ 46 kcal exothermic and might





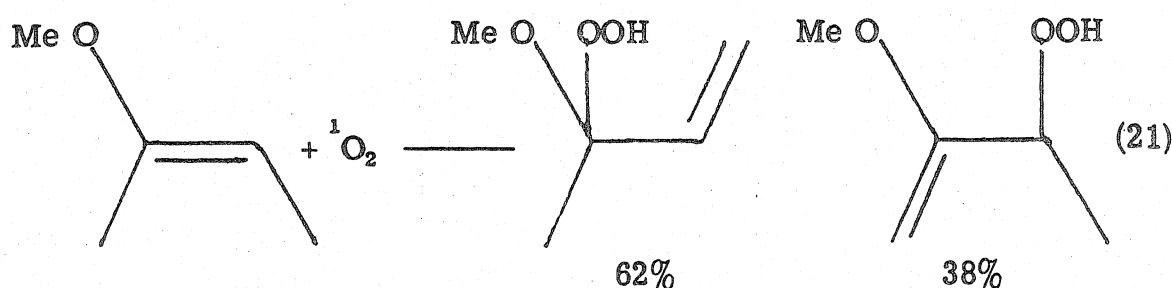
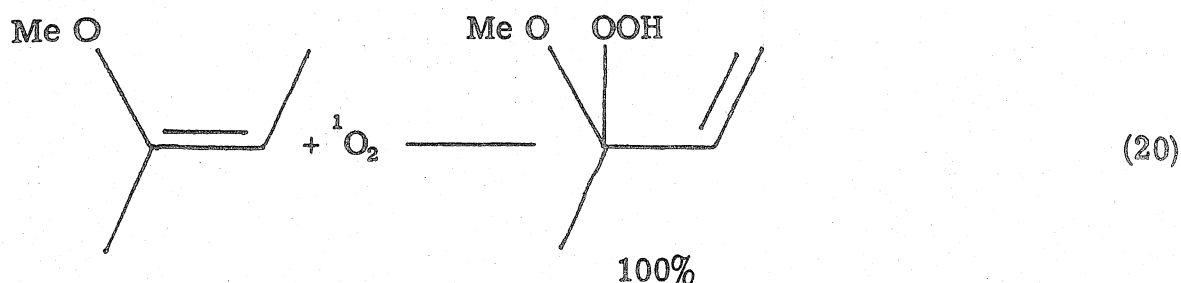
be a facile process. In fact, Bartlett<sup>57</sup> has found that epoxide products are accompanied by the production of ozone. This evidence is by no means conclusive though, particularly since epoxide production is apparently dependent on both the wavelength of light used and on the sensitizer.<sup>59</sup> In particular, sensitizers with low-lying carbonyl  $n \rightarrow \pi^*$  states produce unusually large amounts of epoxide.<sup>60</sup> Bartlett concludes that in at least some cases, the source of epoxides is not  $^1\text{O}_2$ .

Biradical intermediates, if sufficiently long lived, are also expected to initiate free radical polymerizations. Thus, the presence of polymeric products in  $^1\text{O}_2$  hydroperoxidations<sup>61,62</sup> is also consistent with a biradical intermediate (although, again, other sources of polymer are possible). Further evidence for the presence of an intermediate under some conditions is discussed in Section VE.

#### D. Polar Substituent Directing Effects

The results presented in Section IVB contain two important predictions; (i) A highly electronegative substituent (MeO) will direct the attack of  $^1\text{O}_2$  to a position alpha to the polar substituent, and (ii) A polar group will also direct the H-absorption step to occur preferentially from the substituent cis to the polar group. There is now experimental support for both of these conclusions.

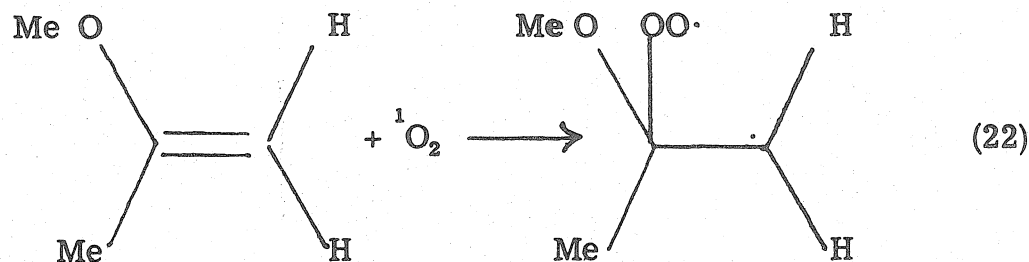
First, in order to test our predictions, Hammond<sup>63</sup> recently carried out gas phase experiments yielding the following results,



In reaction (20) the only observed product results from initial  $\alpha$  addition followed by cis abstraction, consistent with both predictions (i) and (ii). In reaction (21) there are no abstractable hydrogens cis to the methoxy group and, therefore, the preferred mode is not available. The result is that now two competing modes are detectable, one being  $\alpha$  addition (followed by trans abstraction) and the second being  $\beta$  addition.

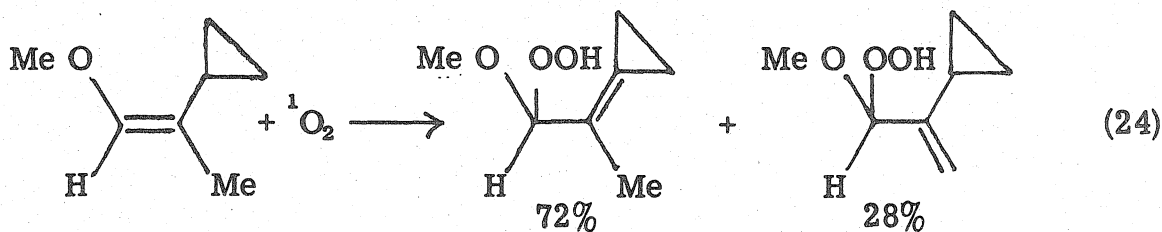
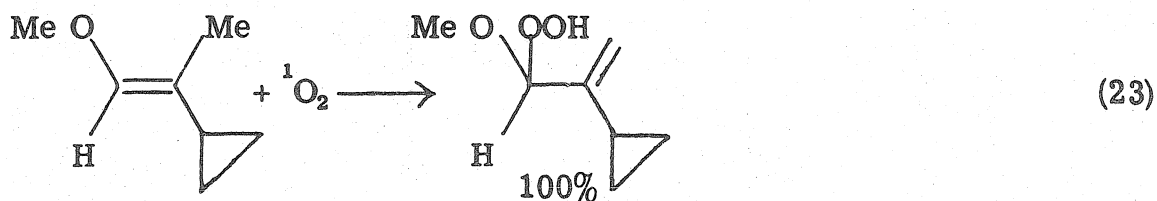
Related work by Cross,<sup>64</sup> using crossed molecular beams, has shown that gas phase addition of  $^1\text{O}_2$  to 2-methoxypropene leads to luminescence, presumably from decomposition of a dioxetane. Cross notes that this is an unexpected result since activation energies for 2+2 cycloaddition (forming dioxetane) are typically much larger than those for the ene process. However,

the results in Table IV indicate the preferred biradical is the  $\alpha$  adduct,



which cannot undergo the ene reaction.

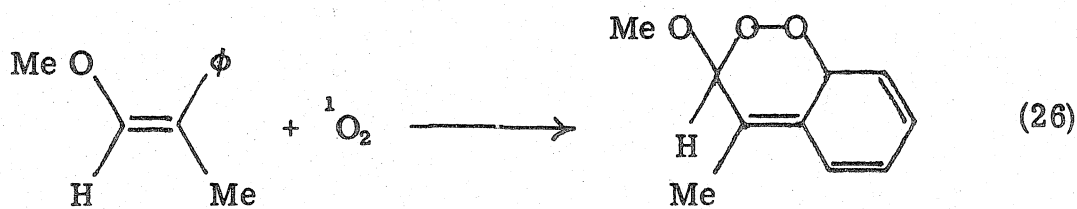
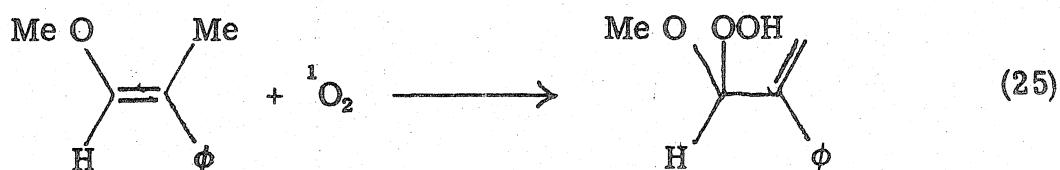
Additional support for this interpretation comes from work by Conia *et al.*<sup>65</sup> Conia's results are summarized in equations (23) and (24). Again the products show a clear bias toward H-abstraction



from the substituent cis to the methoxy group. In the latter reaction, (24), the dominant (cis abstraction) product is 9 kcal less stable than the minor product (trans abstraction) indicating that the effect is indeed an important one. Conia also notes that replacement of the methoxy group by methyl removes the directing effect. In

this case products resulting from abstraction of the cyclopropyl hydrogen are not observed (from either isomer).

Finally, recent studies by Foote et al.<sup>66</sup> also show the importance of this directing effect. In this work, the observed reactions are



In both cases, the only observed products are those resulting from attack of the oxygen radical center on the group cis to the methoxy.

It is found then, that a methoxy substituent exerts an important directing influence on the course of  ${}^1\text{O}_2$  reactions with various (quite different) olefins and under a variety of reaction conditions.

Furthermore, this effect can be understood in terms of the biradical intermediate, the conformation of which is controlled by the anomeric effect.

### E. Solution Phase Mechanism

In the previous sections we presented and discussed estimates for the energies of gas phase 1,4-biradicals and 1,4-zwitterions relative to the  $^1\text{O}_2$ -olefin reactants. In this section we will consider the effects of solvation on these relative energies and on the mechanism of  $^1\text{O}_2$ -olefin reactions.

As a simple model for solvation, assume the intermediate to be in a spherical cavity of radius  $R(\text{\AA})$ , surrounded by a dielectric medium with dielectric constant  $\epsilon$ . The stabilization of the zwitterion relative to the biradical can then be estimated using the formula,<sup>67,68</sup>

$$\Delta E(\text{kcal}) = 14.4 \frac{(\epsilon - 1)}{(2\epsilon + 1)} \frac{[\mu_{\text{zwit}}^2 - \mu_{\text{birad}}^2]}{R^3} \quad (27)$$

where  $\mu_{\text{zwit}}$  is the dipole moment (debye) of the zwitterionic state and  $\mu_{\text{birad}}$  is the dipole moment of the biradical. It is further assumed that  $\mu_{\text{zwit}}^2 \gg \mu_{\text{birad}}^2$  and that  $\mu_{\text{zwit}}$  can be approximated with the dipole resulting from two point charges separated by a distance of  $2.65\text{\AA}$ , the approximate distance between the carbon and oxygen radical centers of a gauche 1,4-biradical (see Appendix A).

The assumptions then are:

(i) The primary effect of the solvent can be approximated by a structureless dielectric medium.

(ii) The dominant term in the dielectric interaction is the dipole term (the effect of the quadrupole and higher moments are neglected), and

(iii) The dipole moments of the two states can be approximated as noted above. Although these assumptions are only partially correct, this procedure should yield a valid estimate of the magnitude of the solvent effect and, more importantly, the dependence of this effect on the solvent (dielectric constant).

Using a cavity of radius (2.65Å) and the above approximations, expression (27) reduces to,

$$\Delta E(\text{kcal}) = \frac{\epsilon - 1}{2\epsilon + 1} \times 125.4 \quad (28)$$

or, in the limit of high dielectric constant,  $\Delta E \approx 60$  kcal. Since this is larger than the estimated zwitterion-biradical energy separations (Table II), it is concluded that high dielectric solvents or low dielectric solvents with electron donating olefin substituents, can stabilize the zwitterion with respect to the biradical.

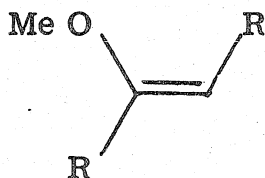
Under these conditions the intermediate will have the character of a 1,4-zwitterion with a smaller biradical component. In solvents of lower polarity the intermediate can have a character intermediate between that of a biradical and a zwitterion.

Similar solvent effects on the energy of the perepoxide are also to be expected. However, the dipole moment of the perepoxide, 5.6 D (see Appendix A), is much smaller than that expected for the open 1,4-zwitterion (~12 Debye). Since the solvent stabilization is proportional to  $\mu^2$ , the stabilization of the open 1,4-zwitterion will be ~ 3 times that of the perepoxide. Thus, in extreme cases

solvent stabilization may lower both the zwitterion and the perepoxide below the biradical, however, the ground state would be an open zwitterion, not a perepoxide.

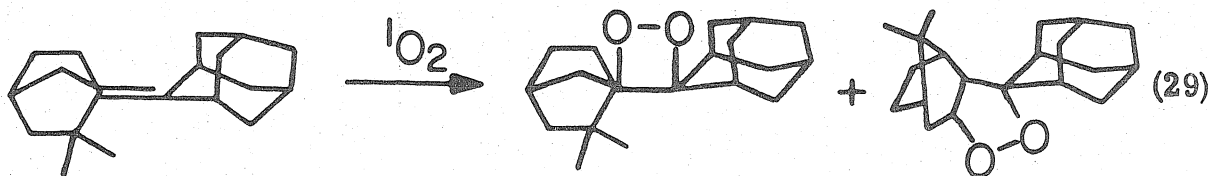
Although there are large uncertainties in the estimates of both the zwitterion energies and the solvation effects, some useful trends can be extracted. Consider first the addition of  $^1\text{O}_2$  to an unsymmetrical alkyl olefin. Biradical energetics indicate the preferred direction of addition is to the most substituted carbon in agreement with gas phase experiments. The zwitterion estimates indicate the preferred direction is to the least substituted carbon. Thus, if a solvent stabilized zwitterionic character is important, the product distribution should shift to larger yields of the less substituted peroxide.<sup>69</sup>

Similarly in the addition of  $^1\text{O}_2$  to an olefin of the form,



estimates of gas phase biradical energies show a clear preference for addition  $\alpha$  to the methoxy group (in agreement with results of gas phase experiments<sup>63</sup>). Zwitterion energetics, however, indicate that addition to the  $\beta$  carbon is 22 kcal lower energy than addition to the  $\alpha$  carbon. Therefore, if solvent stabilized open zwitterions play an important role in this reaction, there should be a large shift in the product distribution as a function of the dielectric constant.<sup>70</sup>

Several intriguing features of solution phase  $^1\text{O}_2$ -olefin chemistry can be understood by assuming a solvent dependent intermediate of varying degrees of biradical and zwitterion character. For example, McCapra's results<sup>25</sup> on the product ratios resulting from photo-oxidation of camphenylidene-adamantane, (29), show an increased yield of dioxalan



product (presumably resulting from a carbonium ion rearrangement of an intermediate zwitterion) with increased solvent dielectric.

It has also been reported that increased solvent polarity increases the amount of 2+2 cycloaddition product (dioxetanes) at the expense of alkylic hydroperoxides.<sup>26</sup> This is understandable since the zwitterionic structure should exhibit a greater tendency toward ring closure than the biradical (see Section VB).

#### F. Concerted vs. Biradical Mechanisms

In the preceding sections we have presented a thermochemical analysis of  $^1\text{O}_2$ -olefin additions in terms of biradical and zwitterionic intermediates. This analysis, of course, does not deny the possibility of a concerted mechanism, it simply shows that the



biradical is an energetically accessible intermediate and that it leads to regiospecificity in agreement with experiment. The possibility of a slightly lower energy, concerted pathway can not be discarded solely on the basis of these estimates. We stress, however, that these estimates indicate the biradical to be roughly degenerate with the gas phase transition state. This is in contrast to the situation for such clearly concerted reactions as the cope rearrangement, 2+4 cycloadditions or the cycloaddition of ozone to olefins. For example, in the latter case formation of a biradical requires 11 kcal while the observed activation energy is 4 kcal.<sup>72</sup>

In summary, theory and experiment are consistent with the saddle point for the reaction being of biradical structure with no bonding between the radical centers. Whether this state is a true saddle point or whether there are very small (~0.5 kcal) barriers to cleavage and abstraction has not been determined. Without such small barriers one might consider the reaction mechanism to be concerted but highly asynchronous (initial C-O bond formation followed by H-abstraction) as suggested by Nickon<sup>14</sup> and Foote.<sup>16</sup>

Finally, we note that whether the reaction is nonconcerted, involving a true biradical intermediate, or concerted, involving a biradical quasi-intermediate does not affect the predictions of regioselectivity discussed here. In either case, the factors (anomeric effect, etc.) which govern the biradical conformations will be of similar importance in determining the conformation of a biradical-like transition state.

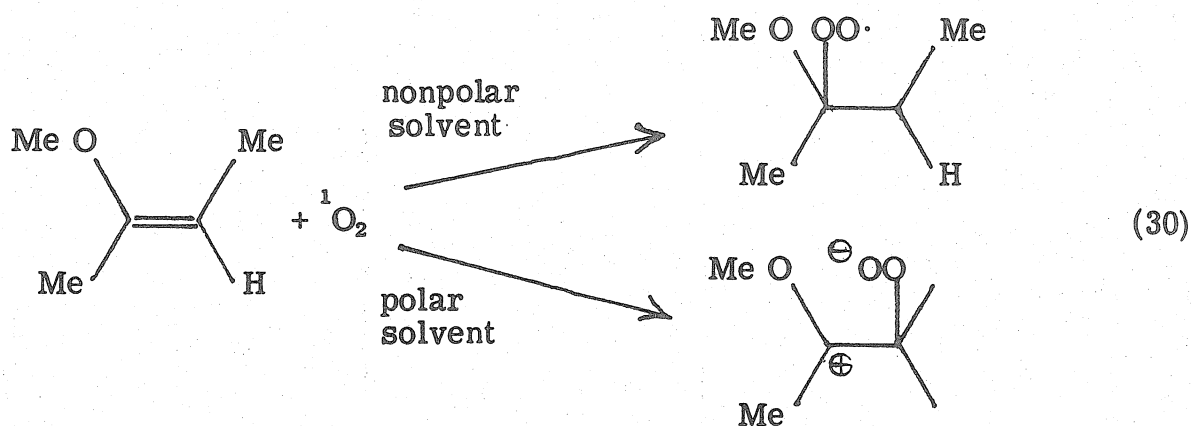
## VI. Summary

An analysis of the  $^1\text{O}_2$ -olefin ene reaction in terms of ab initio energies and thermochemical estimates has been presented. The results indicate that the energetics and regioselectivity of the gas phase reaction can be understood in terms of the peroxy biradical intermediate or quasi-intermediate. It is shown that the often cited lack of Markovnikov directing effects are not inconsistent with a biradical intermediate.

Energetic estimates indicate that both biradical and solvent stabilized zwitterions are energetically accessible intermediates in many solution phase reactions. The precise nature of the intermediate is critically dependent upon the nature of its environment (both solvent and substituent). It is shown that many of the solvent-dependent features of this reaction can be understood assuming an (quasi) intermediate of varying biradical-zwitterion character.

Furthermore, experimental results (formation of epoxides, polymeric product and cation rearrangement products) are cited as evidence for a true intermediate in certain  $^1\text{O}_2$ -olefin reactions.

The results of this analysis also lead to a number of verifiable predictions. The solvent dependent balance between zwitterionic and biradical character indicates that in many cases a marked shift in product distribution should occur as solvent polarity is increased. A particularly appropriate test for this prediction would be 1-methoxy-but-2-ene, (30), since the biradical and



zwitterionic energetics lead to clearly different predictions.

Finally, it is predicted that the observed directing influence of a MeO substituent should be a quite general effect. In particular, F or Cl substitution should lead to a similar directing effect.

#### Acknowledgments

The authors thank C. S. Foote, L. M. Stephenson, J. M. Conia, W. B. Hammond, P. B. Dervan, F. A. Houle and J. L. Beauchamp for preprints of their papers and for helpful discussions. This investigation was supported by NIH research grant number GM-23971 from the National Institute of General Medical Sciences.

### Appendix A. Ab Initio Calculations

The ab initio calculations on  $\text{CH}_2\text{CH}_2\text{O}^\bullet$  used the valence double zeta (DZ) basis of Huzinaga and Dunning<sup>38</sup> [(9s, 5p/4s) primitive Gaussians contracted to (3s, 2p/2s)] augmented with d polarization functions ( $\alpha_{\text{C}} = 0.6760$  and  $\alpha_{\text{O}} = 0.8853$ ) centered on each heavy atom. In addition, a set of diffuse oxygen centered s and p functions ( $\alpha = 0.059$ ) were included to describe the negative ion character correctly.

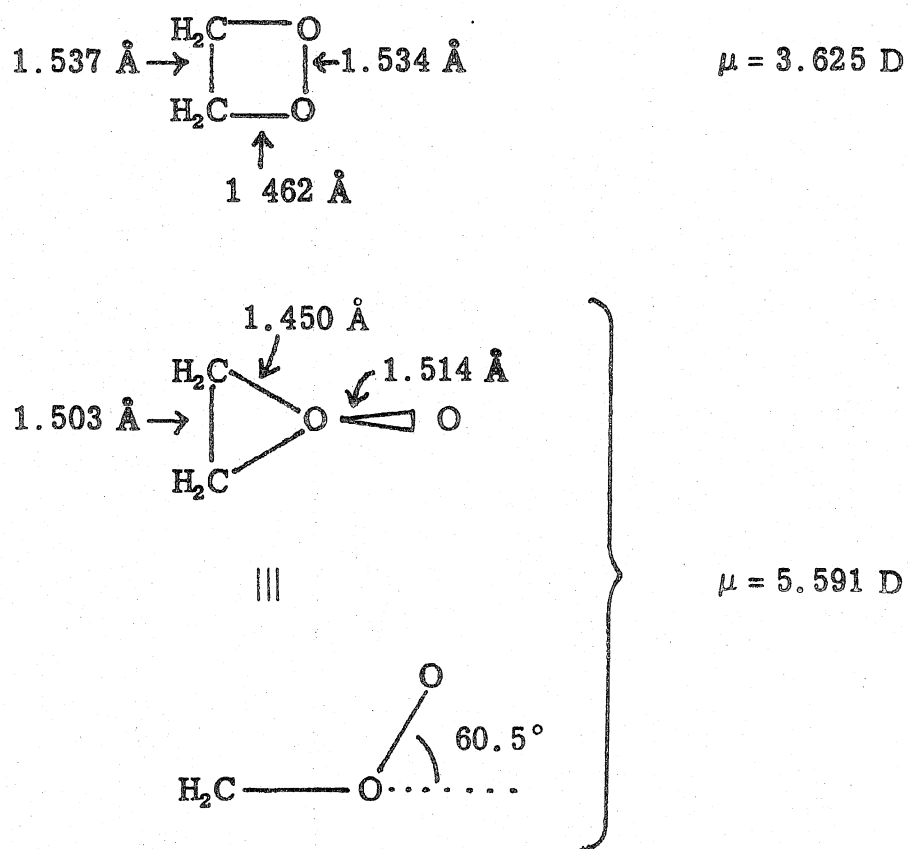
The geometry used for all states was  $R_{\text{CC}} = 1.51 \text{ \AA}$ ,  $R_{\text{CO}} = 1.41 \text{ \AA}$ ,  $R_{\text{CH}} = 1.08 \text{ \AA}$ , all bond angles about the saturated carbon were tetrahedral and all those about the C radical center were  $120^\circ$ . The CO and CC bond lengths were optimized for the biradical state. The remaining geometric parameters are all standard values.

Using this basis and geometry, GVB wavefunctions<sup>37</sup> were optimized in which all valence electron pairs were correlated, each with one correlating natural orbital. These calculations were carried out for each of four states: biradical, positive ion, negative ion, and zwitterion. The latter is the same symmetry as the ground state biradical. For this reason, it was necessary to place a restriction (the tighter of the two carbon radical  $p\pi$  atomic orbitals was required to have a zero coefficient in all orbitals) on the wavefunction of this state. The resulting total energies (hartrees) are, biradical -152.96278, positive ion -152.63100, negative ion -152.96574 and zwitterion -152.86425.

With these wavefunctions, the calculated dipole moments of the biradical and zwitterionic states are 2.36 D and 10.14 D respectively. For comparison, the two radical centers are 2.39 Å apart thus, the simple model of two point charges (see text) leads to a zwitterion dipole moment of 11.46 D. For a 1,3-zwitterion then this model overestimates the dipole moment by ~ 10%. For a 1,4-zwitterion, the errors are expected to be smaller.

Comparable calculations on the unsubstituted dioxetane and perepoxide led to the geometries and dipole moments shown in Figure 1.

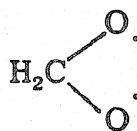
Figure 1. Calculated Geometries and Dipole Moments of Dioxetane and Perepoxyde.



### Appendix B. Anomeric Effect

The exact magnitude of the anomeric effect depends on the nature of the substituents. Thus, for example, calculations<sup>43</sup> on methanediol indicate an anomeric effect ( $V_2$ ) of  $\sim 0.5$  kcal while similar studies on dimethoxy methane led to a value of  $\sim 1.5$  kcal. The calculated preference for gauche over anti, however, was considerably larger for both of these molecules (3.7 and 2.6 kcal, respectively).

Calculations on dioxymethylene,<sup>72</sup> in which the anomeric



effect is exhibited in the separations between the eight possible biradical states, lead to a value of 6 kcal. Although no experimental barriers are available for methanediol or dimethoxymethylene, recent NMR studies<sup>73</sup> of rotational barriers of chloromethylmethyl ether and fluoromethylmethyl ether have led to an anomeric effect of 2-3 kcal.

Thus, both experimental and theoretical studies indicate a clear anomeric preference for gauche conformations over anti in molecules of the form 22, 23, and 24. The magnitude of this effect is variable, 2 to 6 kcal, depending on the particular molecule and the method of analysis. Finally, we note that the product distribution from the gas phase reaction of  $^1\text{O}_2$  with 2-methoxy-but-

2-ene has been found<sup>63</sup> to be consistent with an anomeric interaction of 3 kcal, in good agreement with the values from both theory and experiment on related molecules.



Table I. Carbon Centered Radical Group Functions

<u>Bond Energies</u> <sup>a</sup>		<u>Group Functions</u> <sup>b</sup>	
MeCH <sub>2</sub> -H	98.8	C·(H) <sub>2</sub> (C)	36.5
(Me) <sub>2</sub> CH-H	94.5	C·(H)(C) <sub>2</sub>	37.5
(Me) <sub>3</sub> C-H	92.7	C·(C) <sub>3</sub>	38.7
MeOCH <sub>2</sub> -H	94.1	C·(O)(H) <sub>2</sub>	31.9
(MeO)(Me)CH-H	(89.8) <sup>c</sup>	C·(O)(C)(H)	29.6
(MeO)(Me) <sub>2</sub> C-H	(88.0) <sup>c</sup>	C·(O)(C) <sub>2</sub>	28.7

a) From reference 10 except where noted.

b) Obtained using  $G[C·(X)(Y)(Z)] = G[C(H)(X)(Y)(Z)] + D_0 - 52.1$ .

c) Estimated assuming bond energy lowering on methyl substitution identical to that for corresponding hydrocarbon.

Table II. Biradical-Zwitterion Separations (kcal/mol) for  $R_1R_2C-CH_2-OO$ . Positive  $\Delta E$  indicates that the biradical is lower.

$R_1$	$R_2$	Biradical		Positive Ion		$\Delta E$
		$\Delta H_f^a$	IP	$\Delta H_f$	$E_{\text{zwit}} - E_{\text{birad}}$	
H	H	26.5	193 <sup>c</sup>	220 <sup>b</sup>		49
CH <sub>3</sub>	H	17.6	170 <sup>c</sup>	187		26
CH <sub>3</sub>	CH <sub>3</sub>	8.4	154 <sup>c</sup>	162		10
HO	H	-18.5	155	136 <sup>d</sup>		11
HO	CH <sub>3</sub>	-29.3	145	115 <sup>d</sup>		1

- a) Obtained from the heats of formation of reference 10 and the C-H bond energies of Table I.
- b) From reference 36.
- c) F. A. Houle and J. L. Beauchamp, A.C.S. meeting at Anaheim, March (1978); F. A. Houle and J. L. Beauchamp, J. Am. Chem. Soc. (to be submitted).
- d) From J. F. Wolfe, R. H. Staley, I. Koppel, M. Taagepera, R. T. McIver, Jr., J. L. Beauchamp and R. W. Taft, J. Am. Chem. Soc., 99, 5417 (1977).

**Table III.** Energetics (in kcal/mol) for Addition of  $^1\text{O}_2$  to Alkyl-substituted Olefins. The enthalpy of forming the olefin-dioxygen adducts from olefin and  $^1\text{O}_2$  is listed for the zwitterion, perepoxide and biradical intermediates.  $\Delta H_f(\alpha)$  and  $\Delta H(\beta)$  are the estimated enthalpies (kcal/mol) of addition to the  $\alpha$  and  $\beta$  sides of olefin, respectively.





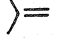


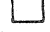





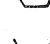


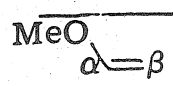
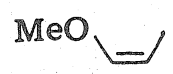
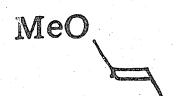
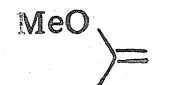
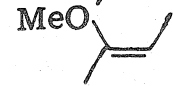
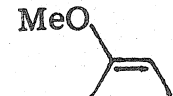
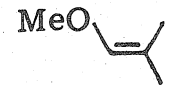
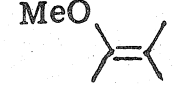
Olefin	Olefin $\Delta H_f$	Zwitterion		Perepoxide $\Delta H$	Olefin Dioxygen Adducts Biradical		Exper $E_a$
		$\Delta H(\alpha)$	$\Delta H(\beta)$		$\Delta H(\alpha)$	$\Delta H(\beta)$	
	+12.5	+59		+16.1		+10.1	--
$\alpha=\beta$ 	+ 4.6	+58	+39	+15.2	+8.7	+8.8	--
	- 2.2	32		+13.7		+ 6.3	6.5
	- 3.2	33		+13.7		7.3	7.3
	- 3.8	56	18	+14.0	7.5	8.2	--
	-10.7	31	16	+12.6	5.2	5.8	4.9
	-17.1	13		+10.4		2.6	3.2
	+37.5	36				5.6	
	+29.0	31	15		4.5	5.1	
	+20.6	14				3.9	4.0
	8.6	33				7.2	7.4
	0.2	32	17		6.0	6.6	6.0
	- 7.3	14				4.5	4.0
	- 0.8	31				5.5	>8.2
	- 9.2	30	15		4.3	5.0	7.5
	-17.0	13				2.8	4.0

Table IV. Energetics (kcal/mol) of Addition of  $^1\text{O}_2$  to Methoxy-substituted Olefins. The enthalpy of forming the olefin-dioxygen adducts from olefin and  $^1\text{O}_2$  is listed for the zwitterion and biradical intermediates (energies in kcal/mol).

Olefin	Olefin $\Delta H_f$	Zwitterion		Biradical	
		$\Delta H(\alpha)$	$\Delta H(\beta)$	$\Delta H(\alpha)^a$	$\Delta H(\beta)$
	-25.7	56	19	6.8	8.1
	-33.6	31	17	5.5	5.7
	-33.6	31	17	5.5	5.7
	-11.6	52	6	2.8	5.5
	-42.1	27	5	1.5	4.1
	-41.1	26	4	0.5	3.1
	-42.1	15	17	5.0	5.6
	-49.6	10	3	0.0	2.0

a) Assumes a conformation consistent with the anomeric effect (see text)

References and Notes

- (1) Presented at the 6th annual Leermakers Symposium, Wesleyan University, May 11, 1978 and at the Mechanisms Conference, Duluth, Minnesota, June 28, 1978.
- (2) R. W. Denny and A. Nickon, Org. Reactions, 20, 133 (1973).
- (3) W. S. Gleason, A. D. Broadbent, E. Whittle, and J. N. Pitts Jr., J. Am. Chem. Soc., 92, 2068 (1970).
- (4) K. L. Demerjian, J. A. Kerr and J. G. Calvert, Adv. in Environ. Sci. and Tech., 4, 1 (1974).
- (5) M. Kasha and A. U. Khan, Ann. N.Y. Acad. Sci., 171, Art. 1, 5 (1970).
- (6) T. Wilson and J. W. Hasting, "Photophysiology," Vol. V, A. C. Giese, Ed., Academic Press, New York, N.Y., p. 49 (1970).
- (7) J. R. Politzer, G. W. Griffen, J. L. Laseter, Chem. Biol. Interactions, 3, 73 (1971).
- (8) C. S. Foote in "Free Radicals in Biology," W. A. Pryor, Ed., Academic Press Inc., New York, N.Y. Vol. II, p. 85 (1976).
- (9) L. B. Harding and W. A. Goddard III, J. Am. Chem. Soc., 99, 4520 (1977).
- (10) (a) S. W. Benson, "Thermochemical Kinetics," 2nd ed., J. Wiley and Sons, New York, N.Y. (1976), (b) S. W. Benson, F. R. Cruickshank, D. M. Golden, G. R. Haugen, H. E. O'Neal, A. S. Rodgers, R. Shaw and R. Walsh, Chem. Rev., 69, 279 (1968).

- (11) C. S. Foote, R. Wexter and W. Ando, Tetra. Lett., 46, 4111 (1965).
- (12) K. Gollnick and G. O. Schenck, Pure Appl. Chem., 9, 507 (1964).
- (13) A. Nickon and J. F. Bagli, J. Am. Chem. Soc., 83, 1498 (1961).
- (14) F. A. Litt and A. Nickon, Adv. in Chem. Ser. No. 77, 118 (1968).
- (15) D. B. Sharp, "Abstracts of Papers", 138th Meeting ACS, Sept. 1960, p. 79.
- (16) (a) C. S. Foote, Accts. Chem. Res., 1, 104 (1968), (b) C. S. Foote, Pure and Appl. Chem., 27, 635 (1971).
- (17) D. R. Kearns, Chem. Rev., 71, 395 (1971) and references therein.
- (18) (a) C. W. Jefford, M. H. Laffer and A. F. Boschung, J. Am. Chem. Soc., 94, 8904 (1972), (b) C. W. Jefford and A. F. Boschung, Helv. Chim. Acta, 57, 2242 (1974), (c) C. W. Jefford and A. F. Boschung, Helv. Chim. Acta, 57, 2257 (1974).
- (19) C. W. Jefford and C. G. Rimbault, J. Org. Chem., 43, 1908 (1978).
- (20) C. W. Jefford and C. G. Rimbault, J. Am. Chem. Soc., 100, 295 (1978).
- (21) N. M. Hasty and D. R. Kearns, J. Am. Chem. Soc., 95, 3380 (1973).
- (22) E. C. Blossey, D. C. Neckers, A. L. Thayer and A. P. Schaap, J. Am. Chem. Soc., 95, 5820 (1973).

- (23) K. R. Kopecky and J. H. Van De Sande, Can. J. Chem., 50, 4034 (1972).
- (24) K. R. Kopecky, W. A. Scott, P. A. Lockwood and C. Mumford, Can. J. Chem., 56, 1114 (1978).
- (25) F. McCapra and I. Beheshti, J. C. S. Chem. Comm., 517 (1977).
- (26) A. A. Frimer, P. D. Bartlett, A. F. Boschung and J. G. Jewett, J. Am. Chem. Soc., 99, 7977 (1977).
- (27) S. Inagaki and K. Fukui, J. Am. Chem. Soc., 97, 7480 (1975).
- (28) S. Inagaki, H. Fujimoto and K. Fukui, Chem. Letts., 749 (1976).
- (29) (a) L. A. Paquette, D. C. Liotta and A. D. Baker, Tetrahedron Letts., 2681 (1976), (b) L. A. Paquette, C. C. Liao, D. C. Liotta and W. E. Firstad, J. Am. Chem. Soc., 98, 6412 (1976), (c) L. A. Paquette, D. C. Liotta, C. C. Liao, T. G. Wallis, N. Eickman, J. Clardy and R. Gleiter, J. Am. Chem. Soc., 98, 6413 (1976).
- (30) (a) M. J. S. Dewar and W. Thiel, J. Am. Chem. Soc., 97, 3978 (1975), (b) M. J. S. Dewar and W. Thiel, J. Am. Chem. Soc., 99, 2338 (1977); (c) M. J. S. Dewar, A. C. Griffin, W. Thiel, and I. J. Turchi, J. Am. Chem. Soc., 97, 4439 (1975).
- (31) R. D. Ashford and E. A. Ogryzlo, J. Am. Chem. Soc., 97, 3604 (1975).
- (32) L. B. Harding and W. A. Goddard III, Tetrahedron Letts., 747 (1978).
- (33) S. K. Shih, S. D. Peyerimhoff and R. J. Buenker, Chem. Phys., 28, 299 (1978).

- (34) (a) K. H. Becker, E. H. Fink, P. Langer and U. Schurath, J. Chem. Phys., 60, 4623 (1974), (b) H. E. Hunziker, and H. R. Wendt, J. Chem. Phys., 60, 4622 (1974), (c) P. A. Freedman and W. J. Jones, J. Chem. Soc. Farad. Trans. II, 76, 207 (1976).
- (35) It is assumed that the EA of the  $\pi^4$  state, (16), of a peroxy radical is approximately the same as that of an alkoxy radical, 1.68 eV.<sup>36</sup> Using a  $\pi^3 \rightarrow \pi^4$  excitation energy of 0.88 eV, then leads to a predicted EA of the  $\pi^3$  state of 0.8 eV.
- (36) H. M. Rosenstock, K. Draxel, B. W. Steiner and J. T. Herron, J. Phys. Chem. Ref. Data, 6, 1-1 (1977).
- (37) (a) W. J. Hunt, P. J. Hay and W. A. Goddard III, J. Chem. Phys., 57, 738 (1972), (b) W. A. Goddard III, T. H. Dunning, Jr., W. J. Hunt and P. J. Hay, Accts. Chem. Res., 6, 368 (1973), (c) The GVB calculations were carried out using the Bobrowicz-Bair-Goddard program GVB2P5.
- (38) T. H. Dunning, Jr. and P. J. Hay in "Modern Theoretical Chemistry: Methods of Electronic Structure Theory," H. F. Schaeffer, ed., Vol. 3, Plenum Press, New York, N.Y., 1977, pp. 1-27.
- (39) J. D. Cox and G. Pilcher in "Thermochemistry of Organic and Organometallic Compounds," Academic Press, New York, N.Y. (1970) p. 208.
- (40) For a review of the experimental literature see N. S. Zefirov and N. M. Shekhtman, Russ. Chem. Rev., 40, 315 (1971).



- (41) C. Romers, C. Altona, H. R. Buys and E. Havinga, Top. Stereochem., 4, 39 (1969).
- (42) S. David, O. Eisenstein, W. J. Hehre, L. Salem and R. Hoffmann, J. Am. Chem. Soc., 95, 3806 (1973).
- (43) (a) G. A. Jeffrey, J. A. Pople and L. Radom, Carbohydr. Res., 25, 117 (1972), (b) G. A. Jeffrey, J. A. Pople, J. S. Binkley and S. Vishveshwara, J. Am. Chem. Soc., 100, 373 (1978).
- (44) D. G. Gorenstein and D. Kar, J. Am. Chem. Soc., 99, 672 (1977).
- (45) (a) L. Radom, W. J. Hehre and J. A. Pople, J. Am. Chem. Soc., 93, 289 (1971), (b) W. A. Lathan, L. Radom, W. J. Hehre and J. A. Pople, J. Am. Chem. Soc., 95, 699 (1972).
- (46) J.-M. Lehn and G. Wipff, Helv. Chim. Acta, 61, 1274 (1978).
- (47) This conclusion conflicts with that of Fukui et al.<sup>48</sup> who, using the complex orbital representation, concluded that the <sup>1</sup>Δ state has no biradical character.
- (48) K. Fukui and K. Tanaka, Bull. Chem. Soc. Japan, 50, 1391 (1977).
- (49) W. A. Goddard III, J. Am. Chem. Soc., 94, 793 (1972).
- (50) K. Yamaguchi, T. Fueno and H. Fukutome, Chem. Phys. Letts., 22, 466 (1973).
- (51) W. S. Gleason, I. Rosenthal and J. N. Pitts, J. Am. Chem. Soc., 92, 7042 (1970).
- (52) J. M. Tedder and J. C. Walton, Accts. of Chem. Res., 9, 183 (1976).

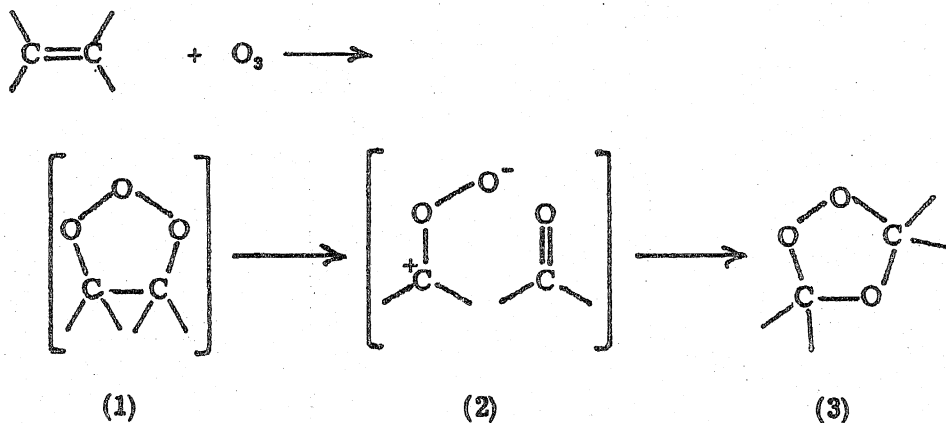
- (53) One explanation for this is that the polar nature of the C-X bond introduces a degree of carbonium ion character at the alpha carbon. Carbonium ions are greatly stabilized by alkyl substituents (to a greater extent than are radicals) and, therefore, the strongest polar bond is to the most substituted carbon.
- (54) A. Nickon, V. T. Chuang, P. J. L. Daniels, R. W. Denny, J. B. Di Giorgio, J. Tsunetsugu, H. G. Vilhuber and E. Werstiuk, J. Am. Chem. Soc., 94, 5517 (1972).
- (55) A. Tsolis, P. P. Hunt, J. K. Kochi and S. Seltzer, J. Am. Chem. Soc. 98, 992 (1976).
- (56) (a) G. Rousseau, P. LePerchec and J. M. Conia, Tetrahedron, 2533 (1976), (b) A. P. Schaap and G. R. Faler, J. Am. Chem. Soc., 95 3381 (1973), (c) P. D. Bartlett and M. S. Ho, J. Am. Chem. Soc., 96 627(1974).
- (57) P. D. Bartlett, personal communication to M. J. S. Dewar.<sup>58</sup>
- (58) M. J. S. Dewar, in "Further Perspectives in Organic Chemistry," North-Holland Publishing Co., New York, N.Y. (1978) pp. 107-129.
- (59) P. D. Bartlett in "Organic Free Radicals," W. A. Pryor, ed., ACS Symposium Series, 69, pp. 15-32 (1978).
- (60) N. Shimizu and P. D. Bartlett, J. Am. Chem. Soc., 98, 4193 (1976).
- (61) A. A. Frimer, D. Rot and M. Specher, Tetrahedron Letts., 1927 (1977).
- (62) C. W. Jefford and C. G. Rimbault, Tetrahedron Letts., 2479 (1976).
- (63) W. B. Hammond, Tetrahedron Letts., submitted for publication.

- (64) K. T. Alben, A. Auerbach, W. M. Ollison, J. Weiner and R. J. Cross, Jr., J. Am. Chem. Soc., 100, 3274 (1978).
- (65) G. Rousseau, P. LePerchec, and J. M. Conia, Tetrahedron Letts., 2517 (1977).
- (66) D. Lerdal and C. S. Foote, preprint from authors.
- (67) R. Huisgen, Acc. Chem. Res., 10, 117 (1977).
- (68) K. J. Laidler and H. Eyring, Ann. N.Y. Acad. Sci., 39, 303 (1940).
- (69) Solution phase hydroperoxidations of trimethylethylene<sup>14</sup> do show a small shift toward the secondary hydroperoxide relative to the gas phase result.<sup>51</sup> It is not known if this shift is dependent on solvent polarity.
- (70) Conia et al.<sup>71</sup> have recently proposed an open zwitterionic intermediate for a similar reaction in nonpolar solvent. Our estimates indicate that in the gas phase the zwitterion state is ~10 kcal above the biradical, and the net solvent ( $\epsilon = 2.8$ ) stabilization of the zwitterion is ~35 kcal. Therefore, we expect the solvated state to involve a mixture of zwitterionic and biradical character.
- (71) G. Rousseau, A. Lechevallier, F. Huet and J. M. Conia, Tetrahedron Letts., in press.
- (72) (a) W. R. Wadt and W. A. Goddard III, J. Am. Chem. Soc., 97, 3004 (1975), (b) L. B. Harding and W. A. Goddard III, J. Am. Chem. Soc., 100, 0000 (1978).
- (73) F. A. L. Anet and I. Yavari, J. Am. Chem. Soc., 99, 6752 (1977).

**PART B: MECHANISMS OF GAS PHASE AND LIQUID  
PHASE OZONOLYSIS**

# I. Introduction

The reaction of ozone and olefins has been of continuing interest to chemists for over 100 years. Most recently the gas phase reaction has received considerable attention due to its importance in photochemical smog formation.<sup>2</sup> Nearly 30 years ago Criegee proposed<sup>3</sup> the following mechanism,



in order to explain the isolation of 1,2,4-trioxolanes (3) from ozone-olefin reaction mixtures and to explain the incorporation of foreign aldehydes into these products. Since then a great deal of experimental evidence (solution phase) has been reported, supporting the Criegee mechanism<sup>4</sup> with only minor modifications.<sup>5</sup>

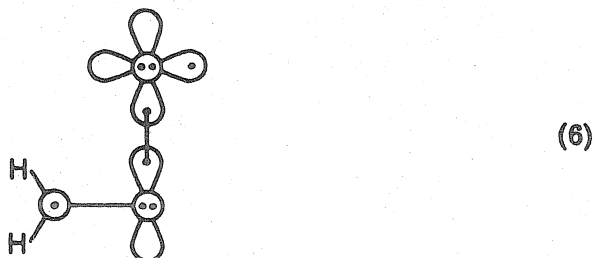
Recent *ab initio* calculations<sup>1</sup> on the peroxymethylene intermediate ( $\text{CH}_2\text{OO}$ ) have established the electronic structure of the planar gas phase species to be that of a singlet biradical (4) similar to ozone.



As discussed in the earlier paper,<sup>1</sup> the  $\pi$  system of the planar ground state consists of a doubly-occupied p orbital on the central oxygen and singly-occupied p orbitals on both of the terminal atoms, (5). The terminal p orbitals

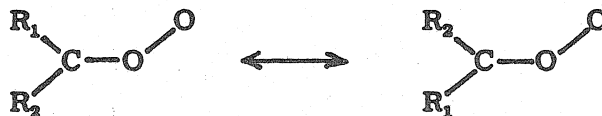


are found to overlap considerably ( $S = 0.346$ ), leading to a ground state singlet,  $^1A'(4\pi)$ , and a low-lying excited state triplet,  $^3A'(4\pi)$  (corresponding to triplet coupling the two singly-occupied orbitals). Two other low-lying excited states of the planar molecule,  $^1A''(5\pi)$  and  $^3A''(5\pi)$ , derive from configuration (6),



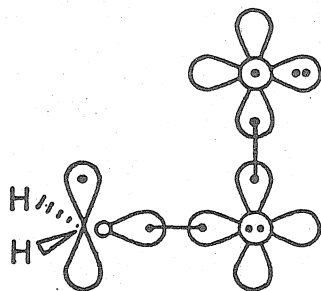
in which the  $p\pi$  orbital of the terminal oxygen is doubly-occupied.

Of considerable importance in understanding the mechanism of ozonolysis is the barrier to interconversion of the syn and anti peroxyethylene intermediates

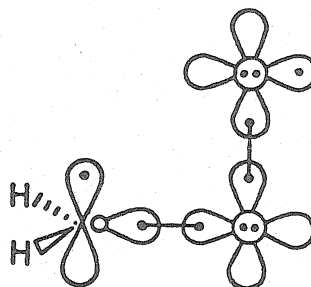


The transition state for this interconversion is expected to be a peroxyethylene species in which the plane of the carbon has been rotated  $90^\circ$  (making the  $R_2CR_1$  plane perpendicular to the COO plane).<sup>6</sup>

Rotating the  $\text{CH}_2$  group of (5) and (6), we obtain (7) and (8), respectively,



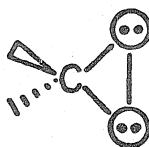
(7)



(8)

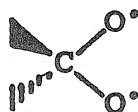
Of these we expect the singlet and triplet states corresponding to (7),  $^1\text{A}''(3\pi)$  and  $^3\text{A}''(3\pi)$ , to be lower in energy due to the three-electron O-O  $\pi$  bond.

The singlet state of (8),  $^1\text{A}''(4\pi)$ , can undergo ring closure forming dioxirane, (9). The weakest bond of



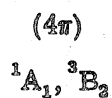
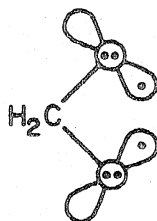
(9)

dioxirane is the O-O bond, and cleaving this bond leads to the reactive intermediate dioxymethylene (10).

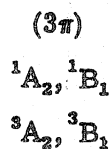
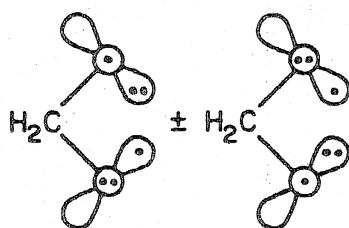


(10)

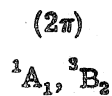
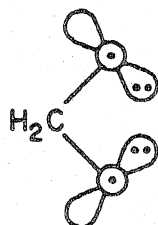
There are altogether eight biradical states corresponding to (10), four singlets and four triplets (11)-(13),



(11)



(12)



(13)

all of which are expected to lie fairly close (10 kcal) in energy.

It is the purpose of this paper to examine with accurate ab initio calculations (large basis set, correlated wavefunctions) the electronic structure and relative energies of configurations (5)-(13) and to discuss the implications of these results on the mechanism of ozonolysis. In Section II details concerning the geometries, basis set, and wavefunctions are presented. The results of the calculations are presented in Section III and discussed in Section IV.



## II. Computational Details

A. Basis Set and Geometries. All calculations used the valence double zeta (DZ) basis of Huzinaga and Dunning<sup>7</sup> [(9s, 5p/4s) primitive Gaussians contracted to (3s, 2p/2s)] augmented with d polarization functions ( $\alpha_C = 0.6760$ ,  $\alpha_O = 0.8853$ ) centered on each heavy atom. The hydrogen exponents were scaled by 1.44 (corresponding to a Slater function with  $\zeta = 1.2$ ).

The geometries employed in these calculations are shown in Figure 1. In all configurations CH bonds were assumed to be 1.08 Å and all trivalent carbon bond angles were taken to be 120°. Optimized parameters are indicated by an underline in Figure 1.

For the planar ground state of peroxyethylene [configuration (5)], the three remaining parameters,  $r(\text{CO})$ ,  $r(\text{O-O})$ , and COO angle, were optimized. The results are shown in Figure 1A.

For perpendicular peroxyethylene [configurations (7) and (8) and Figure 1B], the C-O bond length was assumed to be that of dimethyl ether,<sup>8</sup> 1.41 Å, and the COO bond angle was taken to be 103°, intermediate between that of dimethyl peroxide (105°) and hydrogen peroxide (100°).<sup>9</sup> The O-O bond length was optimized for each of the four valence states.

For the ring state [configuration (9) or Figure 1C] the C-O bond length and the HCH angle were taken to be 1.436 Å and 116°, respectively, as in ethylene oxide.<sup>10</sup> The O-O bond distance was taken as 1.45 Å, as is found in the ring state of ozone.<sup>11</sup>

Finally, for dioxymethylene, the C-O distance was assumed to be 1.41 Å (from dimethyl ether)<sup>8</sup> and the OCO and HCH angles were chosen to be 106° and 113°, respectively (from 1,2,4-trioxolane<sup>12</sup>). We optimized the bond lengths of a closely related diradical,  $\text{CH}_2\text{CH}_2\text{O}$ , obtaining a C-O bond length of 1.411 Å; this supports the choice of 1.41 Å chosen for dioxymethylene.

B. GVB(3) Calculations. Previous calculations on ozone have shown the Hartree-Fock (HF) wavefunction to lead to a qualitatively inaccurate description of the low-lying states (for example, HF predicts the ground state of ozone to be a triplet).<sup>11</sup> The cause of this failure is the orbital occupancy restrictions placed on the HF wavefunction which leads to a poor description of states with considerable singlet biradical character [such as (5)].

The GVB method corrects the major deficiencies in the HF wavefunctions by allowing singlet-paired electrons to split or correlate with singly-occupied nonorthogonal orbitals. This corresponds to the following replacement,

$$\phi_{\text{HF}}(1)\phi_{\text{HF}}(2) \rightarrow \phi_{\ell}(1)\phi_{\text{r}}(2) + \phi_{\text{r}}(1)\phi_{\ell}(2) = \lambda_1\phi_a^2 - \lambda_2\phi_b^2,$$

where  $\phi_{\ell}$  and  $\phi_{\text{r}}$  are the nonorthogonal valence bond-like orbitals and  $\phi_a$  and  $\phi_b$  form the equivalent natural orbital representation. Calculations on a large number of well-characterized small molecules<sup>13-16</sup> have shown that for the purpose of calculating excitation energies of valence states it is necessary to have a consistent level of correlation in the ground and excited state wavefunctions. [Hartree-Fock calculations in which the ground and excited states usually have differing numbers of open-shell orbitals are not consistent.]

From the valence bond diagrams, (5)-(8), we conclude that a consistent level of description for peroxymethylene biradical is one in which three pairs are allowed to correlate, the C-O and O-O sigma bonds and the  $\pi$  pair. We will denote these wavefunctions as GVB(3/PP) indicating three pairs have been correlated and the perfect pairing restriction has been applied.<sup>17, 18</sup>

In order to obtain accurate excitation energies, it is necessary to relax the perfect pairing restriction and to include the important interpair correlation terms neglected in the GVB(3/PP) wavefunction. By using the self-consistent GVB(3/PP) orbitals this can be accomplished with a relatively

small configuration interaction (CI) calculation<sup>19</sup> [the CI calculations also included four additional virtual p orbitals, one corresponding to each occupied p orbital; thus, for example, the CI basis for the states of planar peroxy-methylene would include three p- $\pi$  virtuals (one on each oxygen and carbon) and a p- $\sigma$  virtual centered on the terminal oxygen]. In all cases the GVB(3/PP) orbitals used in the CI calculations were solved self-consistently for the lowest states of each appropriate symmetry.

C. The GVB(7) Calculations. Although the GVB(3)-CI calculations are sufficiently accurate for the purposes of calculating valence excitation energies or one-electron properties (e.g., dipole moments), they do not lead to sufficiently accurate bond energies. For example, the equivalent calculations on the A-B bond energies of  $\text{CH}_3\text{-CH}_3$ ,  $\text{CH}_3\text{-OH}$ , and  $\text{HO-OH}$  lead to results that are consistently low, the errors being 10, 22, and 21 kcal, respectively.<sup>20</sup> There are primarily two sources of error in these calculations; the neglect of all but the dominant intrapair correlation and the neglect of interpair correlations between the bond pair being broken and other adjacent bond pairs and lone pairs.

In order to include the intrapair terms it is necessary to optimize additional correlating natural orbitals for the bond pair to describe the radial and angular correlations in addition to the dominant (left-right) correlation. Calculations on simple molecules have shown three additional natural orbitals to be sufficient.

In order to include the interpair terms it is necessary to correlate not only the bond being broken but also all of the adjacent bond pairs and lone pairs. An extensive CI calculation within the resulting set of orbitals serves to include the important intra- and interpair terms.<sup>21</sup> The equivalent calculations on the bond energies of  $\text{CH}_3\text{-CH}_3$ ,  $\text{CH}_3\text{-OH}$ , and  $\text{HO-OH}$  lead to errors of 3, 1, and -4 kcal, respectively.

Calculations of this level of accuracy are essential for comparing energies of species with differing numbers (or types) of bond pairs (for example, to obtain the relative energy of the ring state to any of the open states).

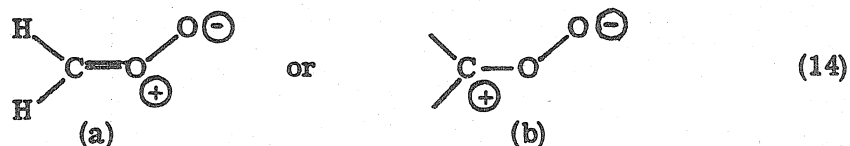
### III. Results

A. Peroxymethylene. As noted earlier, the ground state of gas phase peroxymethylene is a planar singlet biradical,  $^1A'(4\pi)$ . The  $\pi$  electronic structure of this state is very similar to that of ozone, consisting of a doubly-occupied  $p-\pi$  orbital on the central oxygen and two singly-occupied, singlet-coupled  $p\pi$  orbitals on the terminal atoms. The calculated geometry is found to be very close to that predicted earlier.<sup>1, 22</sup>

The lowest vertical excited state of peroxymethylene,  $^3A'(4\pi)$ , arises from triplet coupling of the terminal  $p-\pi$  orbitals and is calculated to lie 1.20 eV above the ground state (see Table I). This is slightly lower than the corresponding state of ozone, 1.59 eV,<sup>11, 23</sup> indicating a smaller degree of  $\pi$  delocalization (smaller overlap between the terminal  $p-\pi$  orbitals). By analogy to ozone we expect the triplet state to lead to longer bond lengths, a smaller angle, and an adiabatic excitation energy considerably below the vertical value (for ozone the adiabatic excitation energy is  $\sim 0.9$  eV; thus, the value for peroxymethylene may be as low as 0.5 eV).

The remaining two low-lying biradical states,  $^3A''(5\pi)$  and  $^1A''(5\pi)$ , are calculated to be 1.63 and 1.71 eV, respectively, above the ground state. These also are slightly lower than the corresponding states of ozone.

Of particular interest is the energy of the zwitterionic state, (14), commonly assumed to be the ground state.



The GVB-CI calculations lead to a vertical excitation energy of 3.99 eV for this state,  $2^1A'(4\pi)$  considerably below that of the analogous state of ozone, 5.81 eV.<sup>23, 24</sup> Apparently the lower electronegativity of carbon stabilizes the

zwitterionic structure (14b) relative to the corresponding state of ozone.  
[See Section IV.D for further discussion of the zwitterion-biradical character.]

In the case of substituted peroxyethylene, the planar ground state can exist as either of two isomers, syn or anti, depending on which side the substituent is placed. In order to determine the stereochemical consequences of this, it is necessary to know the barrier to interconversion of these two isomers, i.e., the barrier to rotation about the C-O bond.<sup>6</sup> The GVB-CI calculations lead to a barrier for this process of 29.1 kcal, indicating that in solution phase reactions, at least, the isomers will not interconvert. However, this will not necessarily be true in gas phase reactions where the Criegee intermediate may be formed with sufficient vibrational energy to surmount this barrier (we estimate that the reaction leading to the Criegee intermediate is exothermic by >40 kcal/mol).

The calculated energies of the other states of perpendicular peroxyethylene are summarized in Table I.

B. Dioxymethylene. The calculated GVB-CI energies of the eight biradical states of dioxymethylene (open geometry) are shown in Table I. Averaging over spin states, the relative energies are

$2\pi$ (13)	0.0 kcal
$3\pi$ (12)	8.9 kcal
$4\pi$ (11)	11.8 kcal.

There are two surprising aspects of these results. First, we would normally expect the singlet  $4\pi$  state to be lowest since in this state the  $p_\sigma$  orbitals can overlap, leading to increased bonding (decreasing the OCO angle of the singlet  $4\pi$  state leads directly to the ground state of dioxirane). Second, the total separation, 12 kcal, between the  $2\pi$  and  $4\pi$  states is much too large for normal 1,3-biradical couplings.

The explanation for these effects lies in the interaction of a doubly-occupied oxygen sigma lone-pair with an adjacent C-O bond, see (11)-(13). The C-O bond, being highly polarized toward the oxygen, effectively stabilizes adjacent lone pairs lying in the same plane as the C-O bond. Thus the  $2\pi$  states, having two stabilized lone pairs, are lowest in energy and the  $4\pi$  states, having no stabilized lone pairs, are highest.

From the magnitude of the  $2\pi$ - $3\pi$ - $4\pi$  splittings, we conclude that this lone-pair stabilization effect is worth  $\sim 6$  kcal per lone pair. An experimental estimate of the energy involved in lone-pair stabilization can be obtained by comparing the C-O bond energy of methanediol with that of ethanol. First though, consider the effect of an adjacent oxygen on typical C-H bond energies,<sup>25, 26</sup>

$$D_0(\text{CH}_3\text{CH}_2\text{CH}_2\text{-H}) = 97.9 \text{ kcal}$$

$$D_0(\text{CH}_3\text{OCH}_2\text{-H}) = 94.1 \text{ kcal.}$$

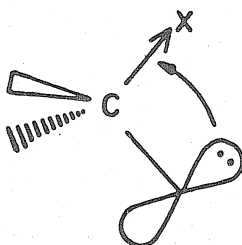
We conclude that an oxygen lone pair adjacent to a carbon radical center stabilizes the radical by 3.8 kcal. Now, consider the analogous C-O bond energies,<sup>25</sup>

$$D_0(\text{CH}_3\text{CH}_2\text{-OH}) = 92.1 \text{ kcal}$$

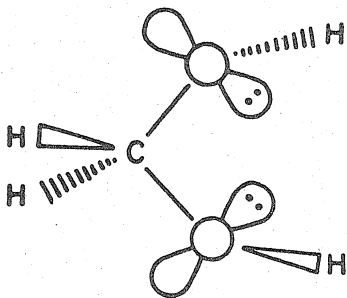
$$D_0(\text{HOCH}_2\text{-OH}) = 96.9 \text{ kcal.}$$

Thus replacement of  $\text{CH}_3$  by OH strengthens the adjacent C-O bond by 4.8 kcal. Since the OH stabilizes the radical center by 3.8 kcal, the lone-pair stabilization of the diol must be 8.6 kcal, in reasonable agreement with that estimated for dioxymethylene (12 kcal). Because of the large magnitude of the lone-pair stabilization effect, it plays an important role in the mechanisms of many reactions, including the ozonolysis of olefins (e.g., see Section IV.B), the ozonolysis of acetals<sup>27</sup> and the  $^1\text{O}_2$ -olefin ene reaction.<sup>28</sup>

This lone pair stabilization is a very general phenomenon, often referred to in the literature as the anomeric effect.<sup>29-31</sup> As noted here and elsewhere<sup>28, 29, 31, 32</sup> the effect results from a delocalization of a heteroatom lone pair into the region of an adjacent polar bond as shown below,



The result is an increased stability ( $\sim 5$  kcal each) of configurations in which a lone pair is in the same plane as an adjacent heteroatom. As an example, consider methanediol. The O-H bonds are roughly perpendicular to the oxygen lone pairs and thus orienting the lone pairs in the OCO plane (to maximize lone pair stabilization) forces the O-H bonds to be perpendicular to this plane. In fact, it is found<sup>32</sup> that the most stable configuration of methanediol is one in which both O-H bonds are perpendicular to the OCO plane as shown,



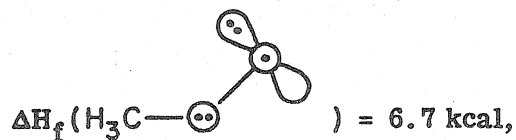


C. Thermochemistry. The C-O and O-O bond energies of the ring state from GVB(7/17)-CI calculations are shown in Table II. These results together with the GVB(3)-CI energies, Table I, accurately determine ( $\pm 4$  kcal) the relative heats of formation of all of the states corresponding to configurations (5)-(13). In order to obtain absolute heats of formation it is necessary to estimate independently the heat of formation of one of these states. As a starting point, consider methanediol,  $\Delta H_f = -93.5$  kcal (all  $\Delta H_f$  will be for 298°K).<sup>26</sup> The O-H bond energies of methanediol are expected to be nearly independent of each other and approximately equal to the O-H bond energy of methanol, 103.6 kcal.<sup>26</sup> Therefore we estimate as follows,

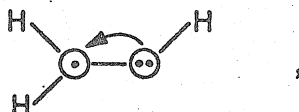
$$\Delta H_f(\text{H}_2\text{C} \begin{array}{c} \diagup \text{O}^\bullet \\ \diagdown \text{O}^\bullet \end{array}) = -93.5 + 2(103.6) - 2(52.1) \\ = 9.5 \text{ kcal.}$$

Now, methanediol is stabilized by the lone pair-C-O bond interaction discussed in Section III.B. Therefore the estimated  $\Delta H_f$  corresponds to an average over those biradical states with similar stabilizing interactions, i.e., an average of the  $^1(2\pi)$  and  $^3(2\pi)$  states. Using this estimate and the results of the GVB-CI leads to the heats of formation shown in Table III.

As a check on the consistency of the calculations, we can independently estimate the heat of formation of one of the COO biradical states. For example, starting with the peroxy methane radical,<sup>26</sup>



we first estimate the C-H bond energy. In order to minimize any 1,3-diradical interaction we break a C-H bond in the COO plane, forming the ( $3\pi$ ) biradical states of perpendicular peroxyethylene. The C-H bond strength of methanol is 94 kcal, 4 kcal less than that of ethane. The decrease is due to a three-electron bonding interaction in the biradical,



an effect that is not present in the perpendicular geometry of peroxyethylene biradical. Therefore we use a C-H bond energy of 98 kcal leading to the following expression for the biradical heat of formation,

$$\begin{aligned}\Delta H_f(\text{H}_2\text{COO}) &= 6.7 + 98 - 52.1 \\ &= 52.6.\end{aligned}$$

This represents the average of the singlet and triplet ( $3\pi$ ) biradical states of perpendicular peroxyethylene. Excitation energies from GVB-CI calculations lead to  $\Delta H_f[^1A''(3\pi) \text{ perpendicular peroxyethylene}] = 54.7$  kcal, in good agreement with the previous estimate of 58.2 kcal (Table III).

Using the group additivity method of Benson<sup>26</sup> together with the GVB-CI heat of formation for the ring state (-5.7 kcal) leads to a predicted ring strain, for (9), of 21 kcal/mol. This is slightly less than the strain energy for other three-membered rings (27.6 kcal for cyclopropane and 26.9 kcal for ethylene oxide).

Using a combination of experimental, group additivity, and GVB-CI heats of formation leads to the ozonolysis thermochemistry shown in Figure 2. The heats of formation of the four  $\text{C}_2\text{H}_4\text{O}_3$  biradicals were calculated using the following radical group functions;  $\cdot\text{C}(\text{C})(\text{H})_2 = 36.1$ ,  $\cdot\text{C}(\text{O})(\text{H})_2 = 31.9$ ,  $\cdot\text{O}(\text{C}) = 13.6$ ,  $\cdot\text{O}_2(\text{C}) = 16.7$ , and  $\cdot\text{O}_2(\text{O}) = 35.2$ . The ring strain of the 1,2,3-trioxalane

structure was assumed to be 6 kcal (based on cyclopentane), while that of the 1,2,4-trioxalane was assumed to be  $\sim 16$  kcal due to the loss of lone-pair stabilizations upon ring formation. Finally, the group function for  $\text{O}(\text{O})_2$  was taken to be 14 kcal, from an extrapolation of the heats of formation of  $\text{CH}_3\text{OCH}_3$  and  $\text{CH}_3\text{OOCH}_3$  rather than the value suggested by Benson (19 kcal), which is an average of the  $\text{CH}_3\text{O}_n\text{CH}_3$  and  $\text{HO}_n\text{H}$  extrapolations.

#### IV. Discussion

A. Gas Phase Mechanism. From Figure 2 we see that the steps in the Criegee mechanism are energetically plausible. Note, however, that the step leading to epoxide and  $O_2$  ( $^1\Delta$ ) is also energetically acceptable as are the steps leading to dioxymethane in the open or closed forms. Epoxide is a well-known product; however, there is apparently no strong evidence in favor of intermediacy of dioxymethane.

In gas phase ozonolysis the slower quenching of vibrationally excited intermediates allows several additional reaction pathways and a number of additional products have been observed experimentally.<sup>33, 34</sup> For example, Pitts has reported the formaldehyde  $^1A''(n\pi^*) \rightarrow ^1A_1$  and  $OH\ ^2\Sigma^+ \rightarrow ^2\Pi$  chemiluminescence from ozonolysis of ethylene. Emission from  $^3A_u$  glyoxal has been observed from the ozonolysis of cis and trans 2-butene. O'Neal and Blumstein<sup>35</sup> have proposed a competing pathway for the gas phase ozonolysis of ethylene involving H abstraction by the primary ozonide biradical (Path D of Figure 3) leading directly to an  $\alpha$ -hydroperoxy aldehyde intermediate. The Pitts' experiments have been interpreted to support this mechanism.

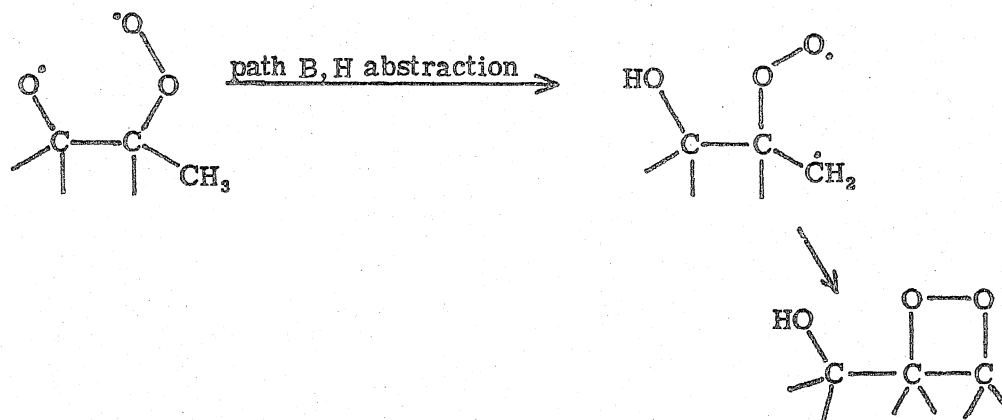
In Figure 3 we show four possible pathways for decomposition of the primary ozonide biradical. Path B involves a splitting of the form proposed by Criegee, while Path D is the H-abstraction of O'Neal and Blumstein. We suggest a third possibility, Path A, consisting of a 1,2-hydrogen shift leading to a biradical which can then undergo ring closure, forming a dioxetane. The dioxetane intermediate would then be expected to cleave, forming an electronically excited formaldehyde ( $^1A''$ ) and a ground state formic acid. The key step in Pathway A is the initial 1,2 H-migration. The activation energy for this process is expected to be only slightly less than the C-H bond strength

(~16 kcal), unless the H-migration and ring closure are concerted. While significantly larger than previous estimates for the H-abstraction pathway (~9 kcal),<sup>35</sup> this is still well below the available vibrational energy of the biradical (~33 kcal).

The activation energy for the Criegee splitting process, B, is in considerably greater doubt. O'Neal and Blumstein<sup>35</sup> have suggested an activation energy of 16.5 kcal based on the experimental activation energy for decomposition of t-BuO radical. They note, however, that this does not include any "polarization" stabilization of peroxyethylene. The GVB-CI calculations indicate this stabilization to be > 20 kcal (comparing with the perpendicular biradical states). Assuming then that the transition state is stabilized by one-half this amount leads to a predicted activation energy of < 6.5 kcal, well below that estimated for any of the competing mechanisms.

We also note in Figure 3 a pathway, C, leading to the formation of  $O_2(^1\Delta_g)$ . It has been shown<sup>36</sup> that  $O_2(^1\Delta_g)$  reacts with ethylene in the gas phase leading to  $^1A''$  formaldehyde chemiluminescence. Thus Pathway C provides an alternative explanation for the observed excited state formaldehyde.

A number of additional products can be formed from bimolecular reactions involving some of the proposed intermediates; however, in Figure 3 we have restricted ourselves to unimolecular processes. In addition, excitation energy transfer may lead to some of the observed chemiluminescence. O'Neal and Blumstein have suggested that the observed  $^1A''$  formaldehyde chemiluminescence may result from a dioxetane intermediate formed as follows:



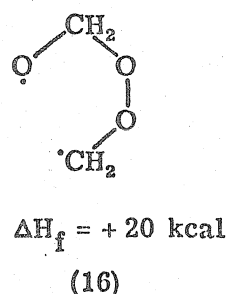
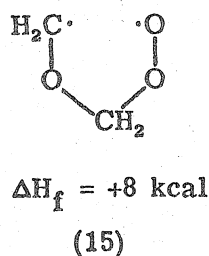
This mechanism requires a substituted ethylene and hence does not explain the observed chemiluminescence of  $^1A''$   $\text{CH}_2\text{O}$  in the ozonolysis of ethylene.<sup>34</sup> However, this chemiluminescence can be understood on the basis of the 1,2 H-migration mechanism as shown in Figure 3 (Path A).

Thus far we have considered primarily the mechanism of ethylene ozonolysis. The effect of alkyl substituents on the C-C double bond will be threefold; (i) additional pathways for decomposition of the primary ozonide biradical will become available ( $\beta$  and  $\gamma$  H-abstraction),<sup>33</sup> (ii) excess vibrational energy will be dissipated to some extent, leading to an increased importance of processes with smaller activation energies (regardless of the A-factors involved), and (iii) the C-C bond strength will be decreased, leading to a decrease in the activation energy for Criegee splitting.

B. Solution Phase Mechanism. In solution the ozonolysis intermediates, although formed vibrationally "hot", will be rapidly quenched, leading to a decrease in the number of competing pathways and to an increase in stereospecificity. Indeed, solution phase ozonolysis of olefins is known to proceed to high yields of secondary ozonide, in some cases stereospecifically.<sup>5,37</sup>

Conformational analysis of the primary ozonide<sup>5</sup> (see Figure 4) indicates that axial substituents should exhibit a preference for forming the *syn* peroxymethylene conformation, while equatorial substituents should be preferentially incorporated into the *anti* position. Furthermore, the *anti* peroxymethylene conformation is the more stable one (by 1-2 kcal) and hence should be formed with some preference, other factors being equal. For sizeable substituents, the *trans* di-substituted primary ozonide will prefer a diaxial conformation, while the *cis* ozonide will prefer an axial-equatorial conformation.<sup>5</sup> Thus we expect *trans*-disubstituted olefins to preferentially form *syn*-peroxymethylene, while *cis* olefins should form *anti*.

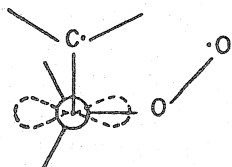
The final step in the ozonolysis reaction involves the addition of peroxymethylene to an aldehyde. The estimated thermochemistry of this addition is shown in Figure 2. Assuming the addition to involve a biradical intermediate, there are two possible biradicals to consider, (15) and (16).



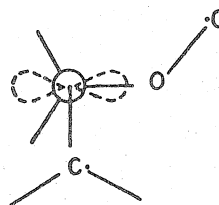
However, since the  $\cdot\text{COCOO}\cdot$  form (15) is expected to be 9 kcal more stable than the alternative  $\cdot\text{OCOOC}\cdot$  form, and since the addition of aldehyde to peroxymethylene forming the  $\cdot\text{COCOO}\cdot$  biradical (15) is only 4 kcal endothermic, we expect that the addition will proceed through the  $\cdot\text{COCOO}\cdot$  biradical intermediate.

Considering in more detail the 1,5- $\cdot\text{COCOO}\cdot$  biradical (15), the lone-pair stabilization (anomeric) effect (Section III.B) implies that this biradical will exist

in either of two preferred conformations, (17) and (18), with a  $\sim 5$  kcal barrier to interconversion. Furthermore, rotation about the  $\text{—C—OO}^\bullet$  bond will be hindered



(17)



(18)

due to the lone-pair stabilization. Thus conformation (18) will have an additional 5 kcal barrier to ring closure and should either dissociate or generate free radical products. We predict therefore that the secondary ozonides are formed via the  $\cdot\text{COCOO}\cdot$  biradical with the conformation shown in (17) and that the stereochemistry of this reaction can be understood on the basis of this intermediate.

Considering now the specific case of a symmetrical, disubstituted olefin, the predicted reaction pathways are shown in Figure 5. We have assumed here that the dominant factor in determining the course of the reaction for bulky substituents will be nonbonded, steric repulsions. Thus, for large substituents, biradicals A-D will ring-close in such a way that the bulky carbonyl substituent is rotated away from all neighboring group interactions. The result is that these steric interactions cause the syn peroxymethylene to favor production of trans product, while the anti form should lead to cis product. Hence, for bulky substituents, cis and trans olefins are expected to lead stereospecifically to cis and trans secondary ozonides, respectively.

An additional effect on the biradical closure should be considered. Since the peroxymethylene biradical is isoelectronic to ozone, orbital phase arguments<sup>38</sup> indicate that it will exhibit a preference for suprafacial  $4\pi_s + 2\pi_s$



addition. For biradicals B and D (Figure 5) the steric and orbital phase considerations lead to the same prediction. However, for biradicals A and C, opposite results are predicted (steric considerations imply antarafacial addition). Of these two biradicals the steric repulsions will be much larger for A ( $R \cdots R$  interaction) than for C ( $R \cdots H$  interaction). Thus, orbital phase considerations are expected to be most important (relative to the steric effects) for the ring closure of C, and hence for small substituents (e.g.,  $R = CH_3$ ) orbital phase effects could dominate this ring closure. In fact, ozonolysis of both cis and trans 2-butenes is observed to produce primarily trans secondary ozonide,<sup>5</sup> as expected on the basis of orbital phase considerations.

Several additional features of solution phase ozonolysis reactions can be understood on the basis of this mechanism. For example, steric considerations predict that addition of a carbonyl to a peroxyethylene having a bulky group in the syn position will lead preferentially to biradical (18). This biradical will have large rotational barriers preventing ring closure, and thus formation of (18) is expected to lead to an increase in radical reactions (polymeric products) and a decrease in ozonide yield. In fact, ozonolysis of trans olefins (via syn peroxyethylene) is observed to proceed with much lower yields of secondary ozonide than the corresponding cis olefins.<sup>5,37</sup>

A second conclusion from the biradical mechanism is that the cis-secondary ozonides result from the thermodynamically more stable peroxyethylene intermediate (anti). Thus syn-anti equilibration of the peroxyethylene species will lead to an increase of cis product. Recently, Bailey *et al.*<sup>39</sup> reported the results of experiments on the effect of complexing agents on the stereospecificity of ozonolysis reactions. They found that complexing agents lead to an increase in the relative yield of cis-secondary ozonide from

both cis and trans olefins. Furthermore, at increased temperatures (or increased solvent polarities), in the absence of a complexing agent, they found a decrease in the stereospecificity of the reaction. On the basis of the proposed biradical mechanism, we interpret these results as follows:

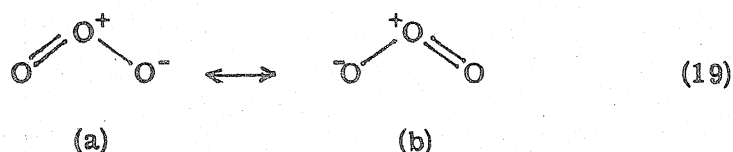
1. In the absence of complexing agent, little or no syn-anti equilibration occurs (the calculated barrier to interconversion is 29 kcal).
2. The complexing agent greatly increases the rate of syn-anti equilibration (probably by reversibly binding to one end of the peroxyethylene), leading to an increased concentration of the more stable (anti) peroxyethylene and thus to an increase in cis ozonide product.<sup>40</sup>
3. At higher temperatures the final ring-closure step is less stereospecific (due to increased rates of bond rotation relative to the rate of ring closure). It is expected that this would favor the more stable product (trans) as observed.
4. An increase in the solvent polarity may increase the lifetime of the 1,5-biradical, again leading to a loss of stereospecificity.

In conclusion, the biradical mechanism proposed here explains a large body of experimental results on solution phase ozonolysis.

C. Comparison with Previous Calculations. Recently, Hiberty<sup>41</sup> has reported the results of calculations on the mechanism of ozonolysis. These calculations employed a double zeta basis set and Hartree-Fock wavefunctions, augmented in some cases with limited CI calculations. The present calculations involve a much more flexible basis set (double zeta plus d-polarization functions) and extensive CI calculations. Comparison of the present DZd-GVB results with earlier DZ-GVB calculations<sup>1</sup> indicates that d functions have large effects (10-20 kcal) on the relative energies of various intermediates. For example, without d functions the barrier to syn-anti interconversion is pre-

dicted to be 19 kcal, while comparable DZd calculations predict a barrier of 29 kcal (Hiberty predicts a barrier of 12 kcal). In addition, the DZ calculations predict some states of the open  $\cdot\text{OCO}\cdot$  biradical to be below the ring state, while the DZd calculations predict the ring state to be at least 10 kcal below all of the biradical states. In light of these differences, we conclude that calculations employing DZ basis sets, while adequate for predicting the qualitative nature of the intermediates, are not sufficiently accurate to predict relative energies of key intermediates.

D. Singlet Biradicals vs Zwitterions. Calculations reported here and elsewhere<sup>1, 14</sup> indicate that peroxymethylene and ozone are most accurately described as 1, 3 singlet biradicals. In the past, the observed reactivity of these species has been interpreted to indicate a zwitterionic mode of bonding. For example, ozone has most often been described as a resonance of structures 19a and 19b.



The zwitterion model of ozone has received indirect support from experiments implying an electrophilic nature for ozone. For example, the relative reactivities of substituted aromatic compounds with ozone fit the trends expected of an electrophilic agent.<sup>42</sup> Similar studies on the ozonolysis of chlorinated olefins have also been interpreted to support the electrophilic character of ozone and the zwitterionic model of bonding in ozone.<sup>43</sup> Similarly, it has been shown that addition of peroxymethylene to carbonyls occurs in a manner consistent with the zwitterion model.

A key misconception in the interpretation of these experiments is in the assumed behavior of 1, 3-biradicals. The electrophilic nature of oxygen-centered radical species is well-established and is consistent with the large electron affinities observed for oxygen-centered radicals [ $\text{EA}(\text{C}_2\text{H}_5\text{O}\cdot) = 1.68 \text{ eV}$ ,  $\text{EA}(\text{O}_3) = 1.92 \text{ eV}$ ].<sup>44</sup> For example, the electronic structure of  $\text{O}_2$  ( $^1\Delta$ ) involves two perpendicular, singly-occupied, "radical" orbitals and yet  $^1\text{O}_2$  exhibits electrophilic character in reactions with olefins.<sup>45</sup> Thus the chemistry of ozone and of peroxymethylene is quite consistent with the 1, 3-biradical character derived from the ab initio wavefunctions, and there is no need to postulate zwitterionic structures.

There are two important qualifications to the preceding discussion. The calculations reported here describe an unsubstituted, gas phase (i.e., not solvated) peroxyethylene molecule. Both solvation and substitution should alter the relative energies of the biradical and zwitterionic states and may alter the character of the ground state.

In Section III.A it was noted that the present ab initio calculations place the zwitterionic state of peroxyethylene 3.99 eV above the biradical ground state. However, in these calculations the excited zwitterionic state is forced to be orthogonal to the lower biradical state. In order to discuss the effects of solvation and substitution, it is more relevant to consider the energy of a zwitterionic state that is not constrained to be orthogonal to the biradical state. The actual optimum wavefunction will, of course, be a combination of both states, emphasizing whichever state is of lower energy.

To estimate the energy of a nonorthogonalized zwitterion state, we will start with the 1,3-biradical and construct the 1,3-zwitterion by ionizing the electron of the carbon radical center and attaching this electron to the oxygen radical center. The energy change for this process is given approximately by the relationship,

$$\Delta E(\text{eV}) = \text{IP}(\text{C}\cdot) - \text{EA}(\text{O}\cdot) - 14.40/R_{\text{CO}}, \quad (20)$$

where

$\text{IP}(\text{C}\cdot)$  = ionization potential (eV) of the carbon radical center

$\text{EA}(\text{O}\cdot)$  = electron affinity (eV) of the oxygen radical center

$R_{\text{CO}}$  = distance (Å) between the carbon and oxygen radical centers  
= 2.23 Å.

In order to account accurately for the effect of coupling between the radical centers, the energy of the zwitterionic state is calculated relative to that of the  $^1(5\pi)$  biradical state in which the radical orbitals are rigorously orthogonal.

The energy of the zwitterionic state relative to the  $^1(4\pi)$  biradical state can then be obtained using the GVB-CI  $^1(4\pi) \rightarrow ^1(5\pi)$  excitation energy.

In order to evaluate the zwitterionic energy from (20), we must estimate appropriate "local" radical center ionization potentials and electron affinities. In the calculations reported here, the following values are assumed,<sup>44, 46</sup>

$$EA(O\cdot) = 1.68 \text{ eV} = EA(\text{CH}_3\text{CH}_2\text{O}\cdot)$$

$$IP(C\cdot) = IP(R_1R_2\dot{C}OH) ,$$

and the results are given in Table IV.<sup>47</sup> These calculations indicate, as expected, that alkyl substituents significantly stabilize the zwitterionic state relative to the biradical state. In fact, the calculations predict that the biradical and zwitterionic states of gas phase dimethyl substituted peroxymethylene are approximately degenerate. Thus the ground state of this species will have a large degree of both biradical and zwitterionic character. Stronger  $\pi$ -donating substituents (amino, alkoxy, etc.) are expected to swing this balance even further toward the zwitterionic state.

Consider now the effect of solvation on the electronic structure of peroxymethylene. As a model, assume the molecule to be in a spherical cavity of radius  $R(\text{\AA})$  surrounded by a dielectric medium with dielectric constant  $\epsilon$ . The stabilization of the zwitterion relative to the biradical can then be estimated using the formula,<sup>48, 49</sup>

$$\Delta E(\text{kcal}) = \left( \frac{\epsilon - 1}{2\epsilon + 1} \right) \frac{\mu_Z^2 - \mu_B^2}{R^3} \times 14.4 ,$$

where  $\mu_Z$  is the dipole moment (debye) of the zwitterionic state and  $\mu_B$  is the dipole moment of the biradical state. Taking  $\mu_B = 3.50 \text{ D}$  (from the GVB-CI wavefunction),  $\mu_Z = 10.7 \text{ D}$  (unit charges separated by a distance of  $2.23 \text{ \AA}$ ) and  $R = 2.5 \text{ \AA}$ , we obtain the following expression,

$$\Delta E = \frac{\epsilon - 1}{2\epsilon + 1} \times 94.2 \text{ kcal/mol.}$$

Therefore, for unsubstituted peroxymethylene, a solvent dielectric constant of  $\geq 2.5$  will bring the zwitterionic state below the biradical.

We conclude then that the ground state of gas phase peroxymethylene is most accurately described as a 1,3-singlet biradical. However, the energy separation between the nonorthogonalized biradical and zwitterionic states is small and can be significantly affected by substituents or solvation. Thus the electronic structure of Criegee intermediates will depend critically on the nature of their environment. However, since the chemistry of the two species [singlet-biradical and zwitterion] is expected to be very similar (*vide supra*), the distinction may well be unimportant for mechanistic considerations.

## V. Conclusion

The qualitative model of ozonolysis previously suggested<sup>1</sup> involving a singlet peroxymethylene biradical intermediate has been confirmed with more accurate calculations (larger basis set, more extensively correlated wavefunctions). In addition, the calculations reported here are of sufficient quality to determine accurately the relative heats of formation of the various proposed intermediates in ozonolysis. It was found that formation of the Criegee intermediate (peroxymethylene) is 10 kcal endothermic from the primary ozonide (1, 2, 3-trioxolane) or ~10 kcal exothermic from a postulated 1,5-biradical intermediate. Peroxymethylene was calculated to have a 29 kcal barrier to rotation about the C-O bond, indicating that syn and anti isomers will be configurationally stable in solution. In addition, it was found that the ring state of methylene peroxide (dioxirane) is 36 kcal below the open peroxy-methylene form.

These results are used to propose a mechanism for the gas phase ozonolysis of ethylene involving four pathways to decomposition of the postulated 1,5-OCCOO biradical intermediate. One pathway, 1,2 H-migration, is found to lead to a dioxetane intermediate, the cleavage of which would lead to chemiluminescence from <sup>1</sup>A" CH<sub>2</sub>O (as recently observed).

In addition, it is shown that many facets of solution phase ozonolysis (including stereospecificity, relative yields, and effects of complexing agents) can be understood on the basis of the biradical mechanism.

## Acknowledgment


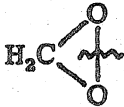
This work was supported in part by a grant (CHE73-05132) from the National Science Foundation. Acknowledgment is made to the Donors of The Petroleum Research Fund, administered by the American Chemical Society, for partial support of this research.



Table I. Calculated Excitation Energies for Peroxymethylene Biradical and Dioxymethane (eV)

State		GVB(3/PP)	GVB(3)-CI	GVB(7/17)-CI
(A) Open Planar COO; see (5) and (6)				
4 $\pi$	1 $^1A'$	1.86	1.29	
	1 $^3A'$	2.45	2.49	
	2 $^1A'$		5.28	
	2 $^3A'$		9.58	
5 $\pi$	1 $^3A''$	2.86	2.92	
	1 $^1A''$	2.92	3.00	
	2 $^3A''$		9.27	
	2 $^1A''$		9.51	
(B) Open Perpendicular COO; see (7) and (8)				
3 $\pi$	1 $^3A''$	2.40	2.37	
	1 $^1A''$	2.50	2.55	
4 $\pi$	1 $^1A'$	2.50	2.70	3.13
	1 $^3A'$	2.81	2.95	
(C) Open Perpendicular OCO; see (11), (12), and (13)				
2 $\pi$	1 $^1A_1$	0.05	0.48	
	1 $^3B_2$	0.05	0.52	
3 $\pi$	1 $^3A_2$		0.60	
	1 $^1A_2$		0.78	
	1 $^3B_1$		0.94	
	1 $^1B_1$		1.14	
4 $\pi$	2 $^1A_1$	0.45	0.97	1.33
	2 $^3B_2$	0.55	1.04	
(D) Ring; see (9)				
4 $\pi$	$^1A_1$	0.00	0.00	0.00
Total Energy (h)		-188.74026	-188.80355	

Table II. Calculated Bond Dissociation Energies (kcal/mol) of Dioxirane.<sup>a</sup>  
 These calculated energies assume  $4\pi$  states for the dissociation species; since this is not the lowest state, the adiabatic bond energies are smaller (see Table III).

Bond	Calculated $D_e$	Estimated Zero-Point Correction	Estimated <sup>b</sup> Error in Theoretical $D_e$	Estimated $D_0$
	72.1 <sup>c</sup>	-5.6	+0.8	67.3
	30.7 <sup>d</sup>	-0.5	-4.2	26.0

<sup>a</sup> Based on GVB(7/17)-CI wavefunctions for dioxirane and for the  $^1(4\pi)$  state of the biradicals.

<sup>b</sup> Taken from equivalent calculations on the bond energies of  $\text{CH}_3\text{-OH}$  and  $\text{HO-OH}$ .

<sup>c</sup> Total energy of ring state, -188.8437.

<sup>d</sup> Total energy of ring state, -188.8515.

Table III. Calculated Heats of Formation ( $T = 298^\circ$ ) of Peroxymethylene Biradical, Dioxirane, and Dioxymethylene (kcal)

Geometry	State	$\Delta H_f^0_{298^\circ}$
Planar COO (Figure 1A)	$^1A' (4\pi)$	29.1
	$^3A' (4\pi)$	56.8
	$^1A'' (5\pi)$	68.5
	$^3A'' (5\pi)$	66.7
Perpendicular COO (Figure 1B)	$^1A' (3\pi)$	58.2
	$^3A' (3\pi)$	54.0
	$^1A'' (4\pi)$	61.6
	$^3A'' (4\pi)$	67.4
Ring (Figure 1C)	$^1A' (4\pi)$	-5.7
Perpendicular OCO (Figure 1D)	$1^1A_1 (2\pi)$	9.0
	$1^3B_2 (2\pi)$	10.0
	$^1A_2 (3\pi)$	16.0
	$^3A_2 (3\pi)$	11.8
	$^1B_1 (3\pi)$	24.3
	$^3B_1 (3\pi)$	19.6
	$2^1A_1 (4\pi)$	20.3
	$2^3B_2 (4\pi)$	21.9

Table IV. Substituent effects on the energy,  $\Delta E$ , of the zwitterionic state of peroxymethylene ( $R_1R_2\text{COO}$ ) relative to the biradical state.<sup>a</sup>

$R_1$	$R_2$	$\Delta H_f(R_1R_2\text{COH}^+)$ kcal	$\Delta H_f(R_1R_2\dot{\text{C}}\text{OH})$ kcal	IP(C•) eV	$\Delta E$ kcal
H	H	160 <sup>b</sup> , 172 <sup>c</sup>	-6.0	7.5	23
CH <sub>3</sub>	H	136 <sup>b</sup> , 145 <sup>c</sup>	-18.5	7.0	12
CH <sub>3</sub>	CH <sub>3</sub>	115 <sup>b</sup> , 125 <sup>c</sup>	-29.3	6.5	0

<sup>a</sup> See Section IV.D for explanation of parameters.

<sup>b</sup> From ref 44b, assuming the proton affinity of NH<sub>3</sub> is 205 kcal.

<sup>c</sup> From ref 44a.

### References and Notes

- (1) (Paper I) W. R. Wadt and W. A. Goddard III, J. Am. Chem. Soc., 97, 3004 (1975). Peroxymethylene was referred to as methylene peroxide in this paper.
- (2) K. L. Demerjian, J. A. Kerr, and J. G. Calvert, Advan. Environ. Sci. Tech., 4, 1 (1974).
- (3) (a) R. Criegee and G. Wenner, Justus Liebigs Ann. Chem., 546, 9 (1949); (b) R. Criegee, Rec. Chem. Progr., 18, 111 (1957).
- (4) R. Criegee, Angew. Chem. Int. Ed., 14, 745 (1975), and references cited therein.
- (5) (a) N. L. Bauld, J. A. Thompson, C. E. Hudson, and P. S. Bailey, J. Am. Chem. Soc., 90, 1822 (1968); (b) P. S. Bailey and T. M. Ferrel, ibid., 100, 899 (1978).
- (6) Another possibility for this transition state is a linear C-O-O geometry. By analogy to ozone, we estimate this transition state to be 50 to 90 kcal above the planar ground state.
- (7) (a) S. Huzinaga, J. Chem. Phys., 42, 1293 (1965); (b) T. H. Dunning, Jr., and P. J. Hay in "Modern Theoretical Chemistry: Methods of Electronic Structure Theory," H. F. Schaefer, Ed., Vol. 3, Plenum Press, New York, N.Y., 1977, pp. 1-27.
- (8) G. Herzberg, "Molecular Spectra and Molecular Structure," Vol. 3, Van-Nostrand, Princeton, N.J., 1967.
- (9) L. E. Sutton, "Tables of Interatomic Distances," The Chemical Society, London, 1958.
- (10) G. L. Cunningham, Jr., A. W. Boyd, R. J. Meyers, W. D. Gwinn, and W. I. LeVan, J. Chem. Phys., 19, 676 (1951).

- (11) P. J. Hay, T. H. Dunning, Jr., and W. A. Goddard III, Chem. Phys. Lett., 23, 457 (1973).
- (12) C. W. Gilles and R. L. Kuczkowski, J. Am. Chem. Soc., 94, 6337 (1972).
- (13) W. J. Hunt, P. J. Hay, and W. A. Goddard III, J. Chem. Phys., 57, 738 (1972).
- (14) W. A. Goddard III, T. H. Dunning, Jr., W. J. Hunt, and P. J. Hay, Acc. Chem. Res., 6, 368 (1973).
- (15) (a) L. B. Harding and W. A. Goddard III, J. Am. Chem. Soc., 97, 6293 (1975); (b) ibid., 97, 6300 (1975).
- (16) L. B. Harding and W. A. Goddard III, J. Am. Chem. Soc., 98, 6093 (1976).
- (17) F. W. Bobrowicz and W. A. Goddard III in "Modern Theoretical Chemistry: Methods of Electronic Structure Theory," H. F. Schaefer, Ed., Vol. 3, Plenum Press, New York, 1977, pp. 79-127.
- (18) The GVB calculations were carried out with the Bobrowicz-Wadt-Goddard-Yaffe program (GVB TWO) using the basic methods of ref 12.
- (19) The CI calculations were carried out with the Bobrowicz-Walch program (CITWO).
- (20) L. B. Harding and W. A. Goddard III, to be published.
- (21) The CI calculations include up to quadrupole excitations consisting of products of single excitations within all GVB pairs with double excitations within the bond pair being broken.
- (22) In ref 1 the predicted geometry was  $r(\text{C-O}) = 1.35 \text{ \AA}$ ,  $r(\text{O-O}) = 1.37$ , and  $\text{OOC angle} = 103^\circ$ . The calculated results are 1.343, 1.362, and  $116.6^\circ$ , respectively.

- (23) (a) P. J. Hay, T. H. Dunning, Jr., and W. A. Goddard III, J. Chem. Phys., 62, 3912 (1975); (b) P. J. Hay and T. H. Dunning, Jr., ibid., 67, 2290 (1977).
- (24) The GVB-CI calculations on the excitation energy to the zwitterionic state of ozone are apparently high, possibly by as much as 1.3 eV. If a similar error exists in the peroxymethylene biradical calculations, the energy of the  $2^1A_1(4\pi)$  state could be as low as 2.7 eV.
- (25) In these calculations, heats of formation for the various species were obtained from ref 26, except for  $\Delta H_f(\cdot\text{CH}_2\text{OH})$ . The latter was obtained by assuming  $D_0(\text{HOCH}_2\text{-H}) = D_0(\text{CH}_3\text{OCH}_2\text{-H}) = 94.1$  kcal. This leads to  $\Delta H_f(\cdot\text{CH}_2\text{OH}) = -6.0$  kcal.
- (26) (a) S. W. Benson, "Thermochemical Kinetics," Wiley, New York, N. Y., 1976; (b) S. W. Benson, F. R. Cruickshank, D. M. Golden, G. R. Haugen, H. E. O'Neal, A. S. Rodgers, R. Shaw, and R. Walsh, Chem. Rev., 68, 279 (1968).
- (27) P. Deslongchamps, P. Atlani, D. Frehel, A. Malaval, and C. Moreau, Can. J. Chem., 52, 3651 (1974).
- (28) L. B. Harding and W. A. Goddard III, Tetrahedron Lett., 797 (1978).
- (29) C. Romers, C. Altona, H. R. Buys, and E. Havinga, Top. Stereochem., 4, 39 (1969).
- (30) N. S. Zefirov and N. M. Shekhtman, Russ. Chem. Rev., 40, 315 (1971).
- (31) S. David, O. Eisenstein, W. Hehre, L. Salem, and R. Hoffmann, J. Am. Chem. Soc., 95, 3806 (1973).
- (32) G. A. Jeffrey, J. A. Pople, and L. Radom, Carbohydr. Res., 25, 117 (1972).
- (33) R. Atkinson, B. J. Finlayson, and J. N. Pitts, Jr., J. Am. Chem. Soc., 95, 7592 (1973).

- (34) B. J. Finlayson, J. N. Pitts, Jr., and R. Atkinson, J. Am. Chem. Soc., 96, 5356 (1974).
- (35) H. E. O'Neal and C. Blumstein, Int. J. Chem. Kinetics, 5, 397 (1973).
- (36) D. L. Bogan, R. S. Sheinson, and F. W. Williams, J. Am. Chem. Soc., 98, 1034 (1976).
- (37) R. W. Murray, R. D. Youssefyeh, and P. R. Story, J. Am. Chem. Soc., 89, 2429 (1967).
- (38) W. A. Goddard III, J. Am. Chem. Soc., 92, 7520 (1970).
- (39) P. S. Bailey, A. Rustaiyan, and T. M. Ferrell, J. Am. Chem. Soc., 98, 638 (1976).
- (40) Bailey et al.<sup>39</sup> interpreted their results in exactly the opposite way. They concluded that in the absence of complexing agent a syn-anti equilibration occurs and that this equilibration is impeded by the presence of complexing agent.
- (41) P. C. Hiberty, J. Am. Chem. Soc., 98, 6088 (1976).
- (42) J. P. Wibaut, F. L. J. Sixma, L. W. F. Kampschmidt, and H. Boer, Rec. Trav. Chim. Pays-Bas, 69, 1355 (1950).
- (43) D. G. Williamson and R. J. Cvetanovic, J. Am. Chem. Soc., 90, 4248 (1968).
- (44) (a) H. M. Rosenstock, K. Draxl, B. W. Steiner, and J. T. Herron, J. Phys. Chem. Ref. Data, 6, 1-1 (1977); (b) J. F. Wolf, R. H. Staley, I. Koppel, M. Taagepera, R. T. McIver, Jr., J. L. Beauchamp, and R. W. Taft, J. Am. Chem. Soc., 99, 5417 (1977).
- (45) C. S. Foote and R. W. Denny, J. Am. Chem. Soc., 93, 5162 (1971).
- (46) The values for  $IP(R_1R_2COH)$  were obtained from reported heats of formation of the positive ions<sup>44</sup> and estimated heats of formation of the radical species.<sup>26</sup>



- (47) Note that the energy of the zwitterionic state of peroxymethylene from these calculations (23 kcal) is much lower than the GVB-CI energy (92 kcal). This difference is primarily due to the removal of orthogonality constraints and differences in geometries; however, the GVB-CI calculation was not designed to accurately describe the zwitterionic state, and up to 30 kcal of this difference may be due to inaccuracies in the calculations.<sup>24</sup>
- (48) R. Huisgen, Acc. Chem. Res., 10, 117 (1977).
- (49) K. J. Laidler and H. Eyring, Ann. N. Y. Acad. Sci., 39, 303 (1940).

### Figure Captions

Figure 1. Geometric parameters used in calculations. All bond lengths are in angstroms. All CH bond lengths were taken to be 1.08 Å. Underlined parameters are the optimum values from GVB-CI calculations.

Figure 2. The thermochemistry of ozonolysis. The calculated heats of formation (kcal/mol) are shown below each set of molecules. The dashed lines trace out the Criegee mechanism.

Figure 3. Possible mechanisms for gas phase ozonolysis of ethylene. Species formed with a large excess of vibrational energy are marked with ‡; those formed in excited electronic states are denoted by \*. Pathways A and C are new mechanisms, Pathway B involves an initial Criegee-like splitting, and Pathway D was proposed by O'Neal and Blumstein (ref 24).

Figure 4. Stereoselective decomposition of cis and trans disubstituted primary ozonides. This analysis is based on the C (O-O) envelope conformation, which is most appropriate for very large substituents (e.g., t-butyl). A similar analysis leads to the same result for all six envelope and half-chair conformations, with the exception of the trans O (C-C) envelope. This latter conformation is not expected to be low energy (Ref. 42).

Figure 5. Proposed biradical mechanism for the stereospecific ozonolysis of cis and trans disubstituted olefins. In the drawings A, B, C, and D, the carbonyl oxygen is directly above the peroxyethylene carbon and the conformations are such that the dotted p orbital has a lone-pair stabilization (anomeric interaction) with the peroxyethylene CO bond. Arrows around the biradical C-O bonds indicate the sterically preferred direction of rotation to closure (such that the bulky R-group will move away from all neighboring groups). Orbital phase considerations predict suprafacial addition and hence lead to the same closure

direction for biradicals B and D but the opposite direction for A and C. For large groups (e.g.,  $R = t\text{-Bu}$ ) the steric effects dominate for all four cases. For small groups (e.g.,  $R = \text{CH}_3$ ), C is expected to follow the orbitally allowed (suprafacial) addition as indicated with dotted lines; even here, the other three cases should follow the steric pathways.

$\frac{r}{\text{Å}}$	
1(4 $\pi$ )	1.44
3(4 $\pi$ )	1.48
1(3 $\pi$ )	1.36
3(3 $\pi$ )	1.38

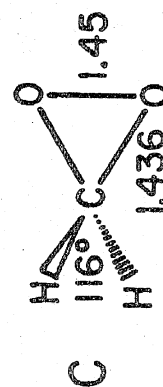
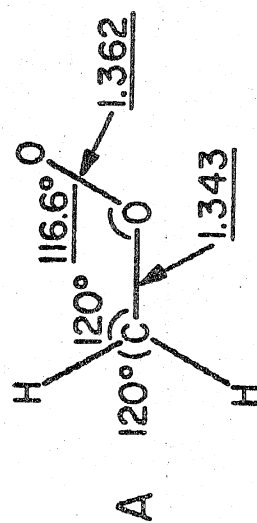
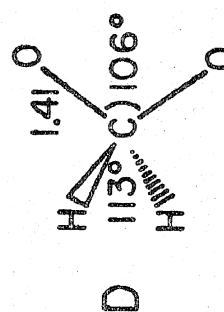
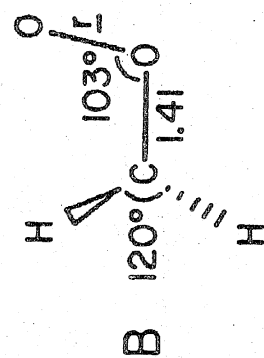


Figure 1.

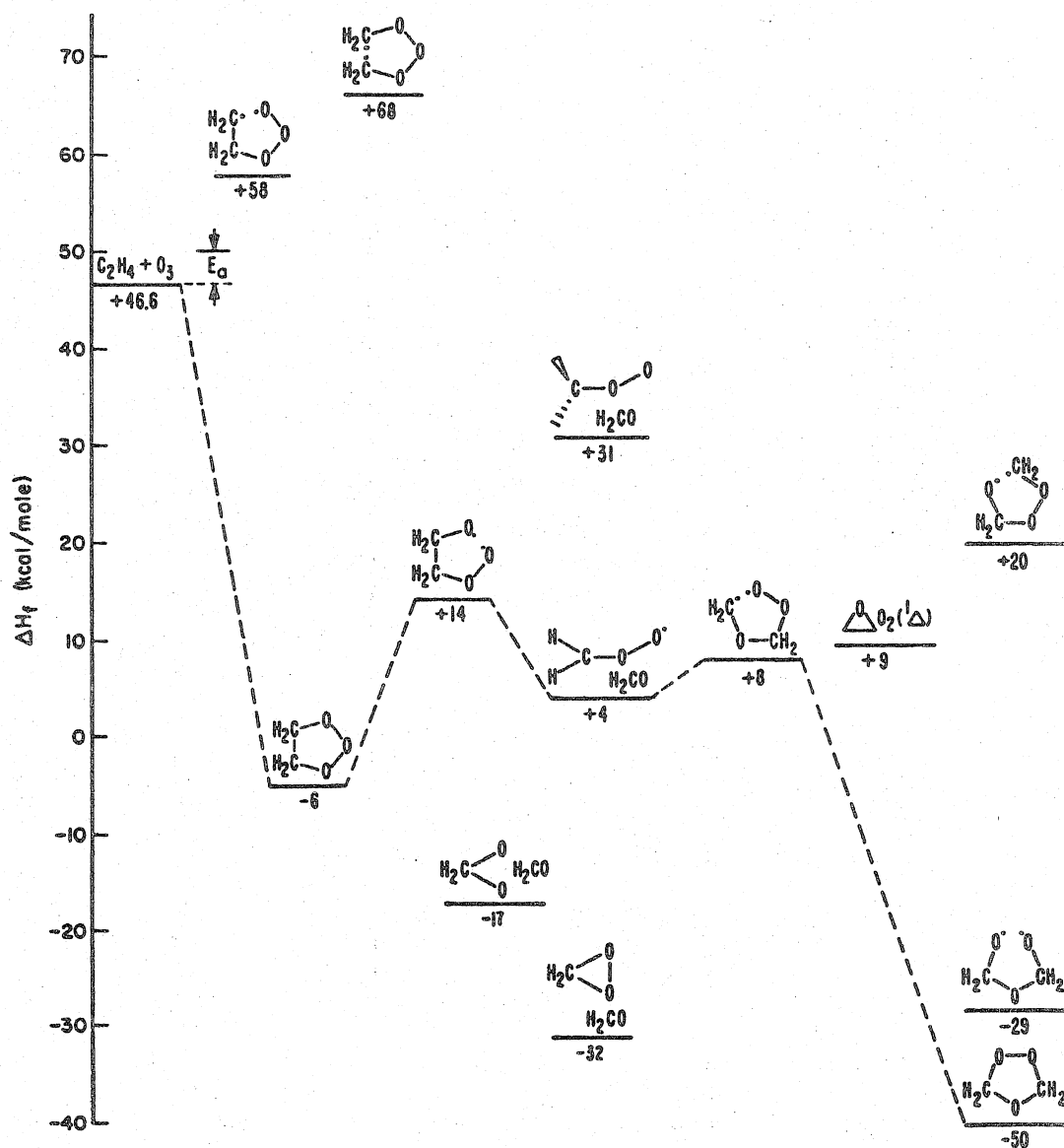
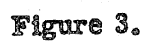


Figure 2.



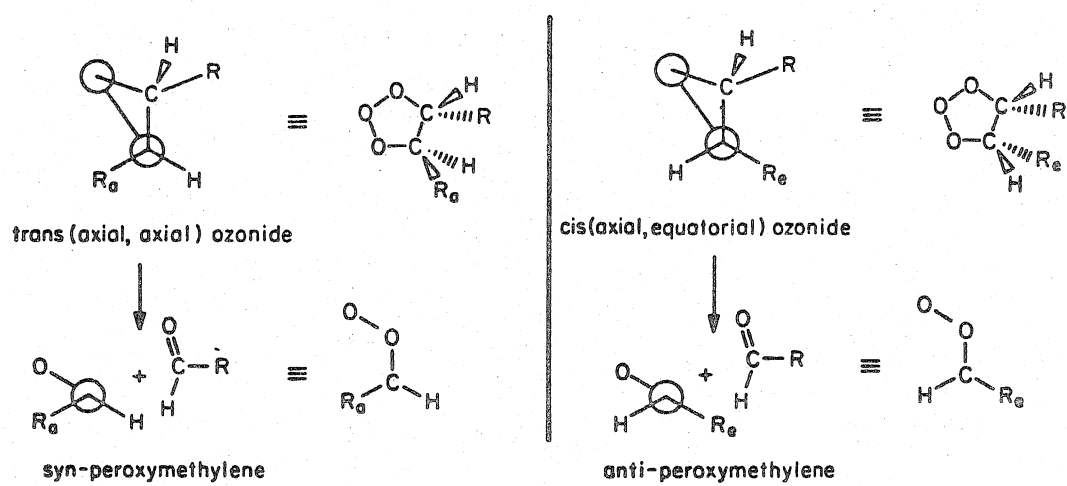


Figure 4.

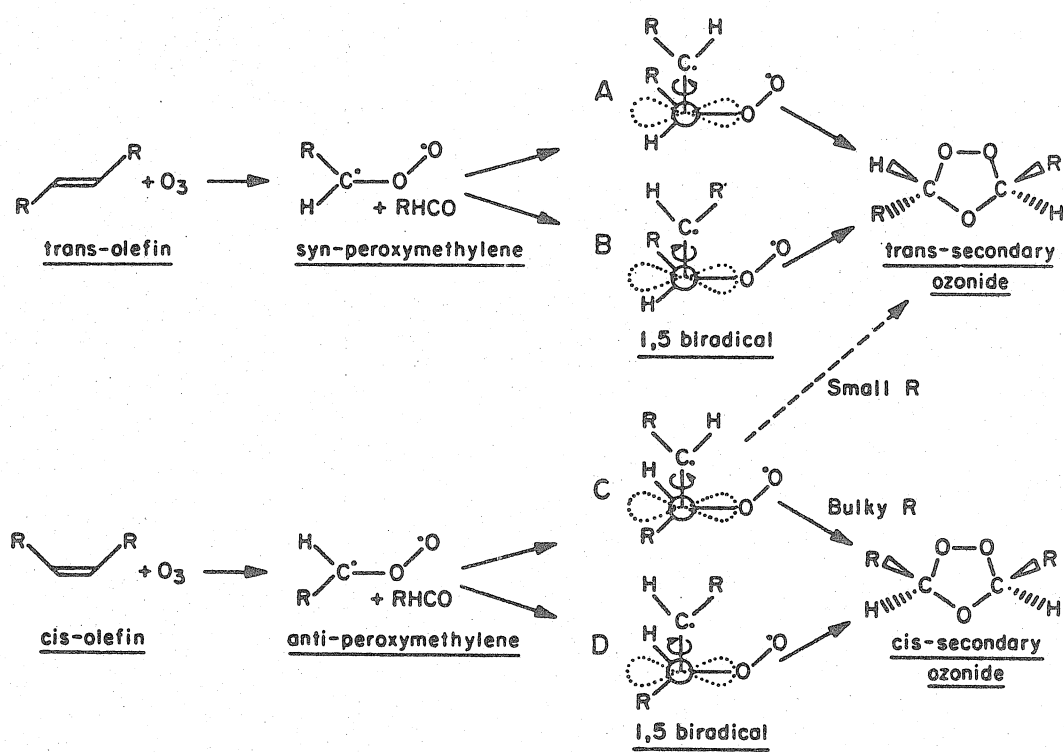


Figure 5.



**PART C: METHYLENE: AB INITIO VIBRONIC  
ANALYSIS AND REINTERPRETATION OF THE  
SPECTROSCOPIC AND NEGATIVE ION PHOTO-  
ELECTRON EXPERIMENTS**

# METHYLENE: AB INITIO VIBRONIC ANALYSIS AND REINTERPRETATION OF THE SPECTROSCOPIC AND NEGATIVE ION PHOTOELECTRON EXPERIMENTS\*

Lawrence B. HARDING and William A. GODDARD III

*Arthur Amos Noyes Laboratory of Chemical Physics \*\*, California Institute of Technology, Pasadena, California 91125, USA*

Received 19 December 1977

Revised manuscript received 10 February 1978

The potential curves from extensive ab initio configuration interaction calculations on the three lowest states of methylene ( $^3B_1$ ,  $^1A_1$ , and  $^1B_1$ ) and one state ( $^2B_1$ ) of  $CH_2^-$  are reported. The Franck-Condon factors from the vibrational wavefunctions obtained using these potential curves lead to excellent agreement with the observed  $^1B_1 \leftarrow ^1A_1$  spectrum (Herzberg) and also lead to an excellent fit with the photoelectron spectra of  $CH_2^-$  (Lineberger), showing that the lowest three bands in the observed negative ion spectrum are hot bands (from vibrationally excited  $CH_2^-$ ). Reassignment of the observed spectrum based on these calculations leads to the prediction of a  $^1A_1 \leftarrow ^3B_1$  splitting of  $0.39 \pm 0.05$  eV (9 kcal); theoretical value: 0.45 eV.

Despite numerous experimental [1-10] and theoretical [11-15] studies, there remains a continuing controversy concerning the relative energies of the three lowest states ( $^3B_1$ ,  $^1A_1$ , and  $^1B_1$ ) of methylene. In the first experimental studies on methylene, Herzberg [1,2] assigned the lowest observed band in the visible spectrum ( $10823\text{ cm}^{-1}$ ) as  $^1B_1(0, 6 \pm 2, 0) \leftarrow ^1A_1(0, 0, 0)$  based on an extrapolation of the  $^{13}C$  isotope shifts. This extrapolation also led to the prediction of the 0-0 transition (unobserved) at  $0.88 \pm 0.06$  eV. Since then, several theoretical studies have been reported, the most extensive of which led to a 0-0 separation of 1.08 eV [15].

The greatest controversy has centered around the  $^1A_1 \leftarrow ^3B_1$  splitting of methylene. Recent theoretical studies [15]<sup>†</sup> led to the prediction of a 0-0 singlet-triplet separation of 0.45 eV, in good agreement with previous calculations [11-14] and in reasonable agree-

ment with recent photochemical studies (0.39 eV) [4,5]. However, the first direct measurement [7] of this separation (from photoionization of  $CH_2^-$ ) led to a  $^1A_1 \leftarrow ^3B_1$  splitting of 0.84 eV, quite at variance with both theory and the (indirect) photochemical studies.

In this communication we report the results of a detailed vibronic analysis of both the visible spectrum ( $^1B_1 \leftarrow ^1A_1$ ) of  $CH_2$  and the photoelectron spectrum of  $CH_2^-$  ( $^2B_1$ ), using potential curves obtained from accurate, highly correlated wavefunctions.

The computational details were reported previously [15]. Briefly, the calculations employ a flexible basis set (35 basis functions) and involve an extensive level of electron correlation (generalized valence bond using 14 natural orbitals and configuration interaction allowing up to selected quadruple excitations using the entire basis) referred to as GVB POL CI.

\* This work was supported in part by a grant (CHE73-05132) from the National Science Foundation. Acknowledgement is made to the donors of the Petroleum Research Fund, administered by the American Chemical Society for partial support of this research.

\*\* Contribution No. 5633.

<sup>†</sup> This paper corrected only for bending contributions to the zero-point energy leading to 0.48 eV. Using force constants from the calculations reported here, we find total zero-point energies of 0.437, 0.452, 0.445, and 0.443 eV for the  $^2B_1$ ,  $^3B_1$ ,  $^1A_1$ , and  $^1B_1$  states, respectively. Correcting for the 0.007 eV difference between  $^3B_1$  and  $^1A_1$  leads to a 0-0 separation of 0.45 eV.

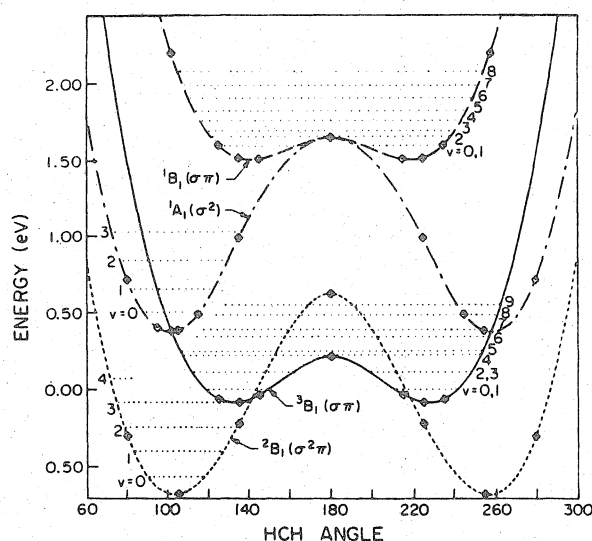


Fig. 1. Potential curves and vibronic energies for the bending mode of  $\text{CH}_2$  and  $\text{CH}_2^-$  (from GVB POL CI calculations).

The GVB POL CI potential curves\* are shown in fig. 1 together with the calculated vibrational energy levels for each state. The resulting equilibrium geometries ( $^3\text{B}_1$ :  $R_e = 1.084 \text{ \AA}$ ,  $\theta_e = 133.2^\circ$ ;  $^1\text{A}_1$ :  $R_e = 1.113 \text{ \AA}$ ,  $\theta_e = 101.8^\circ$ ;  $^1\text{B}_1$ :  $R_e = 1.085 \text{ \AA}$ ,  $\theta_e = 140.9^\circ$ ; and  $^2\text{B}_1$ :  $R_e = 1.121 \text{ \AA}$ ,  $\theta_e = 102.9^\circ$ ) lead to rotational constants within 1% of those reported by Herzberg [1,2].

Comparing the calculated vibrational spacings and isotope shifts with experiment, we find excellent agreement if the lowest observed  $^1\text{B}_1 \leftarrow ^1\text{A}_1$  transition is reassigned as  $5-0^\dagger$  (calculated position, 1.375 eV; observed, 1.342 eV). The low extrapolated value for the  $0-0$  transition (0.88 eV) is found to be due to the use of a slope of 0.0055 for the isotope shift versus

\* In these curves the optimum bond distance for each state is used at each angle. The level of correlation employed in these calculations leads to accurate geometries and excitation energies; however, calculated electron affinities are typically low by 0.5 eV. Thus in fig. 1 we have shifted the negative ion curve by  $-0.02926 \text{ h}$  in order to match the  $^1\text{A}_1 \leftarrow ^2\text{B}_1$   $0-0$  transition with experiment.

$^\dagger$  Because of the large inversion barrier in the  $\text{CH}_2(^1\text{A})$  and  $\text{CH}_2(^2\text{B}_1)$  states, the first 12 vibrational states of the double well potential consist of six pairs of nearly degenerate ( $\Delta E < 0.5 \text{ cm}^{-1}$ ) levels. Thus, for simplicity we treat these as simple (single) wells with no degeneracies. As a result, both even and odd  $\Delta v$  are allowed for transitions to the  $^{1,3}\text{B}_1$  states.

frequency plot (based on a parabolic potential curve), whereas theory (and experiment, if  $v = 8$  is excluded) $^{\dagger\dagger}$  leads to a slope of 0.0065. Thus we estimate

$$\Delta E_{00}(^1\text{B}_1 - ^1\text{A}_1) = 1.08 \pm 0.05 \text{ eV}.$$

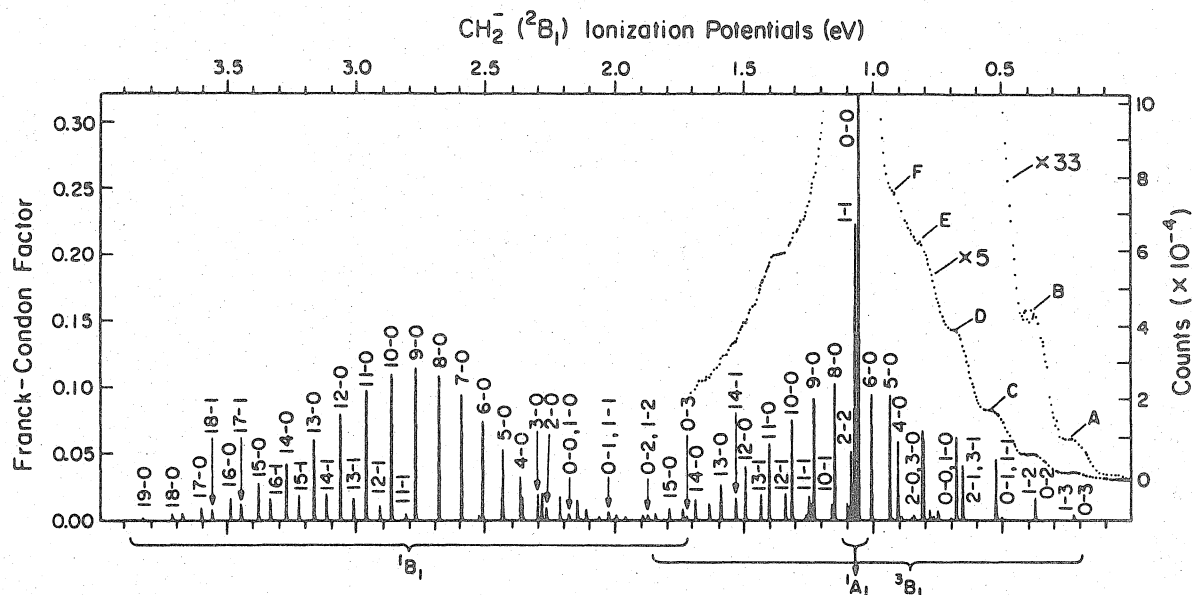
Also shown in fig. 1 are the calculated vibronic energies of the negative ion state ( $^2\text{B}_1$ ). These vibrational wavefunctions lead to Franck-Condon factors from the  $v = 0, 1$ , and  $2$  levels of the negative ion to the  $v = 0$  level $^\ddagger$  of the neutral ( $^3\text{B}_1$ ) state of 0.032, 0.096, 0.141, and 0.237, respectively. Assuming populations of 0.751, 0.185, 0.050, and 0.014 for the  $v = 0, 1, 2$ , and  $3$  levels of the negative ion (this corresponds approximately to a Boltzmann distribution for a temperature of 1370 K), the calculated Franck-Condon factors are converted into the predicted relative intensities $^\diamond$  shown in fig. 2. Superimposed on the GVB POL CI spectrum is the observed photoelectron spectrum of Lineberger et al. [7]. We find the positions and intensities of the "hot" bands,  $0-3$ ,  $0-2$ , and  $0-1$ , to be in good agreement with the first three observed peaks (labeled A, B, and C). The position of the fourth peak (D) is in excellent agreement with the predicted  $0-0$  transition (of 0.45 eV), implying a  $^1\text{A}_1 - ^3\text{B}_1$  separation of 0.39 eV $^\ddagger$ . (The predicted separations of the first five peaks are $^\star$  0.150,

$^{\dagger\dagger}$  As noted by Herzberg [2], the presence of large perturbations in the  $^1\text{B}_1$  vibronic states leads to highly irregular  $^1\text{B}_1$  vibrational spacings. This makes an accurate assignment of the observed transitions difficult.

$^\diamond$  The spin factors for transitions from  $^2\text{B}_1$  to  $^3\text{B}_1$ ,  $^1\text{A}_1$ , and  $^1\text{B}_1$  are 1.5, 1.0, and 0.5. Thus, ignoring the dependence of photoionization cross sections upon energy above threshold and upon whether a  $\sigma$  or  $\pi$  orbital is being ionized, the observed spectrum should be the square of the spin factor times the Franck-Condon factor. The observed spectra suggest that the ratio of intensity to  $^1\text{A}_1$  and to  $^3\text{B}_1$  is 0.76 rather than 0.44, suggesting that the other factors are lower for  $^1\text{A}_1$  than for  $^3\text{B}_1$ .

$^\star$  The assignment of D as the  $0-0$  band implies that our calculated  $^1\text{A}_1 - ^3\text{B}_1$  separation is in error by 0.06 eV. Consequently, all of the  $^3\text{B}_1 - ^2\text{B}_1$  peaks of fig. 2 have been shifted to higher energy by 0.06 eV to correct for this error.

$^\ddagger$  Comparison of the calculated ( $1451 \text{ cm}^{-1}$ ) and experimental ( $1353 \text{ cm}^{-1}$ ) vibrational frequencies for the  $^1\text{A}_1$  bending mode indicates an error of 0.012 eV. We expect a similar error in the  $^2\text{B}_1$  frequency and have therefore included the appropriate correction in these spacings. The calculated vibrational spacings for the  $^1\text{B}_1$  state are in excellent agreement with experiment [2] and hence no corrections are expected to be necessary for the  $^3\text{B}_1$  levels.



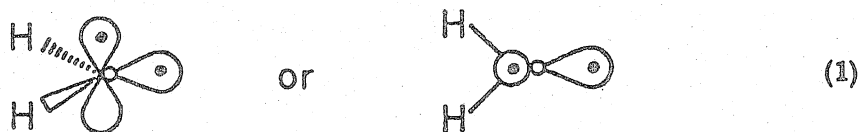
- [1] G. Herzberg, *Proc. Roy. Soc. A* 262 (1961) 291.
- [2] G. Herzberg and J.W.C. Johns, *Proc. Roy. Soc. A* 295 (1966) 107.
- [3] R.W. Carr Jr., T.W. Ede and M.G. Topor, *J. Chem. Phys.* 53 (1970) 4716.
- [4] H.M. Frey, *J. Chem. Soc. Chem. Commun.* (1972) 1024; H.M. Frey and G.J. Kennedy, *J. Chem. Soc. Chem. Commun.* (1975) 233.
- [5] F. Lahmani, *J. Phys. Chem.* 80 (1976) 2623.
- [6] E. Wasserman, W.A. Yager and U.J. Kuck, *Chem. Phys. Letters* 7 (1970) 409; E. Wasserman, J.V. Kuck, R.S. Hutton and W.A. Yager, *J. Am. Chem. Soc.* 92 (1970) 7491.
- [7] P.F. Zittel, G.B. Ellison, S.V. O'Neil, E. Herbst, W.C. Lineberger and W.P. Reinhardt, *J. Am. Chem. Soc.* 98 (1976) 3721.
- [8] J.F. Harrison and L.C. Allen, *J. Am. Chem. Soc.* 91 (1969) 807.
- [9] J.F. Harrison, *Accounts Chem. Res.* 7 (1974) 378, and references therein.
- [10] G. Herzberg and J.W.C. Johns, *J. Chem. Phys.* 54 (1971) 2276.
- [11] P.J. Hay, W.J. Hunt and W.A. Goddard III, *Chem. Phys. Letters* 13 (1972) 30.
- [12] C.F. Bender, H.F. Schaefer III, P.R. Franceschetti and L.C. Allen, *J. Am. Chem. Soc.* 94 (1972) 6888.
- [13] J.A. Pople, J.S. Binkley and R. Seeger, *Intern. J. Quantum Chem.* 10S (1976) 1.

- [14] R.R. Lucchese and H.F. Schaefer III, private communication.
- [15] L.B. Harding and W.A. Goddard III, J. Chem. Phys. 67 (1977) 1777.
- [16] W.C. Lineberger, private communication.
- [17] B.O. Roos and P.M. Siegbahn, J. Am. Chem. Soc. 99 (1977) 7716.
- [18] R.R. Lucchese and H.F. Schaefer III, J. Am. Chem. Soc. 99 (1977) 6766.
- [19] C.W. Bauschlicher and I. Shavitt, J. Am. Chem. Soc., to be published.

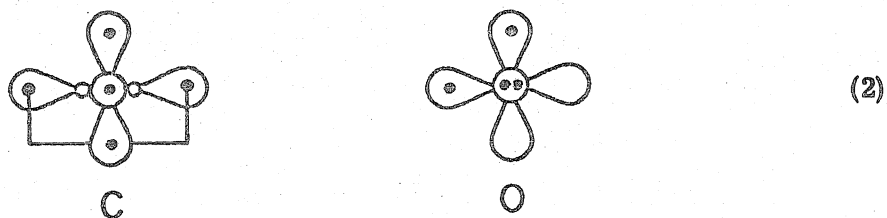
PART D: THE GENERALIZED VALENCE BOND  
DESCRIPTION OF THE LOW-LYING STATES OF  
KETENE

# I. Introduction

The ground state of  $\text{CH}_2$  ( $^3\text{B}_1$ ) has the form<sup>2-5</sup>

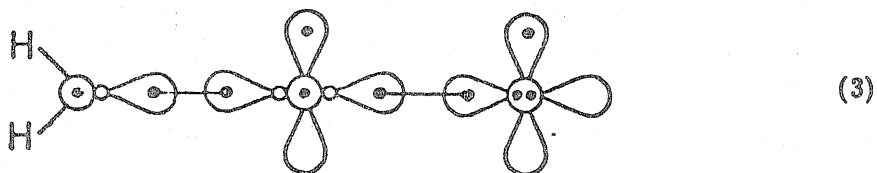


consisting of two C-H bonds, a singly-occupied p-like  $\pi$  orbital and an sp hybridized  $\sigma$  orbital (where  $\infty$  and  $\bigcirc$  represent p orbitals in the plane and perpendicular to the plane, respectively). The ground state of atomic carbon and oxygen have the forms

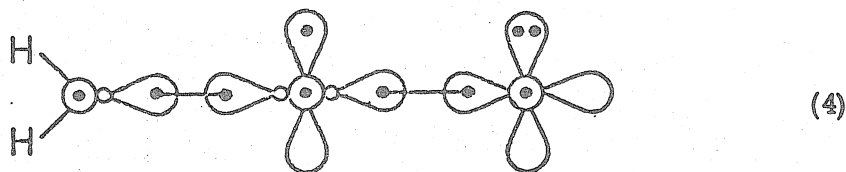


where the line connecting the singly-occupied orbitals indicates singlet pairing.

Combining (1) and (2) we find only two orientations leading to two covalent sigma bonds:



and



We will denote orbitals antisymmetric under reflection through the plane of the molecule (i.e.,  $b_1$  symmetry) as  $\pi$  and orbitals antisymmetric under reflection through the symmetry plane perpendicular to the molecule (i.e.,  $b_2$  symmetry) as  $\bar{\pi}$ . (Reference 6 uses  $\pi'$  in place of  $\bar{\pi}$ .)

Using (3) and allowing all possible couplings of the four singly-occupied  $\pi$  and  $\bar{\pi}$  orbitals leads to six states: two singlets, three triplets and a quintet. Of these three, a singlet, triplet and the quintet result from triplet coupling of both the  $\pi$  and the  $\bar{\pi}$  pairs and are therefore expected to be high-lying. The remaining three states consist of the  $^1A_1$  ground state (resulting from singlet-coupling both the  $\pi$  and  $\bar{\pi}$  pairs leading to a total of four bonds) and two  $^3A_1$  states,  $^3(\pi - \pi^*)$  and  $^3(\bar{\pi} - \bar{\pi}^*)$  (resulting from triplet coupling the  $\pi$  pair with singlet coupling of the  $\bar{\pi}$  pair, and vice versa, respectively).

Similarly, configuration (4) leads to six states of which we will consider only the lowest singlet and triplet. These two states will be denoted  $^1A_2$  or  $^1(n - \bar{\pi}^*)$  and  $^3A_2$  or  $^3(n - \bar{\pi}^*)$ .

The above<sup>type</sup> analysis of the states of ketene in terms of atomic wavefunctions is referred to as a valence bond (VB) analysis. In this paper we report the results of generalized valence bond (GVB)<sup>7,8</sup> calculations in which the orbitals of valence bond-type wavefunctions are solved for self-consistently. The results indicate that (3) and (4) correctly describe the qualitative nature of the states but that polarization and delocalization effects are important for a quantitative description.



We also report configuration interaction (GVB-CI) calculations which include the most important orbital coupling and correlation effects neglected in the GVB wavefunction.

Some of the details of the calculations are discussed in Section II, an analysis of the GVB orbitals is contained in Section III, and the calculated excitation energies and dipole moments are reported in Section IV.

## II. Computational Details

A. Basis Set and Geometry. The double zeta (DZ) basis of Huzinaga<sup>9</sup> and Dunning,<sup>10</sup> (9s, 5p/4s) primitive Gaussians contracted to (4s, 2p/2s), was used in all calculations.

The geometry used was the experimental ground state geometry.<sup>11</sup>  $R_{CO} = 1.161 \text{ \AA}$ ,  $R_{CC} = 1.314 \text{ \AA}$ ,  $R_{CH} = 1.083 \text{ \AA}$ ,  $\angle HCH = 123^\circ$ ,  $\angle CCO = 180^\circ$ .

B. The GVB Calculations.<sup>12</sup> The ground state HF wavefunction of ketene consists of eleven doubly-occupied orbitals.

$$\psi_{HF} = \mathcal{A}[\phi_1^2 \phi_2^2 \cdots \phi_{11}^2 \alpha\beta \cdots \alpha\beta] \quad (5)$$

The HF wavefunction of the low-lying excited states, though, consists of ten doubly-occupied orbitals and two singly-occupied orbitals. In general the correlation error in a closed shell HF ground state is significantly greater than the correlation error in open shell excited states. This differential correlation effect then leads to erroneously low HF excitation energies.

In the GVB wavefunction all orbitals are singly occupied and the spin function is completely general; for ketene this would lead to twenty-two non-orthogonal orbitals. However, one can also deal with intermediate cases in which some electrons are paired into doubly-occupied orbitals as in the HF method while other electron pairs are allowed to split or correlate into nonorthogonal singly-occupied orbitals. In addition, it has been found that two restrictions (perfect pairing and strong orthogonality)<sup>7,13</sup> can be imposed

on the GVB wavefunction leading to a significant reduction in computational complexity without serious effects upon the quality of the wavefunction. The first approximation, perfect pairing, restricts the spin function to be the one in which as many orbital pairs as possible are singlet-coupled for the given spin state. The strong orthogonality restriction requires orbitals of different singlet pairs to be orthogonal.

In the calculations reported here the four pairs corresponding to  $\sigma$ ,  $\pi$  and  $\bar{\pi}$  bonds in the CO and CC regions were allowed to split into non-orthogonal, singly occupied, singlet coupled orbitals. This wavefunction is denoted as GVB(4/PP) to indicate that four pairs of electrons are split (correlated) and that the perfect pairing and strong orthogonality restrictions (PP) are imposed. Thus the GVB(4/PP) ground state wavefunction is of the form

$$\begin{aligned} \alpha [ & \phi_1^2 \phi_2^2 \cdots \phi_7^2 (\phi_8 \phi_9 + \phi_9 \phi_8) \cdots (\phi_{14} \phi_{15} + \phi_{15} \phi_{14}) \\ & \times \alpha\beta \alpha\beta \cdots \alpha\beta ] \end{aligned} \quad (6)$$

The perfect pairing restriction is generally adequate for systems with a single important VB structure. For systems with two or more important VB structures, such as allyl radical or benzene, the optimum orbital coupling often differs greatly from perfect pairing.<sup>14</sup> In the  $n \rightarrow \bar{\pi}^*$  states, the  $\pi$  system is formally that of allyl, and hence such effects could be expected to be important. For this reason we carried out additional calculations in which the PP restriction was relaxed (imposing only the strong orthogonality restriction on the  $\pi$  and  $\bar{\pi}$  orbitals). These calculations are denoted as GVB(4/SO).<sup>13</sup> As expected there was little effect (0.0001 h) on the ground state but a significant effect (0.010 to 0.012 h) on the  $n \rightarrow \bar{\pi}^*$  states. However, we found (see section C) that CI calculations based on either PP or SO orbitals led to nearly identical absolute energies, indicating that the SO calculations are not necessary if an adequate CI is performed.

C. The CI Calculations.<sup>15</sup> Wavefunctions of the valence bond form,

$$\phi_a \phi_b + \phi_b \phi_a,$$

where  $\phi_a$  and  $\phi_b$  are nonorthogonal, may be transformed to an equivalent natural orbital (NO) representation,

$$c_1 \phi_1^2 - c_2 \phi_2^2 \quad (7)$$

where the NO's,  $\phi_1$  and  $\phi_2$  are orthogonal. Generally the dominant NO of a GVB pair may be interpreted as a bonding orbital and the remaining NO as an antibonding or correlation orbital.

The basis for the GVB-CI calculations reported herein consists of all the GVB natural orbitals except the three lowest orbitals (one 1s-like orbital on each carbon and oxygen) together with all three virtual (unoccupied)  $\pi$  functions and virtual  $\bar{\pi}$  functions on the two centers of the carbonyl. In all cases self-consistent orbitals for each state were used in the CI's. Within this basis all configurations resulting from single excitations from each of the configurations listed in Table 1 were included. These calculations relax the perfect pairing and strong orthogonality restrictions and include the important correlation effects neglected in the GVB wavefunction.

For the  $A_2$  states, GVB-CI calculations using the GVB(4/PP) and the GVB(4/SO) orbitals were found to yield identical excitation energies (to 0.0004 h).

### III. The GVB Orbitals

A. The Ground State. The ground state GVB(4) orbitals of ketene are shown in Figure 1. The C—C and C—O  $\sigma$  bonds are found to be very similar to those of ethylene<sup>4</sup> and formaldehyde.<sup>17</sup> The C—O  $\bar{\pi}$  bond is more strongly polarized toward the oxygen than the analogous  $\pi$  bond of formaldehyde. In addition the C—H bonds are noticeably polarized in the same direction resulting in a net  $\bar{\pi}$  polarization toward the oxygen.

The  $\pi$  system consists of two singly-occupied CC bonding orbitals and a doubly-occupied orbital centered on the oxygen but somewhat delocalized into the CO  $\pi$  bonding region. In the VB model this latter orbital would correspond to a doubly-occupied oxygen p orbital analogous to the n orbital of formaldehyde and other carbonyls. We therefore denote this orbital as n, noting however, that the GVB orbital is found to have some  $\pi$  bonding character.

B. The (n -  $\bar{\pi}^*$ ) states. The CH and  $\bar{\pi}$  orbitals of the  $A_2$  states are shown in Figure 2. In these plots the CH and  $\bar{\pi}$  doubly-occupied orbitals are obtained from approximate GVB(5) calculations.<sup>18</sup>

As expected from (4) the resulting CO  $\bar{\pi}$  orbital is localized primarily on the oxygen; however, it does exhibit considerable CO  $\bar{\pi}$  bonding character. The CO  $\bar{\pi}^*$  orbital is centered primarily on the central carbon with some antibonding delocalization onto both the oxygen and the CH<sub>2</sub> group. With three electrons in the CO  $\bar{\pi}$  bond region, the CH bonds cannot effectively delocalize toward the carbonyl, and hence the CH bonds are more localized in the n -  $\bar{\pi}^*$  states than in ground state.

In the  $\pi$  system, Figure 3, we find the singly-occupied p orbital on the oxygen to be singlet paired with and highly overlapping (see Table 2) the p orbital on the adjacent carbon, leading to a significant CO  $\pi$  bonding effect. Due to the strong orthogonality constraints, the remaining carbon p

orbital must be orthogonal to the CO  $\pi$  bond and hence this orbital has C—O antibonding character. It should be emphasized that the strong orthogonality restriction results in an over-emphasis of the more favorable orbital coupling (in this case, singlet coupling of the carbonyl p orbitals) at the expense of the less favorable coupling (singlet coupling of the two carbon p orbitals).

C. The  $^3(\pi - \pi^*)$  State. The  $\sigma$  and  $\bar{\pi}$  orbitals of the  $^3(\pi - \pi^*)$  state, Figure 2, are nearly identical to those of the ground state, as expected from the VB description, (3).

In the  $\pi$  system, Figure 3, the oxygen lone pair has slightly more CO  $\pi$  bonding character than the ground state lone pair. As a result both the CC  $\pi$  and  $\pi^*$  orbitals are found to have a considerable amount of CO antibonding character.

D. The  $^3(\bar{\pi} - \bar{\pi}^*)$  State. The CO  $\bar{\pi}$  orbitals of the  $2^3A_1$  state are slightly more delocalized into the C—H region than are the corresponding ground state orbitals. A much larger effect is the decrease in CO  $\bar{\pi}$  bond polarity. A similar effect has been noted<sup>17</sup> in the  $^3(\pi - \pi^*)$  state of formaldehyde.

The  $\pi$  orbitals of this state (Figure 3) are slightly more localized than the ground state  $\pi$  orbitals, possibly representing a decrease in the  $\pi$  polarization away from the oxygen in conjunction with the decrease in  $\bar{\pi}$  polarization toward the oxygen.

#### IV. Discussion

A. Excitation Energies. The calculated GVB energies are listed in Table 2 along with GVB pair overlaps and splitting energies. In Table 3 the calculated excitation energies are compared with previous theoretical results and experiment. The  $^1A_2$  and  $1\ ^3A_1$  excitation energies from GVB-CI are in excellent agreement with the results of recent electron impact experiments by Frueholz et al.<sup>19</sup> and, for the  $^1A_2$  state, with the results of optical spectra.<sup>20, 21</sup> We expect comparable accuracy in the  $^3A_2$  and  $2\ ^3A_1$  excitation energies from GVB-CI, although neither of the states has been conclusively assigned in either the optical or electron impact spectra.<sup>19</sup>

Of particular interest is the calculated singlet-triplet splitting, 0.07 eV, of the  $A_2$  ( $n-\bar{\pi}^*$ ) states. Previous calculations<sup>6</sup> and assignments of the optical spectra<sup>20, 21</sup> have led to a splitting of 0.5 eV, comparable to the singlet-triplet ( $n-\pi^*$ ) splitting in formaldehyde (0.47 eV) and other carbonyls. To a first approximation (not including orbital readjustments between the two states) the singlet-triplet splitting is equal to twice the exchange integral between the two "active" orbitals. In formaldehyde this exchange integral is 0.16 eV, in ketene it is only 0.07 eV. The exchange integral is much smaller in ketene because the  $\bar{\pi}^*$  orbital (Figure 2) has a node through the carbon on which the relevant  $\pi$  orbital is centered (Figure 3). Basically then, the small splitting is due to the  $\bar{\pi}^*$  orbital being localized in the carbonyl region and the  $\pi$  orbital (to which it is either singlet or triplet coupled) being localized on the  $CH_2$  carbon.

Excited states of closed shell systems are often treated in CI calculations including only single-excitations from the higher-lying ground state occupied MO's to the lower-lying virtual MO's. Del Bene<sup>6</sup> has found that with a minimum basis set (MBS), this method leads to a singlet-triplet  $A_2$  splitting of 0.59 eV. In order to test the possible basis set dependence of this result

we have carried out similar calculations with our DZ basis and find a splitting of 0.42 eV.<sup>22</sup> In light of the explanation proposed above for the anomalously small splitting (0.07 eV) it is not surprising that calculations based on delocalized, ground-state, HF orbitals would lead to an erroneously large singlet-triplet splitting.

Laufer and Keller<sup>23</sup> have reported an extensive study of the low-energy optical spectrum of ketene using oxygen enhancement techniques. They find no evidence for a singlet-triplet transition in the 2-4 eV range and conclude that the  $^3A_2$  transition is obscured by the  $^1A_2$  transition.

Frueholz et al.<sup>19</sup> have recently reported the results of electron impact experiments at varying angles and impact energies. They were unable to resolve the  $^3A_2$  transition from the  $^1A_2$  transition and concluded the splitting to be much smaller than that normally found for carbonyl ( $n \rightarrow \pi^*$ ) states. Their results indicate a singlet-triplet splitting of less than 0.2 eV and probably no bigger than 0.1 eV. These results are in agreement with our results but contradict those of Dixon and Kirby,<sup>21</sup> McGlynn and co-workers,<sup>20</sup> and Del Bene.<sup>6</sup>

McGlynn<sup>20</sup> has proposed the existence of two low-energy triplet states in the 2-4 eV range. Our results contradict this contention, indeed our calculations and the results of electron impact experiments place the second triplet state above 5 eV.

B. Dipole Moments. The calculated GVB(4/PP) and GVB-CI dipole moments are listed in Table 4. The ground state GVB-CI dipole moment, 1.62 D, is found to be 0.21 D above the reported experimental value of 1.41 D.<sup>24</sup> A similar error (0.25 D) in the DZ GVB-CI dipole moment of formaldehyde was found to be due to a lack of d functions in the basis set.<sup>17</sup>

The ground state GVB-CI dipole moment, 1.62 D, is in significantly



better agreement with experiment (1.41 D) than the GVB(4/PP) and HF results, 1.95 D and 2.00 D, respectively. Previous HF calculations<sup>25</sup> with a different basis set led to the same dipole moment.

Partitioning the HF and GVB dipole moments into  $a_1$ ,  $b_1$ , and  $b_2$  components and associating with each the appropriate nuclear contributions [based on (3) and (4)], we find good agreement between the HF and GVB  $a_1$  components, -0.89 and -0.87 a.u., respectively. The HF  $b_1$  or  $\pi$  component, 1.40 a.u., is 0.31 a.u. more positive than the GVB  $b_1$  component, 1.09 a.u. The HF  $b_2$  or  $\bar{\pi}$  component, -1.30 a.u., is 0.31 a.u. more negative than the GVB  $b_2$  component. Thus in spite of the close agreement between the GVB(4/PP) and HF total dipole moments, the HF wavefunction contains appreciably more ionic character in both the  $\pi$  and  $\bar{\pi}$  systems.

C. Comparison of Theoretical Excitation Energies. In previous calculations on  $\text{CH}_2\text{O}$ <sup>17</sup> and  $\text{H}_2\text{NCHO}$ ,<sup>26</sup> it was noted that the most important effects included in the GVB-CI wavefunctions but neglected in the GVB(/PP) wavefunctions were orbital coupling and interpair correlation terms. Of these the GVB(/SO) wavefunctions include only the important orbital coupling or resonance effects. From the results of Table 3, we see the allylic resonance of the singlet and triplet ( $n \rightarrow \bar{\pi}^*$ ) states lowers these states by 5.4 and 6.2 kcal, restrictively, indicating a resonance energy of  $\sim 6$  kcal. For comparison, in allyl radical, where the two resonance structures are completely equivalent the resonance stabilization was found to be 11.4 kcal.<sup>14</sup>

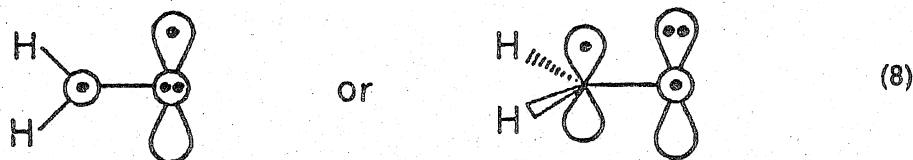
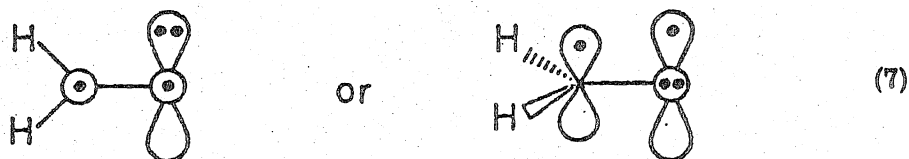
Considering now the GVB-CI excitation energies, we find only a small change in the  $^1,^3(n \rightarrow \bar{\pi}^*)$  excitation energies relative to the GVB(4/SO) results. This is in agreement with calculations on  $\text{CH}_2\text{O}$  and  $\text{H}_2\text{NCHO}$  in which it was found the ( $n \rightarrow \pi^*$ ) excitation energies were not greatly affected by the additional correlation effects in the CI.

Comparing the GVB(4/PP)  $^3(\pi \rightarrow \pi^*)$  and  $^3(\bar{\pi} \rightarrow \bar{\pi}^*)$  excitation energies to the GVB-CI results, we find the  $^3(\pi \rightarrow \pi^*)$  energy to be unaffected by the CI whereas the  $^3(\bar{\pi} \rightarrow \bar{\pi}^*)$  energy is increased by 0.55 eV. In calculations on formaldehyde<sup>17</sup> it was found that  $\sigma$ - $\pi$  interpair correlations resulted in a lowering of the ground state energy 0.5 eV relative to the  $^3(\pi \rightarrow \pi^*)$  state. The explanation for this differential effect is that  $\sigma$ - $\pi$  interpair correlation corresponds to a concerted (correlated) movement of the two  $\sigma$  electrons to one center and the two  $\pi$  electrons to the opposite center. When the  $\pi$  pair is triplet coupled, the movement of both  $\pi$  electrons onto one center is unfavorable. In formamide<sup>26</sup> it was found that delocalization of the nitrogen  $\pi$  lone pair in the  $^3(\pi \rightarrow \pi^*)$  state led to interpair correlation terms that

cancelled those in the ground state. In ketene the oxygen  $\pi$  lone pair is found to be greatly delocalized in the  $^3(\pi \rightarrow \pi^*)$  state while no equivalent effect is found in the  $^3(\bar{\pi} \rightarrow \bar{\pi}^*)$  state. Thus we would expect, as is found, a large ( $\sim 0.5$  eV) CI effect on the  $^3(\bar{\pi} \rightarrow \bar{\pi}^*)$  excitation energy and little if any effect on the  $^3(\pi \rightarrow \pi^*)$  excitation energy.

### V. Comparisons to Formaldehyde and Ethylene

The VB diagrams for the valence states of formaldehyde are shown in (7) and (8).

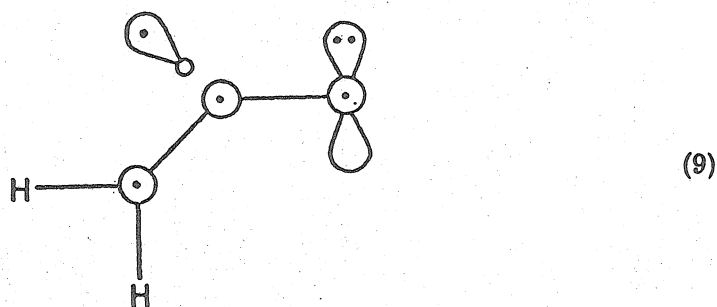


Coupling the two singly-occupied orbitals into either a singlet or a triplet leads to the  $^1A_1$  or ground state and  $^3A_1$  or  $^3(\pi - \pi^*)$  state for (7) and the  $^1A_2$  or  $^1(n - \pi^*)$  and  $^3A_2$  or  $^3(n - \pi^*)$  states for (8).

In the  $A_2$  states of formaldehyde it has been found that the hydrogens bend out of the plane of the molecule allowing the singly-occupied  $\pi$  orbital to hybridize away from the doubly-occupied  $\pi$  orbital thereby reducing the antibonding interaction.

Comparing (7) to (3) then, we find the oxygen  $b_2$  or  $\bar{\pi}$  lone pair of formaldehyde corresponds to a  $b_1$  or  $\pi$  orbital of ketene. Similarly, the  $\pi$  bond of formaldehyde corresponds to the  $\bar{\pi}$  bond of ketene. Making this comparison we find the lone pair of ketene to have considerably more CO bonding character than the lone pair of formaldehyde (Figure 4).

Similarly comparing (8) to (4) we would expect the antibonding character of the singly-occupied  $\bar{\pi}$  orbital to lead to a change in geometry analogous to that found in formaldehyde. In ketene this effect will lead to a decrease in the CCO angle as shown in (9).



Such an effect was in fact found in the calculations reported by Del Bene.<sup>6</sup>

In ref 20, comparisons are made between the  $2b_2$  orbital of formaldehyde and the  $2b_2$  orbital of ketene discussing the relative amounts of bonding and nonbonding character; from a simple VB analysis we conclude it is far more appropriate to compare the  $b_2$  long pair of formaldehyde and the  $b_1$  lone pair of ketene. Similarly, Del Bene<sup>6</sup> argues that since the  $A_2$  states of formaldehyde arise from a  $b_2 \rightarrow b_1$  transition, while the  $A_2$  states of ketene arise from a  $b_1 \rightarrow b_2$  transition, the  $A_2$  states of ketene are not analogous to the  $A_2$  states of formaldehyde. We find this argument to be incorrect.

It is also of interest to compare the excitation energies of ketene to those of the constituent chromophores ethylene and formaldehyde. From this analysis, Table 5, we find a correct prediction of the ordering of the states. In particular, we find fairly good agreement between the  $(n \rightarrow \pi^*)$  excitation energies but the  $^3(\pi \rightarrow \pi^*)$  energies of ketene are significantly higher than those of  $C_2H_4$  and  $CH_2O$ . The difference in  $^3(\pi \rightarrow \pi^*)$  excitation energies may be due to shorter CO and CC bond lengths in ketene. In the  $(n \rightarrow \pi^*)$  states this effect is canceled by the previously mentioned allylic resonance stabilization.

## VI. Summary

The GVB wavefunction leads to a consistent description of the valence states of ketene, and the GVB orbitals provide simple explanations of the character of the states. In addition, CI calculations based on the GVB orbitals include additional correlation and orbital coupling effects necessary for quantitatively accurate valence excitation energies.

Table 1. Configurations for the GVB-CI Calculations. The occupation numbers are shown for the orbitals of variable occupancy. Six other orbitals are doubly-occupied.

State	GVB Natural Orbitals				
	CO	CC	O	CC	CO
	$\sigma \sigma^*$	$\sigma \sigma^*$	$n(\pi)$	$\pi \pi^*$	$\bar{\pi} \bar{\pi}^*$
<sup>1</sup> A <sub>1</sub> ground state	2 0	2 0	2	2 0	2 0
	1 1	2 0	2	2 0	2 0
	2 0	1 1	2	2 0	2 0
	2 0	2 0	2	1 1	2 0
	2 0	2 0	2	2 0	1 1
A <sub>2</sub> ( $n - \pi^*$ )	2 0	2 0	1	2 0	2 1
	1 1	2 0	1	2 0	2 1
	2 0	1 1	1	2 0	2 1
	2 0	2 0	1	1 1	2 1
	2 0	2 0	0	2 1	2 1
	2 0	2 0	2	1 0	2 1
	2 0	2 0	1	2 0	1 2
<sup>3</sup> A <sub>1</sub> ( $\pi - \pi^*$ ) and ( $\bar{\pi} - \bar{\pi}^*$ )	2 0	2 0	2	1 1	2 0
	1 1	2 0	2	1 1	2 0
	2 0	1 1	2	1 1	2 0
	2 0	2 0	2	1 1	1 1
	2 0	2 0	2	0 2	2 0
	2 0	2 0	2	2 0	2 0
	2 0	2 0	2	2 0	1 1
	2 0	1 1	2	2 0	1 1
	1 1	2 0	2	2 0	1 1
	2 0	2 0	2	2 0	0 2
	2 0	2 0	2	2 0	2 0

Table 2. Energies and GVB parameters for the GVB(4/PP) and GVB(4/SO) wavefunctions of  $\text{CH}_2\text{CO}$ . All quantities are in atomic units.

Character	State	Calculation	Total Energy	GVB Pair Information		
				Pair	Overlap	$\Delta E^a$
Ground State	$^1A_1$	PP	-151.7476	$\text{CO}\sigma$	0.874	0.0234
				$\text{CC}\sigma$	0.893	0.0085
				$\text{CO}\bar{\pi}$	0.696	0.0240
				$\text{CC}\pi$	0.693	0.0330
		SO	-151.7477	$\text{CO}\sigma$	0.874	0.0134
				$\text{CC}\sigma$	0.893	0.0085
				$\text{CO}\bar{\pi}$	0.696	--
				$\text{CC}\pi$	0.693	--
$^3(n - \bar{\pi}^*)$	$^3A_2$	PP	-151.6016	$\text{CO}\sigma$	0.874	0.0133
				$\text{CC}\sigma$	0.891	0.0088
				$\text{CO}\pi$	0.768	0.0210
		SO	-151.6116	$\text{CO}\sigma$	0.875	0.0132
				$\text{CC}\sigma$	0.891	0.0087
				$\text{CO}\pi$	0.782	--
$^1(n - \bar{\pi}^*)$	$^1A_2$	PP	-151.5958	$\text{CO}\sigma$	0.874	0.0133
				$\text{CC}\sigma$	0.891	0.0088
				$\text{CO}\pi$	0.760	0.0222
		SO	-151.6082	$\text{CO}\sigma$	0.875	0.0132
				$\text{CC}\sigma$	0.892	0.0087
				$\text{CO}\pi$	0.769	--
$^3(\pi - \pi^*)$	$1^3A_1$	PP	-151.5494	$\text{CO}\sigma$	0.875	0.0132
				$\text{CC}\sigma$	0.891	0.0088
				$\text{CO}\bar{\pi}$	0.702	0.0313
				$\text{CC}\pi$	0.691	0.0246
$^3(\bar{\pi} - \bar{\pi}^*)$	$2^3A_1$	PP	-151.4968	$\text{CO}\sigma$	0.875	0.0132
				$\text{CC}\sigma$	0.894	0.0083
				$\text{CC}\pi$	0.691	0.0246

<sup>a</sup> Energy increase upon replacing the GVB pair by a HF pair (averaging the GVB orbitals to obtain the HF orbital).



Table 3. Vertical Excitation Energies (eV) for CH<sub>2</sub>CO.

State	Exp't. <sup>a</sup>	GVB-CI	GVB(4/SO)	GVB(4/PP)	HF <sup>b</sup>	Single Excitation CI	
						DZ	MBS <sup>c</sup>
<sup>3</sup> A <sub>2</sub> (n → π*)	--	3.62 <sup>d</sup>	3.70 <sup>d</sup>	3.97 <sup>d</sup>	3.12 <sup>d</sup>	3.84 <sup>d</sup>	3.71
<sup>1</sup> A <sub>2</sub> (n → π*)	3.8	3.69	3.79	4.13	3.32	4.27	4.30
<sup>1</sup> A <sub>1</sub> (π → π*)	5.35	5.39	--	5.39	--	4.95	4.88
<sup>2</sup> A <sub>1</sub> (π → π*)	--	7.37	--	6.82	--	6.62	--

<sup>a</sup> Electron impact results of R. P. Frueholz, W. M. Flicker, and A. Kuppermann, ref 19.<sup>b</sup> H. Basch, Theoret. Chim. Acta, 28, 151 (1973).<sup>c</sup> J. E. Del Bene, ref 6.<sup>d</sup> The calculated ground state (<sup>1</sup>A<sub>1</sub>) energies are -151.8271, -151.7477, -151.7476, -151.6721, and -151.6718 h, respectively.

Table 4. Calculated Total Dipole Moments. <sup>a</sup>

State		Atomic Units		Debye		Exper
		GVB(4/PP)	GVB-CI	GVB(4/PP)	GVB-CI	
<sup>1</sup> A <sub>1</sub>	Ground State	0.77 <sup>b</sup>	0.64	1.95	1.62	1.41
<sup>3</sup> A <sub>2</sub>	<sup>3</sup> (n - $\bar{\pi}^*$ )	1.25	1.09	3.18	2.76	
<sup>1</sup> A <sub>2</sub>	<sup>1</sup> (n - $\bar{\pi}^*$ )	1.19	1.35	3.03	3.43	
<sup>1</sup> <sup>3</sup> A <sub>1</sub>	<sup>3</sup> ( $\pi$ - $\pi^*$ )	1.09	0.96	2.77	2.43	
<sup>2</sup> <sup>3</sup> A <sub>1</sub>	<sup>3</sup> ( $\bar{\pi}$ - $\bar{\pi}^*$ )	0.008	0.11	0.19	0.27	

a. The sign of the dipole moments indicates a shift of electron charge toward the oxygen for all states.

b. The dipole moment for the HF wavefunction is 2.00 Debye.

Table 5. Comparison of GVB-CI vertical excitation energies of  $\text{CH}_2\text{O}$ ,  $\text{C}_2\text{H}_4$  and  $\text{CH}_2\text{CO}$ .

	$\text{CH}_2\text{O}^{\text{a}}$	$\text{C}_2\text{H}_4^{\text{b}}$	$\text{CH}_2\text{CO}$
$^3\text{A}_2$ ( $\text{n} \rightarrow \pi^*$ )	3.62	-	3.62
$^1\text{A}_2$ ( $\text{n} \rightarrow \pi^*$ )	4.09	-	3.69
$1^3\text{A}_1$ ( $\text{CC}\pi - \text{CC}\pi^*$ )	-	4.65	5.39
$2^3\text{A}_1$ ( $\text{CO}\pi - \text{CO}\pi^*$ )	5.95	-	7.37

a. L. B. Harding and W. A. Goddard, ref 17.

b. L. B. Harding and W. A. Goddard, manuscript in preparation.

# REFERENCES

- (1) Partially supported by a grant (MPS73-05132) from the National Science Foundation.
- (2) S. V. O'Neil, H. F. Schaefer III, and C. F. Bender, J. Chem. Phys., 55, 162 (1971).
- (3) P. J. Hay, W. J. Hunt, and W. A. Goddard III, Chem. Phys. Lett., 13, 30 (1972).
- (4) P. J. Hay, W. J. Hunt, and W. A. Goddard III, J. Amer. Chem. Soc., 94, 8293 (1972).
- (5) W. A. Goddard III, T. H. Dunning, Jr., W. J. Hunt, and P. J. Hay, Accts. Chem. Res., 6, 368 (1973).
- (6) J. E. Del Bene, J. Amer. Chem. Soc., 94, 3713 (1972).
- (7) W. J. Hunt, P. J. Hay, and W. A. Goddard III, J. Chem. Phys., 57, 738 (1972).
- (8) W. A. Goddard III and R. C. Ladner, J. Amer. Chem. Soc., 93, 6750 (1971).
- (9) S. Huzinaga, J. Chem. Phys., 42, 1243 (1965).
- (10) T. H. Dunning, J. Chem. Phys., 53, 2823 (1970).
- (11) A. P. Cox, L. F. Thomas, and J. Sheridan, Spectrochim. Acta, 15, 542 (1954).
- (12) The GVB(PP) calculations were carried out with the GVB TWO program of Bobrowicz,<sup>13</sup> Wadt and Goddard (based essentially on the methods of Hunt et al.<sup>7</sup>). The GVB(SO) calculations were carried out with the SOGVB program of Bobrowicz and Goddard.<sup>13</sup>
- (13) F. Bobrowicz, Ph.D. Thesis, California Institute of Technology, 1974.
- (14) G. Levin and W. A. Goddard III, J. Amer. Chem. Soc., 97, 1649 (1975).
- (15) The CI calculations were carried out with the Caltech spin-eigenfunction CI program (Bobrowicz,<sup>13</sup> Winter, Ladner,<sup>16</sup> Moss, Harding, Walch, and Goddard).

- (16) R. C. Ladner, Ph.D. Thesis, California Institute of Technology, 1971.
- (17) L. B. Harding and W. A. Goddard III, J. Amer. Chem. Soc., 97, 6293 (1975).
- (18) In the GVB(4) calculations on the  $A_2$  states, there are two doubly-occupied, and therefore nonunique,  $b_2$  orbitals. In order to obtain significant CH and  $\bar{\pi}$  bond pairs it is necessary to solve for the GVB(5) wavefunction in which the  $CH_{b_2}$  orbital is allowed to correlate. Since we were not otherwise interested in electron correlations involving the CH bond pairs, we approximated the GVB(5) wavefunction in the following way: (a) the  $a_1$ ,  $b_1$ , and  $\bar{\pi}^*$  occupied orbitals of the GVB(4) wavefunction were fixed (not allowed to vary); (b) the  $\bar{\pi}$  orbital and the first NO of the  $CH_{b_2}$  pair were restricted to be linear combinations of the two doubly-occupied GVB(4)  $b_2$  orbitals; (c) the second NO of the new pair was restricted to be a linear combination of the virtual orbitals from the GVB(4) calculation. This procedure leads to a good approximation to the GVB(5) orbitals but at considerably less cost, and thus can be considered as an energy based approach to localizing the doubly-occupied orbitals of a wavefunction.
- (19) R. P. Frueholz, W. M. Flicker, and A. Kuppermann, Chem. Phys. Lett., 38, 57 (1976).
- (20) J. W. Rabalais, J. M. McDonald, V. Scherr, and S. P. McGlynn, Chem. Rev., 71, 73 (1971).
- (21) R. N. Dixon and G. H. Kirby, Trans. Faraday Soc., 62, 1406 (1966).

- (22) In the calculations of reference 6, all single excitations from the six highest occupied MO's to the six lowest virtuals (in this case this includes all of the virtuals) were included. We performed two such calculations; one in which all single excitations from the six highest occupieds to the 12 lowest virtuals were included, and a second consisting of all single excitations from the six highest occupieds to all of the  $b_1$  and  $b_2$  virtual functions plus the two lowest  $a_1$  virtual MO's. For the  $A_2$  states, due to the method of generating the configurations, the later calculation is equivalent to including all virtual functions. The excitation energies from the two calculations were found to be within 0.05 eV of each other.
- (23) A. H. Laufer and R. A. Keller, J. Amer. Chem. Soc., 93, 61 (1971).
- (24) H. R. Johnson and M. W. P. Strandberg, J. Chem. Phys., 20, 687 (1952).
- (25) J. H. Letcher, M. L. Unland, and J. R. Van Waser, J. Chem. Phys., 50, 2185 (1969).
- (26) L. B. Harding and W. A. Goddard III, J. Amer. Chem. Soc., 97, 6300 (1975).

Figure Captions

Figure 1: The Ground State GVB(4/PP) orbitals of  $\text{CH}_2\text{CO}$ . The three 1s orbitals are not shown. The ONE and TWO indicate the number of electrons in the orbital. PAIRED connecting two orbitals indicates that the two orbitals are singlet paired. Long dashes indicate zero amplitude, the spacing between contours is 0.5 a.u., the same conventions are used in all plots.

Figure 2: The CH and  $\bar{\pi}$  orbitals of the valence states of  $\text{CH}_2\text{CO}$  (see ref 18).

Figure 3: The GVB(4/PP)  $\pi$  orbitals of the valence states of  $\text{CH}_2\text{CO}$ .

Figure 4: The  $\bar{\pi}$  lone pair and CO  $\pi$  bond orbitals of  $\text{CH}_2\text{O}$ . All orbitals are from GVB(4/PP) calculations (see ref. 18).

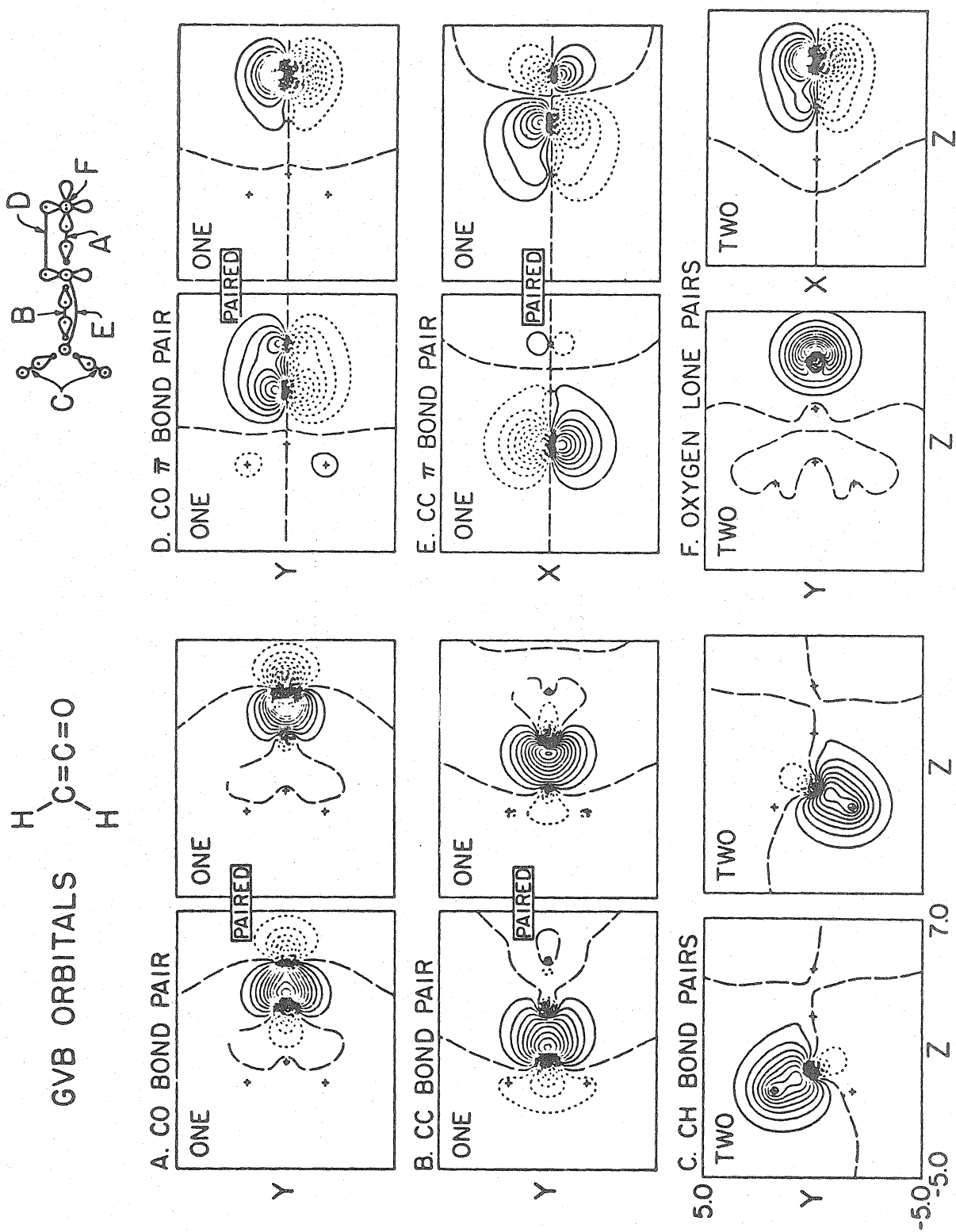


Figure 1



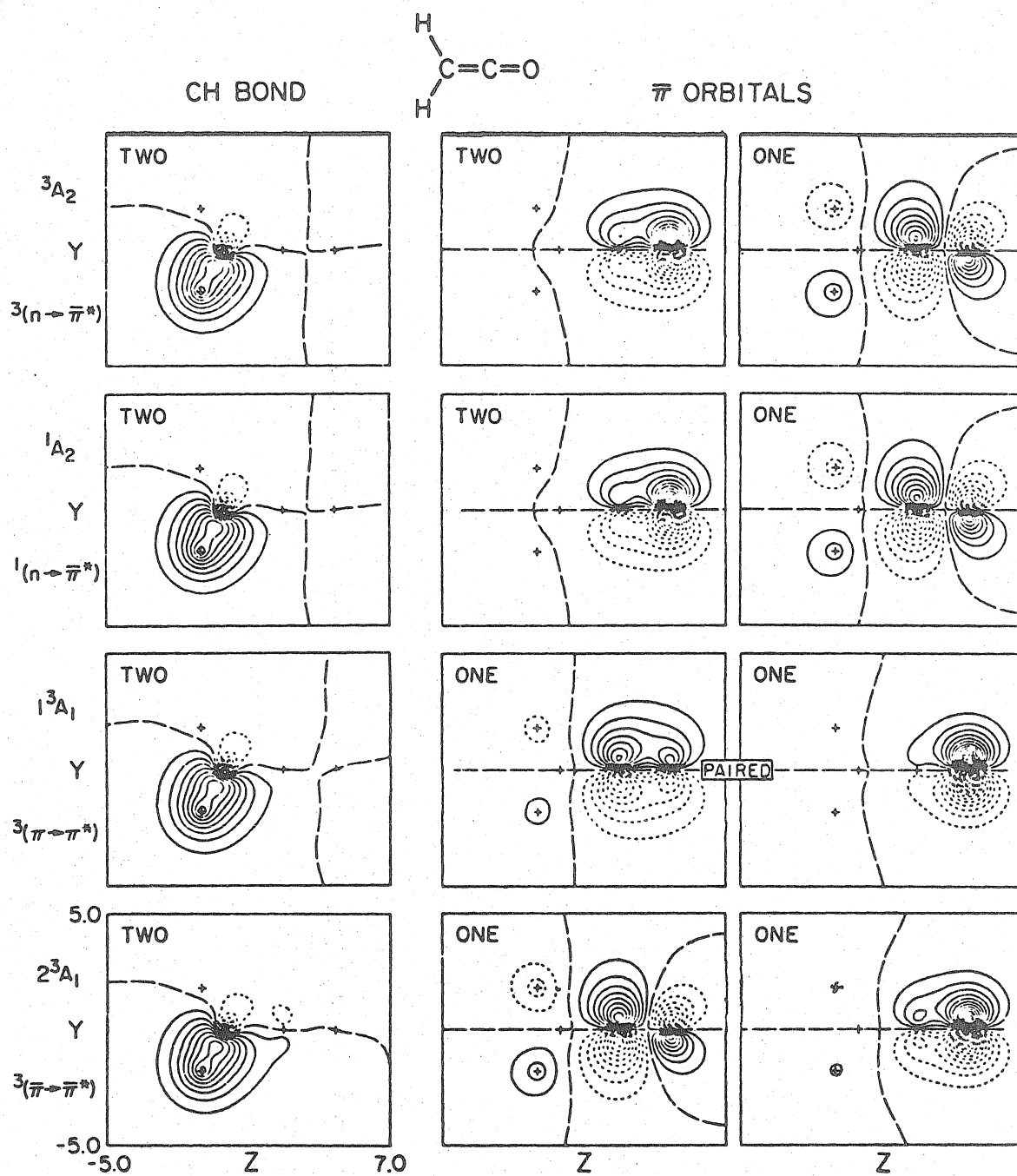


Figure 2



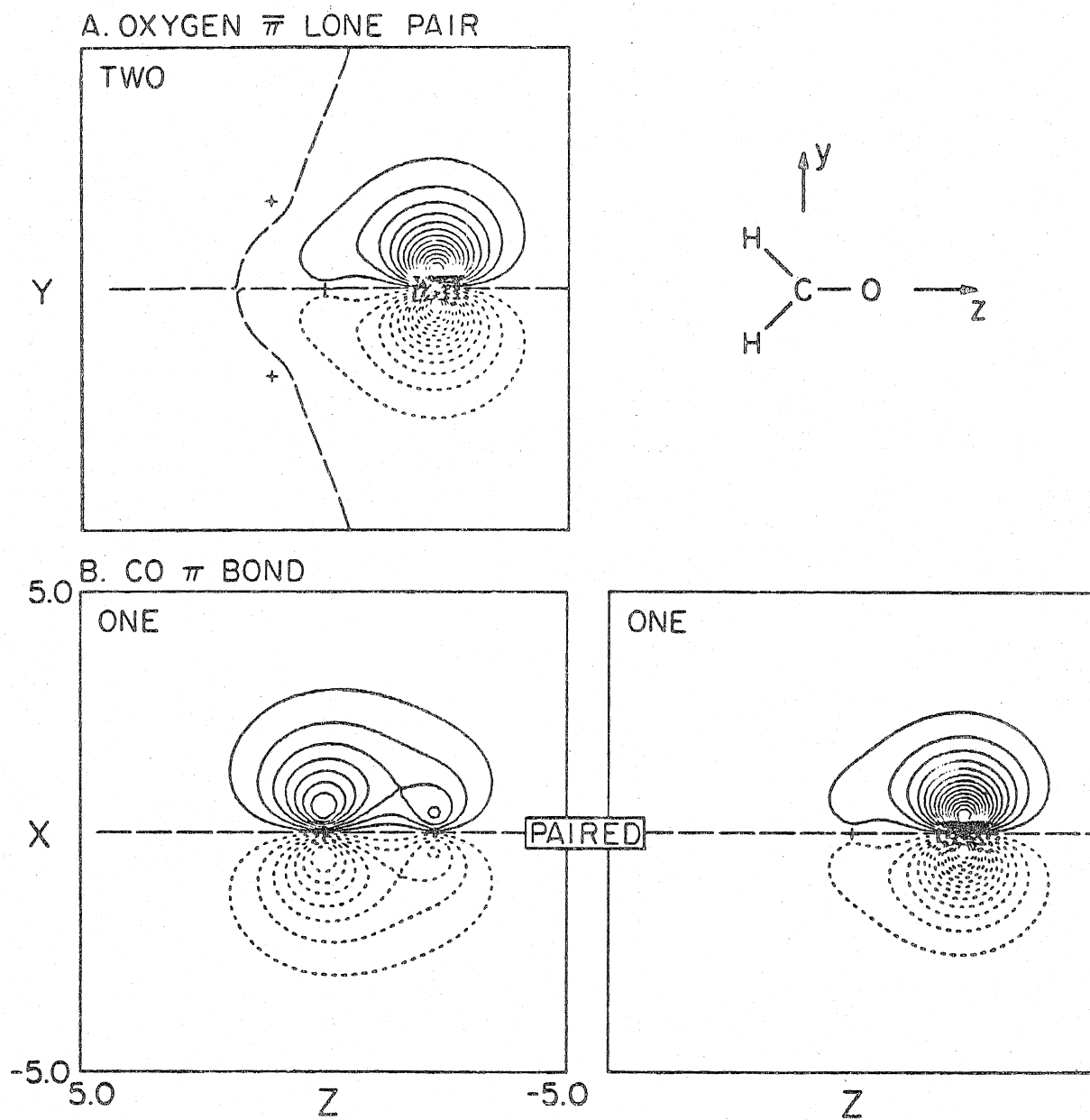
GROUND STATE  $\pi$  AND  $\bar{\pi}$  ORBITALS OF  $\text{CH}_2\text{O}$ 

Figure 4

**PART E: AB INITIO THEORETICAL STUDIES  
OF THE RYDBERG STATES OF FORMALDEHYDE**

## I. Introduction

The electronic states of simple organic molecules can be categorized according to size as either valence or Rydberg. In a previous paper<sup>2</sup> we reported the results of ab initio generalized valence bond (GVB) calculations on the valence states of formaldehyde,  $^3,^1(n \rightarrow \pi^*)$  and  $^3(\pi \rightarrow \pi^*)$ . It is the purpose of this paper to extend this treatment to the Rydberg states.

The Rydberg states of formaldehyde have been the subject of numerous recent experimental<sup>3-9</sup> and theoretical<sup>9-15</sup> investigations. Experimentally, dipole-allowed  $n \rightarrow s$ ,  $n \rightarrow p$ , and  $n \rightarrow d$  Rydberg series have been assigned in both the optical and electron impact spectra. However, there has been no conclusive assignment of a Rydberg state resulting from excitation out of the  $\pi$  orbital (we denote such states as  $\pi$ -Rydberg) in either the optical or electron impact spectra. In fact, no peaks are found in the photoabsorption spectrum of formaldehyde in the 10.5 - 13 eV region where the  $n = 3$  members of the  $\pi$ -Rydberg series are expected. Although poorly resolved peaks are found in this region of the electron impact spectrum, they have not yet been assigned.

Previous theoretical studies of the formaldehyde Rydberg states have been limited either by the number of states considered or the accuracy of the computational method used. Calculations using correlated wavefunctions have been reported<sup>10, 11, 14</sup> on the  $n \rightarrow 3s$ ,  $n \rightarrow 3p$ ,  $\pi \rightarrow 3s$ , and  $\pi \rightarrow 3p_z$  states. In addition, single configuration calculations<sup>9</sup> have been reported on some of the  $n \rightarrow 3d$  and  $\pi \rightarrow 3d$  states. In this paper we report the results of extensive ab initio calculations on all the  $n = 3$  Rydberg states associated with the first two ionization potentials of formaldehyde.

The details of the calculational method are discussed in Sec. II, the results are presented and discussed in Sec. III, and a detailed discussion of the  $^1(\pi \rightarrow \pi^*)$  state is contained in Sec. IV.

## II. Computational Details

A. Basis Sets and Geometry. The double zeta (DZ) basis set of Huzi-naga<sup>16</sup> and Dunning<sup>17</sup> augmented with a set of d basis functions ( $\zeta_c = 0.6769$ ,  $\zeta_o = 0.8853$ ) was used for the ground and ion state calculations. For calculations on Rydberg states, this basis was augmented with two sets each of diffuse s ( $\zeta_c = 0.023$ ,  $\zeta_o = 0.032$ ), p ( $\zeta_c = 0.021$ ,  $\zeta_o = 0.028$ ), and d ( $\zeta_c = \zeta_o = 0.015$ ) primitive gaussians. The exponents of the diffuse functions are those of Dunning,<sup>18</sup> optimized for atomic Rydberg calculations. In addition, to test the completeness of our diffuse d basis, a second set of calculations was carried out on some states using the same diffuse s and p functions but with two sets of diffuse d functions, the exponents and contraction coefficients of which are shown in Table I.

The experimental ground state geometry,<sup>19</sup>  $R_{CO} = 1.2099 \text{ \AA}$ ,  $R_{CH} = 1.1199 \text{ \AA}$ ,  $\angle HCH = 118^\circ$ , was used for all calculations

B. Computational Method. The perfect-pairing GVB method<sup>20</sup> has been described in detail elsewhere. Briefly we define our notation as follows: a GVB(p/q/PP) closed-shell singlet wavefunction can be written

$$\mathcal{A} \left\{ \left[ \prod_{i=1}^k \phi_i^2 \right] \left[ \prod_{i=1}^p (\lambda_{ai} \phi_{ai}^2 - \lambda_{bi} \phi_{bi}^2 - \lambda_{ci} \phi_{ci}^2 \dots) \right] \alpha \beta \alpha \beta \dots \alpha \beta \right\}, \quad (1)$$

where q is defined to be the total number of orbitals involved in the second product (i.e., all orbitals with occupancy,  $2\lambda^2$ , less than two). Similarly, the corresponding GVB(p/q/PP) open-shell singlet or triplet wavefunction can be written, as in (2),

$$\mathcal{A} \left\{ \left[ \prod_{i=1}^k \phi_i^2 \right] \left[ \prod_{i=1}^{p-2} (\lambda_{ai} \phi_{ai}^2 - \lambda_{bi} \phi_{bi}^2 \dots) \right] (\phi_{p-1} \phi_p \pm \phi_p \phi_{p-1}) \alpha \beta \dots \alpha \beta \mp \beta \alpha \right\}. \quad (2)$$

Under the perfect-pairing restriction, all of the orbitals are taken to be orthogonal

and the spin function is taken as indicated. Thus the GVB wavefunctions consist of a core of electron pairs described with doubly-occupied orbitals together with a set of correlated pairs each described by a dominant or bonding natural orbital (NO) and a variable number of correlating NO's. All orbitals and occupation numbers,  $\lambda$ , are solved for self-consistently.<sup>21</sup>

It has been found that the GVB orbitals form an effective basis for relatively small configuration interaction (CI) calculations which both relax the perfect-pairing restriction and include important correlation effects neglected in the GVB wavefunctions.

Consider now formaldehyde as an example to elucidate further the nature of GVB wavefunctions. It was found previously<sup>2</sup> that for the purpose of calculating valence excitation energies very small CI calculations using the GVB(2/4) orbitals (correlating only the CO  $\sigma$  and  $\pi$  pairs with one correlating NO/pair) are sufficient. Calculations of this accuracy lead to  $n-\pi^*$  and  $^3(\pi-\pi^*)$  excitation energies within 0.1 eV of the experimental values. Unfortunately, calculations at the GVB(2/4)-CI level of accuracy lead to ionization potentials that are 0.7 to 1.0 eV below the experimental results.<sup>22</sup> Since Rydberg states involve excitations to orbitals which are large with respect to the molecule, it is expected that calculational methods which yield inaccurate ionization potentials will yield equally inaccurate Rydberg excitation energies.

The error is basically due to a differential correlation effect; that is, the neglected correlation energy of the ground state is greater than the neglected correlation energy of the Rydberg or ion states and hence the calculated excitation energies are too low. In order to correct this error it is necessary either to correct empirically the uncorrelated energies or to use a more accurate wavefunction in which the important differential correlation effects are included. We have chosen the latter option.

The calculations reported here are based on GVB(5/14/PP) wavefunctions. Taking the ground state as an example, the GVB(5/14/PP) wavefunction can be written,

$$\mathcal{A} \{ \phi_{1s_O}^2 \phi_{2s_C}^2 \phi_{2s_O}^2 (\lambda_1 \phi_{CH_\ell}^2 - \lambda_2 \phi_{CH_\ell}^{2*}) (\lambda_1 \phi_{CH_r}^2 - \lambda_2 \phi_{CH_r}^{2*}) (\lambda_3 \phi_N^2 - \lambda_4 \phi_N^{2*}) \\ \times (\lambda_5 \phi_{CO\sigma}^2 - \lambda_6 \phi_{1\sigma^*}^2 - \lambda_7 \phi_{2\sigma^*}^2 - \lambda_8 \phi_{3\sigma^*}^2) (\lambda_9 \phi_\pi^2 - \lambda_{10} \phi_{1\pi^*}^2 - \lambda_{11} \phi_{2\pi^*}^2 - \lambda_{12} \phi_{3\pi^*}^2) \\ \times \alpha\beta\alpha\beta \dots \alpha\beta \} ,$$

where we have labeled the self-consistent orbitals as to their qualitative nature. We see then that in the GVB(5/14/PP) wavefunction the CO  $\sigma$  and  $\pi$  bonds are each correlated with the three natural orbitals (the  $\sigma$  pair with two  $a_1$  orbitals and one  $b_2$  and the  $\pi$  pair with two  $b_1$ 's and one  $a_2$ ). In addition, the CH bonds and  $p_y$  lone pair are each correlated with one NO.

Similar calculations were carried out for the  ${}^2B_2$  ( $n \rightarrow \infty$ ) and  ${}^2B_1$  ( $\pi \rightarrow \infty$ ) ion states and for the  ${}^1B_1$  ( $n \rightarrow 3d_{xy}$ ) and  ${}^1B_2$  ( $\pi \rightarrow 3d_{xy}$ ) Rydberg states. The remaining Rydberg states were solved for using the Improved Virtual Orbital (IVO) method<sup>23, 24</sup> with the self-consistent valence core orbitals from either the  ${}^1(n \rightarrow 3d_{xy})$  or the  ${}^1(\pi \rightarrow 3d_{xy})$  states.

Two sets of CI calculations<sup>25</sup> were carried out, one to describe states resulting from excitations out of the  $n$  orbital and the other to describe excitations out of the  $\pi$  orbital. The CI basis in each case consisted of the appropriate set of GVB(5/14/PP) orbitals plus the lowest nine IVO Rydberg orbitals from the appropriate IVO calculation.<sup>28</sup>

In describing the configurations included in the CI calculations, it is convenient to define a set of active and inactive orbitals (see Table II). For the Rydberg states the active orbitals are defined to be those orbitals involved in the excitation. Thus, for example, the active orbitals in the ( $n \rightarrow a_1$  Rydberg)



calculations are the  $n$  orbital and the  $a_1$  Rydberg orbitals. Similarly, in the ion states the active set consists of the one singly-occupied orbital. These definitions require two ground state calculations, one in which the active set is the  $n$  orbital (for comparison with  $n - \text{Rydberg}$  and  $n - \infty$  states) and a second calculation in which the active set is the  $\pi$  orbital. In all cases the inactive set of orbitals is defined to be the remaining dominant NO's with the exception of the C1s and O1s orbitals which are not included in the CI calculations.

The CI calculations include all configurations resulting from at most a single excitation out of the inactive set together with up to a double excitation out of the active set (i.e., up to an overall triple excitation). The only other restrictions placed on the excitations are: (1) no excitations between the  $\sigma$  and  $\pi$  spaces are allowed and (2) all configurations are restricted to have at most one electron in the Rydberg orbitals.

It has been found that this method of generating configurations includes the most important intrapair and interpair differential correlation effects necessary to describe particular ionizations or Rydberg excitations. It should be noted that this method neglects many important correlation effects involving the orbitals in the inactive set, but it is argued that correlations involving these orbitals will not lead to a significant differential effect. The basic assumption then, is that in order to calculate, for example, the  $n$  ionization potential it is only necessary to include those correlations directly involving the  $n$  orbital.

### III. Results

A. Rydberg Orbitals. The Rydberg orbitals resulting from the IVO calculations are shown in Figs. 1-3. Generally the orbitals are found, as expected, to resemble closely hydrogenic,  $n = 3$ , atomic orbitals.

Considering first the  $n$ -Rydberg states, Figure 1, we find most of the Rydberg orbitals to be centered approximately at the center of charge of the  ${}^2B_2$  ion (in the  $CH_2$  region 0.016 Å from the carbon).<sup>29</sup> Deviations from this are more pronounced in the higher 3d states, in particular the  $3d_{z^2-x^2}$  which is apparently centered in the CO region (see Section D).

The orbital sizes, as indicated by  $\langle r^2 \rangle$  in Table III, are found to be highly dependent on the character, i.e., s, p, or d, of the orbital. For example, we find  $\langle 3s | r^2 | 3s \rangle = 44 a_0^2$ ,  $\langle 3p | r^2 | 3p \rangle = 62 \pm 1 a_0^2$ , and  $\langle 3d | r^2 | 3d \rangle = 115 \pm 2 a_0^2$ , whereas, for comparison, the  $n = 3$  hydrogenic orbitals all lead to  $\langle r^2 \rangle = 126 a_0^2$ . Thus, as expected intuitively, the lower angular momentum Rydberg orbitals incorporate a greater degree of valence character than the higher angular momentum orbitals (for the same  $n$ ).

The  $\pi$ -Rydberg IVO's shown in Figure 2 are found to resemble closely those of the  $n$ -Rydberg states (the center of charge of the  $\pi$  ion core is in the  $CH_2$  region 0.12 Å from the carbon). The largest difference occurs in the  $3d_{y^2}$  orbital which has less density in the  $z$  direction than the  $n$ -Rydberg orbital.

Of particular interest among the  $\pi$ -Rydberg states are the  ${}^1A_1$  states corresponding to  ${}^1(\pi - 2\pi)$  and  ${}^1(\pi - 3\pi)$ . From Figure 3 we find the corresponding triplet states to consist of a valence  ${}^3(\pi - \pi^*)$  state and Rydberg  ${}^3(\pi - 3p_x)$  and  ${}^3(\pi - 3d_{xz})$  states in which the Rydberg orbitals closely resemble the corresponding  $n - \pi$  Rydberg states. The singlet states, however, are found from IVO calculations to be very different, due to an apparent mixing of valence  $(\pi - \pi^*)$  character with Rydberg  $(\pi - 3p_x)$  character. The  ${}^1(\pi - \pi^*)$  state will be discussed in more detail in Section IV.

B. Excitation Energies. The calculated excitation energies are listed in Tables IV and V together with the results of the theoretical calculations and experiments. The GVB-CI  $n \rightarrow$  Rydberg excitation energies (Table IV) are found to be within  $\sim 0.1$  eV of the experimental energies in those cases where accurate experimental numbers are available. Experimental results for the  $\pi \rightarrow$  Rydberg states are inconclusive due to a lack of resolution in the 10-13 eV range. However, broad peaks in the electron impact spectrum centered at 10.6, 11.7, and 12.8 eV correspond very closely to the calculated  $\pi \rightarrow 3s$ ,  $\pi \rightarrow 3p$ , and  $\pi \rightarrow 3d$  regions at 10.7, 11.8, and 12.8 eV, respectively. The lack of resolution in the spectrum and the small separation of individual 3p and 3d states makes assignments of particular transitions impossible.

The only accurate experimental excitation energies for  $\pi$ -Rydberg states are recent photoionization results<sup>30</sup> in which preionized states are observed at 11.46 and 12.48 eV. The first state has been assigned as  $^1(\pi \rightarrow 3p_z)$ , in good agreement with the GVB-CI result (11.66 eV). The second state was assigned as  $^1(\pi \rightarrow 4s)$ , although the GVB-CI results indicate it may be a  $^1(\pi \rightarrow 3d)$  state (Table V).

Also of interest is a direct test of the reliability of the Improved Virtual Orbital method. IVO calculations rely on the assumption that the valence core of a given Rydberg state is not greatly affected by the precise nature of the diffuse orbital. In addition, IVO calculations assume the correlation energies of the Rydberg states are all approximately equal to those of the corresponding ion states. The results in Tables IV and V indicate that IVO excitation energies are generally 0.3 to 0.4 eV above the more accurate GVB-CI results. We do find the error in the IVO excitations to be fairly constant with the exception of the  $^1(\pi \rightarrow \pi^*)$  state, and hence accurate predictions ( $\pm 0.1$  eV) based on corrected IVO excitation energies are possible.

C. Oscillator Strengths. The oscillator strengths calculated from GVB-CI wavefunctions are in poor agreement with experimental results (Table VI). The GVB-CI  $^1(n-3s)$  oscillator strength is approximately a factor of four too small. Similar errors are found in all the allowed  $^1(n-3d)$  transitions.

The GVB-CI  $^1(n-3p)$  oscillator strengths, however, are in good agreement with experiment, the calculated results being  $\sim 20\%$  below the experimental results. The  $(n-3p_y)$  absorption is calculated to be approximately twice as intense as the  $(n-3p_z)$ . This ordering is in agreement with the results of the equations of motion calculations although those calculations led to a considerably smaller difference. These results contradict the reported assignment<sup>8,9</sup> of the  $(n-3p)$  states in which the more intense absorption is assumed to be the  $^1(n-3p_z)$  state.

In order to test possible insufficiency of the diffuse d basis, a second set of calculations was carried out employing a more flexible d basis (see Section II). These calculations resulted in no significant improvement in the accuracy of the oscillator strength results (Table VI).

D. Dipole Moments. The GVB-CI dipole moments of the Rydberg states of formaldehyde are listed in Table VII. There are no experimental results for comparison; however, GVB-CI dipole moments for the ground and valence excited states were found to be in excellent agreement with experiment.<sup>2</sup>

Assuming the valence core of each Rydberg series to be independent of the particular Rydberg state, the variations in the dipole moments of these states can be interpreted as shifts in the center of charge of the Rydberg orbitals. In addition, if the Rydberg orbital were centered (symmetrically)

at the center of charge of the valence core, the net dipole moment would be zero. Therefore, deviations from zero may be interpreted as shifts of the Rydberg orbitals relative to the core center of charge.

Considering first the  $n$ -Rydberg states we find the lowest energy orbitals of  $a_1$  and  $b_2$  symmetry,  $3s$  and  $3p_y$ , respectively, are shifted toward the hydrogen while the higher orbitals of these symmetries are shifted toward the oxygen. All of the Rydberg orbitals of  $b_1$  and  $a_2$  symmetry, however, are shifted slightly toward the oxygen.

A similar effect is found in the  $a_1$  and  $b_2$   $\pi$ -Rydberg orbitals with the exception of the  $3d_{x^2}$  which is found to be shifted in the same direction as the  $3s$  (toward the hydrogens). The  $b_1$  and  $a_2$   $\pi$ -Rydberg orbitals are found to be shifted to a much greater extent than the corresponding  $n$ -Rydberg orbitals. This is probably due to larger exchange interactions with the singly-occupied core orbital ( $\pi$  in this case).

The observed shifts in the sigma Rydberg orbitals can be explained by considering the polarity of the CH bonds. Mullikan population analysis leads to net core charges on each hydrogen of 0.33 ( ${}^2B_2$ ) and +0.29 ( ${}^2B_1$ ). Thus the lowest Rydberg orbital of each sigma symmetry is stabilized by a shift toward the hydrogen while the higher orbitals, due to orthogonality constraints, are shifted in the opposite direction.

#### IV. Discussion

There has been some controversy in the literature concerning the character and location of the  $^1(\pi \rightarrow \pi^*)$  state of formaldehyde and other simple  $\pi$ -bonded molecules. In light of this we include here a brief summary of the results of previous calculations on this state of formaldehyde, an analysis of the results of the GVB-CI calculations, and a discussion of the discrepancies between the GVB-CI results and those of other calculations.

The earliest calculations on the  $^1(\pi \rightarrow \pi^*)$  state of  $\text{CH}_2\text{O}$  were semi-empirical, PPP calculations.<sup>31</sup> These calculations assumed the state to be valence and predicted an excitation energy of 7.4 eV. Buenker and Peyerimhoff,<sup>32</sup> in an ab initio CI calculation without diffuse basis functions found the  $^1(\pi \rightarrow \pi^*)$  state to be 11.71 eV above the ground state. Later they<sup>10</sup> and Whitten and Hackmeyer<sup>11</sup> reported that addition of diffuse functions to the basis set leads to a Rydberg-like  $^1(\pi \rightarrow \pi^*)$  state with an excitation energy of 11.3 to 11.4 eV. In more extensive calculations including  $\sigma$ - $\pi$  correlations and d polarization functions, Whitten<sup>13</sup> concluded the state to be valence-like with an excitation energy of 9.9 eV. More recently, Yeager and McKoy<sup>14</sup> have reported equations of motion calculations that lead to a semi-Rydberg  $^1(\pi \rightarrow \pi^*)$  state located at 10.31 eV. Finally, Langhoff et al.<sup>15</sup> have studied the  $^1(\pi \rightarrow \pi^*)$  state with MC-SCF and CI wavefunctions. They conclude the state to be valence in character with an excitation energy of 11.2 eV.

Our single configuration IVO calculations lead to a fairly diffuse state with  $\langle \pi^* | r^2 | \pi^* \rangle$  being approximately five times that of the triplet  $\pi^*$ , Table III. Considering the overlaps of the singlet and triplet IVO orbitals, Table VIII, we find the single configuration  $^1(\pi \rightarrow \pi^*)$  state to be approximately 66% valence in character and 34% Rydberg. This is a slight overestimate of the valence character of the singlet IVO since the IVO triplet  $\pi^*$  orbital is more diffuse

than the self-consistent orbital (the IVO approximation is not as accurate for valence states). Using the self-consistent triplet orbital leads to the conclusion of 50% valence character in the  $^1(\pi - \pi^*)$  state.

In the CI calculations the  $^1(\pi - \pi^*)$  state is found to contract considerably leading to an effective  $\langle \pi^* | r^2 | \pi^* \rangle^{33}$  less than half that of the IVO result. This contraction results from a CI mixing of the single configuration  $^1(1\pi - 2\pi)$  state with the  $^1(1\pi - 3\pi)$  state. The net effect is a decrease in  $\langle 2\pi | x^2 | 2\pi \rangle$  from an IVO value of  $18.55 a_0$  to an effective CI value of  $8.34 a_0$  with a corresponding increase in  $\langle 3\pi | x^2 | 3\pi \rangle$  from  $28.45 a_0$  to  $40.16 a_0$ . In comparison a purely valence  $\pi^*$  orbital would have an  $\langle x^2 \rangle$  of  $3.1 a_0^2$  whereas a purely Rydberg  $\pi^*$  orbital would have an  $\langle x^2 \rangle$  of  $48.6 a_0^2$  (see Table III). Thus we conclude that the  $^1(\pi - \pi^*)$  state of formaldehyde is essentially ( $\sim 90\%$ ) valence in character.

The GVB-CI  $^1(\pi - \pi^*)$  excitation energy, 10.77 eV, is much lower than expected for either a Rydberg  $3p_x$  state ( $\sim 11.8$  eV) or a purely valence state analogous to the  $^3(\pi - \pi^*)$  state [ $E(\text{triplet}) + 2K_{\pi\pi^*} = 12.5$  eV]. It is also noted that the single configuration IVO treatment of this state is clearly anomalous. For all the pure  $\pi$ -Rydberg states the IVO excitation energy is consistently 0.2 to 0.3 eV above the GVB-CI result. However, the IVO  $^1(\pi - \pi^*)$  excitation energy is 0.53 eV above the CI energy. This is consistent with the conclusion of a large CI mixing of the  $^1(1\pi - 2\pi)$  and  $^1(1\pi - 3\pi)$  IVO states.

Experimental evidence concerning the location of the  $^1(\pi - \pi^*)$  state is inconclusive. Recent electron impact spectra<sup>5,6</sup> show a broad peak from 10.4 to 11.0 eV with a maximum at  $\sim 10.7$  eV. The vibrational progression in this peak, although poorly resolved, is consistent with a C-O stretching frequency of approximately  $1130 \text{ cm}^{-1}$  (the stretching frequency of the  $^2B_1$  ion is reported<sup>34</sup> to be  $1210 \text{ cm}^{-1}$ ). Thus these results are consistent with a  $^1(\pi - \pi^*)$  state located at  $\sim 10.7$  eV. This assignment is complicated by the GVB-CI prediction of a second, more weakly absorbing state,  $^1(\pi - 3s)$ , in this region.

Whitten<sup>13</sup> has argued that d-polarization functions and  $\sigma$  correlation are necessary for an accurate description of the  $^1(\pi - \pi^*)$  state. The calculations

reported here include both of these effects and yet lead to results that differ significantly from those of Whitten. Whitten's conclusions are based primarily on two CI calculations. In the first CI calculation only configurations of the form (a)-(d),

	$\sigma_k$	$\sigma_k^*$	$\pi$	$\pi^*$
a)	2	0	2	0
b)	2	0	0	2
c)	1	1	2	0
d)	1	1	0	2
e)	1	1	1	1

were included. In the calculations reported here in which all configurations resulting from single sigma excitations with any order  $\pi$  excitation were included. It was found that configurations of the form (e), representing  $\sigma$ - $\pi$  interpair correlation effects, are very important in the ground state wavefunction. These configurations account for approximately 1.1 eV of the CI energy lowering. Therefore calculations in which these configurations are excluded are expected to lead to erroneously low excitation energies. In the second of Whitten's CI calculations the  $\sigma^*$  orbitals were chosen primarily to describe readjustments resulting from a highly polarized  $\pi$  system, one with either a doubly-occupied oxygen p orbital or a doubly-occupied carbon p orbital. It is certainly the case that this choice strongly favors the  $^1(\pi - \pi^*)$  state over the ground state and hence this calculation should also lead to an anomalously low excitation energy.

A second point that has been discussed at length in the literature is the possibility of mixing occurring between the  $^1(\pi - \pi^*)$  state and the lower-lying ( $n - p_y$ ) and ( $n - d_{yz}$ ) states of the same symmetry. The only reported calculations on the extent of this mixing are those of Mentall *et al.*<sup>9</sup> These



calculations assume the  $^1(\pi - \pi^*)$  state to be purely valence in character and hence are expected to overestimate greatly the amount of mixing. In our calculations the  $^1(\pi - \pi^*)$  state is not allowed to interact with the Rydberg  $^1(n - 3p_y)$  or  $^1(n - 3d_{yz})$  states. However, the  $^1(\pi - \pi^*)$  state is allowed to interact with a valence  $^1(n - 2p_y^*)$  "state" and, in fact, the resulting wavefunction is found to have  $\sim 1\%$   $(n - 2p_y^*)$  character. We, however, interpret this CI effect as an  $n - \pi$  interpair correlation.

Table I. Exponents and Contraction Coefficients for Diffuse d Functions.

The first three of each type are contracted together with the coefficients given.

Carbon		Oxygen	
Exponents	Coefficients	Exponent	Coefficient
0.2556	0.02175	0.2951	0.03061
0.0752	0.10896	0.0984	0.1437
0.0250	0.92616	0.0328	0.8987
0.0083	1.000	0.0109	1.000

Table II. Summary of CI Calculations.

States	Sym- metry	Valence Dominant NO's			Rydberg Orbitals				Number of Spin Eigenfunctions	
		$\sigma$ core	n	$\pi$	$a_1$	$a_2$	$b_1$	$b_2$	Singlet	Triplet
G.S. (n)	$A_1$	N	A	N					447	
$n - a_1$	$B_2$	N	A	N	A				801	1125
$n - a_2$	$B_1$	N	A	N		A			378	546
$n - b_1$	$A_2$	N	A	N			A		725	1040
$n - b_2$	$A_1$	N	A	N				A	560	768
$n - \infty$	$B_2$	N	A	N					140	
G.S. ( $\pi$ )	$A_1$	N	N	A					434	
$\pi - a_1$	$B_1$	N	N	A	A				864	1251
$\pi - a_2$	$B_2$	N	N	A		A			310	460
$\pi - b_1$	$A_1$	N	N	A			A		680	699
$\pi - b_2$	$A_2$	N	N	A				A	654	936
$\pi - \infty$	$B_1$	N	N	A					123	

A - Active Set

N - Inactive Set

(blank) - not included in calculation

Table III. Orbital  $x^2$ ,  $y^2$ ,  $z^2$  Expectation Values. Singlet states unless noted otherwise.

	n - Rydberg States			$\pi$ - Rydberg States <sup>a</sup>		
	$x^2$	$y^2$	$z^2$	$x^2$	$y^2$	$z^2$
3s	14.09	16.83	13.45	14.04	15.80	13.27
3p <sub>x</sub>	36.18	12.06	14.18	35.98 <sup>a</sup>	11.99 <sup>a</sup>	13.26 <sup>a</sup>
3p <sub>y</sub>	11.98	36.01	12.90	11.97	36.01	12.84
3p <sub>z</sub>	13.42	13.82	35.57	14.78	14.18	34.82
3d <sub>y<sup>2</sup></sub>	37.32	24.49	51.62	47.47	24.95	37.94
3d <sub>z<sup>2</sup>-x<sup>2</sup></sub>	39.94	29.76	47.18	28.29	30.38	61.11
3d <sub>xy</sub>	49.99	49.99	16.55	49.99	49.99	16.43
3d <sub>xz</sub>	48.61	16.20	48.32	47.73 <sup>a</sup>	15.91 <sup>a</sup>	47.23 <sup>a</sup>
3d <sub>yz</sub>	16.42	49.27	49.00	16.29	48.89	48.00
2 $\pi$				18.55	6.18	6.64
3 $\pi$				28.45	9.48	17.69
$\pi^*$				3.12 <sup>a</sup>	1.04 <sup>a</sup>	2.05 <sup>a</sup>

<sup>a</sup> These  $\pi^*$ , 3p<sub>x</sub>, and 3d<sub>xz</sub> orbitals are from transitions out of the  $\pi$  orbital with triplet pairing. (The 2 $\pi$  and 3 $\pi$  orbitals show the results for singlet pairing.)

Table IV. Vertical Excitation Energies (eV) for CH<sub>2</sub>O: n<sup>1</sup> States.

Character	State	Experimental		Present Work		Other Theoretical Work			
		optical <sup>a</sup>	e-impact <sup>b</sup>	GVB-CI <sup>c</sup>	IVO <sup>d</sup>	HF <sup>e</sup>	HF-CI <sup>e</sup>	RPA <sup>f</sup>	EOM <sup>g</sup>
n - $\pi^*$	<sup>3</sup> A <sub>2</sub>		3.5	3.68		2.25	3.41	2.13	3.46
	<sup>1</sup> A <sub>2</sub>		4.1	4.09	5.51	2.62	3.81	3.47	4.04
n - 3s	<sup>3</sup> B <sub>2</sub>		7.09	7.08		6.03	7.32		
	<sup>1</sup> B <sub>2</sub>	7.091	7.13	7.16	7.56	6.07	7.38		7.28
n - 3p <sub>z</sub>	<sup>3</sup> B <sub>2</sub>		7.92	7.99			8.29		
	<sup>1</sup> B <sub>1</sub>	7.97	8.00	8.08	8.40		8.39		8.12
n - 3p <sub>y</sub>	<sup>3</sup> A <sub>1</sub>		8.11	8.05		6.93	8.09		
	<sup>1</sup> A <sub>1</sub>	8.14	8.15	8.09	8.42		8.11		8.15
n - 3p <sub>x</sub>	<sup>3</sup> A <sub>2</sub>		(8.31)	8.31			9.06		
	<sup>1</sup> A <sub>2</sub>			8.32	8.71		9.07		8.35
n - 3d <sub>yz</sub>	<sup>3</sup> B <sub>2</sub>			9.01					
	<sup>1</sup> B <sub>2</sub>	8.88	8.92	9.05	9.35				
n - 3d <sub>z<sup>2</sup>-x<sup>2</sup></sub>	<sup>3</sup> B <sub>2</sub>			9.16					
	<sup>1</sup> B <sub>2</sub>			9.17	9.45				
n - 3d <sub>xy</sub>	<sup>3</sup> B <sub>1</sub>			9.21					
	<sup>1</sup> B <sub>1</sub>			9.21	9.47				
n - 3d <sub>xz</sub>	<sup>3</sup> A <sub>2</sub>			9.23					
	<sup>1</sup> A <sub>2</sub>			9.24	9.53				
n - 3d <sub>yz</sub>	<sup>3</sup> A <sub>1</sub>			9.17					
	<sup>1</sup> A <sub>1</sub>	9.03	9.07	9.23	9.50				
n - $\infty$	<sup>2</sup> B <sub>2</sub>	10.87	10.87	10.55		9.47			

<sup>a</sup> Reference 9.<sup>b</sup> Our assignment of unpublished spectra by A. Chutjian.<sup>c</sup> Ground state E = -113.95686.<sup>d</sup> Experimental ionization potential minus IVO orbital eigenvalue.<sup>e</sup> Reference 10.<sup>f</sup> T. H. Dunning, Jr., and V. McKoy, *J. Chem. Phys.*, **48**, 5263 (1968).<sup>g</sup> Reference 14.

Table V. Vertical Excitation Energies (eV) for CH<sub>2</sub>O:  $\pi^1$  States.

Character	State	Experimental	Present Work		Other Theoretical Work			
		e-impact <sup>a</sup>	GVB-CI <sup>b</sup>	IVO <sup>c</sup>	HF <sup>d</sup>	HF-CI <sup>d</sup>	RPA <sup>e</sup>	EOM <sup>f</sup>
$\pi \rightarrow \pi^*$	$^3A_1$	6.0	5.95 <sup>g</sup>	7.56	4.17	5.56		5.29
	$^1A_1$	10.7	10.77	11.30		11.41	11.22	10.30
$\pi \rightarrow 3s$	$^3B_1$		10.68					
	$^1B_1$	10.7	10.73	11.02				11.2
$\pi \rightarrow 3p_z$	$^3B_1$		11.57					
	$^1B_1$	11.6-11.9	11.66	11.96				12.2
$\pi \rightarrow 3p_y$	$^3A_2$		11.63					
	$^1A_2$		11.78	11.93				
$\pi \rightarrow 3p_x$	$^3A_1$		11.77	12.08				
	$^1A_1$	11.6-11.9	12.00	12.58				
$\pi \rightarrow 3d_{y^2}$	$^3B_1$		12.57					
	$^1B_1$	12.5-12.8	12.58	12.86				
$\pi \rightarrow 3d_{z^2-x^2}$	$^3B_1$		12.68					
	$^1B_1$	12.5-12.8	12.70	12.96				
$\pi \rightarrow 3d_{xy}$	$^3B_2$		12.75	12.98				
	$^1B_2$	12.5-12.8	12.75	12.98				
$\pi \rightarrow 3d_{xz}$	$^3A_1$		12.76	13.02				
	$^3A_2$		12.74					
$\pi \rightarrow 3d_{yz}$	$^1A_2$		12.88	13.02				
$\pi \rightarrow \infty$	$^2B_1$	14.4	14.14					

<sup>a</sup> Our assignment of unpublished spectra by A. Chutjian.<sup>b</sup> Ground state E = -113.98763.<sup>c</sup> Experimental ionization potential minus IVO orbital eigenvalue.<sup>d</sup> Reference 10.<sup>e</sup> T. H. Dunning, Jr., and V. McKoy, *J. Chem. Phys.*, **48**, 5263 (1968).<sup>f</sup> Reference 14.<sup>g</sup> This value is GVB-CI using GVB orbitals for the triplet state. Use of the IVO orbitals plus ground state GVB orbitals as in the rest of the states in this table leads to  $\Delta E = 8.08$  eV.

Table VI. Oscillator Strengths for CH<sub>2</sub>O.

State	$f_{\text{calc}}$ #1	$f_{\text{calc}}$ <sup>a</sup> #2	$f_{\text{obsd}}$ <sup>b</sup>
$n \rightarrow 3s$	0.006	0.007	0.038
$n \rightarrow 3p_z$	0.015	0.014	0.017
$n \rightarrow 3p_y$	0.030	0.031	0.038
$n \rightarrow 3d_{y^2}$	0.005	0.007	0.010
$n \rightarrow 3d_{z^2-x^2}$	0.0004	~0.0	--
$n \rightarrow 3d_{yz}$	0.0002	0.0005	0.012
$n \rightarrow 3d_{xy}$	0.0001	0.0002	--
$\pi \rightarrow 3s$	0.026	--	--
$\pi \rightarrow 1\pi^*$	0.256	0.255	--
$\pi \rightarrow 2\pi^*$	0.036		--
$\pi \rightarrow 3p_z$	0.026	--	--
$\pi \rightarrow 3d_{y^2}$	0.0001	--	--
$\pi \rightarrow 3d_{z^2-x^2}$	0.015	--	--
$\pi \rightarrow 3d_{xy}$		--	--

<sup>a</sup> The results of a more accurate calculation using two sets of diffuse d functions.

<sup>b</sup> Reference 9.

Table VII. GVB-CI Dipole Moments for CH<sub>2</sub>O (ground state geometry, GVB-CI).

Positive sign indicates electrons moved from O end to H end.

	a. u.	Debye
G.S.	-0.93 <sup>a</sup>	-2.36 <sup>a</sup>
<sup>3</sup> (n → π*)	-0.600 <sup>a</sup>	-1.52
<sup>1</sup> (n → π*)	-0.665 <sup>a</sup>	-1.69
<sup>1</sup> (n → 3s)	+1.207	3.068
<sup>1</sup> (n → 3p <sub>z</sub> )	-0.718	-1.825
<sup>1</sup> (n → 3p <sub>y</sub> )	+0.151	0.384
<sup>1</sup> (n → 3p <sub>x</sub> )	-0.149	-0.379
<sup>1</sup> (n → 3d <sub>y<sup>2</sup></sub> )	-1.172	-2.979
<sup>1</sup> (n → 3d <sub>z<sup>2</sup>-x<sup>2</sup></sub> )	-2.441	-6.204
<sup>1</sup> (n → 3d <sub>xy</sub> )	-0.014	-0.036
<sup>1</sup> (n → 3d <sub>xz</sub> )	-0.161	-0.409
<sup>1</sup> (n → 3d <sub>yz</sub> )	-0.433	-1.101
<sup>3</sup> (π → π*)	-0.523 <sup>a</sup>	-1.33
<sup>1</sup> (π → 3s)	1.175	2.986
<sup>1</sup> (π → π*)	-0.130	-0.330
<sup>1</sup> (π → 3p <sub>z</sub> )	-0.749	-1.904
<sup>1</sup> (π → 3p <sub>y</sub> )	0.264	+0.671
<sup>3</sup> (π → 3p <sub>x</sub> )	-0.259	-0.658
<sup>1</sup> (π → 3p <sub>x</sub> )	-2.350	-5.973
<sup>1</sup> (π → 3d <sub>y<sup>2</sup></sub> )	0.123	0.313
<sup>1</sup> (π → 3d <sub>z<sup>2</sup>-x<sup>2</sup></sub> )	-2.261	-5.747
<sup>1</sup> (π → 3d <sub>xy</sub> )	+0.075	0.191
<sup>3</sup> (π → 3d <sub>xz</sub> )	+0.455	1.156
<sup>1</sup> (π → 3d <sub>yz</sub> )	-0.104	-0.264

<sup>a</sup> From ref 2.



Table VIII. Overlaps of Singlet and Triplet ( $\pi \rightarrow \pi$ ) IVO Orbitals.

		Triplet State Orbitals			
		$2\pi$ ( $\pi^*$ )	$3\pi$ ( $3p_x$ )	$4\pi$ ( $3d_{xz}$ )	Other
Singlet State Orbitals	$2\pi$	0.812	0.534	-0.171	0.162
	$3\pi$	0.429	-0.808	-0.384	0.125
	$4\pi$	-0.319	0.240	-0.903	0.288
	Other	0.234	0.066	0.089	

### References

1. Partially supported by a grant (CHE74-05132) from the National Science Foundation.
2. L. B. Harding and W. A. Goddard III, J. Am. Chem. Soc., 97, 6293 (1975).
3. E. P. Gentieu and J. E. Mentall, Science, 169, 681 (1970).
4. A. Chutjian, J. Chem. Phys., 61, 4279 (1974).
5. A. Chutjian, unpublished results.
6. M. J. Weiss, C. E. Kuyatt, and S. Mielczanek, J. Chem. Phys., 54, 4147 (1971).
7. D. C. Moule and A. D. Walsh, Chem. Rev., 75, 67 (1975).
8. C. R. Lassard, D. C. Moule, and S. Bell, Chem. Phys. Lett., 29, 603 (1974).
9. J. E. Mentall, E. P. Gentieu, M. Krauss, and D. Neumann, J. Chem. Phys., 55, 5471 (1971).
10. S. D. Peyerimhoff, R. J. Buenker, W. E. Krammer, and H. Hsu, Chem. Phys. Lett., 8, 129 (1971).
11. J. L. Whitten and M. Hackmeyer, J. Chem. Phys., 51, 5584 (1969).
12. K. Tanaka, Int. J. Quant. Chem., 8, 981 (1974).
13. J. L. Whitten, J. Chem. Phys., 56, 5458 (1972).
14. D. L. Yeager and V. McKoy, J. Chem. Phys., 60, 2714 (1974).
15. S. R. Langhoff, S. T. Elbert, C. F. Jackels, and E. R. Davidson, Chem. Phys. Lett., 29, 247 (1974).
16. S. Huzinaga, J. Chem. Phys., 42, 1293 (1965).
17. T. H. Dunning, Jr., J. Chem. Phys., 53, 2823 (1970).
18. T. H. Dunning, Jr., unpublished results.

19. R. B. Lawrence and M. W. P. Strandberg, Phys. Rev., 83, 363 (1951).
20. W. J. Hunt, P. J. Hay, and W. A. Goddard III, J. Chem. Phys., 57, 738 (1972).
21. The GVB(/PP) calculations were carried out with the Bobrowicz-Wadt-Yaffe-Goddard program (GVBTWO) using the basic methods of ref 20.
22. L. B. Harding and W. A. Goddard III, unpublished results.
23. W. J. Hunt and W. A. Goddard III, Chem. Phys. Lett., 3, 414 (1969).
24. W. A. Goddard III and W. J. Hunt, Chem. Phys. Lett., 24, 464 (1974).
25. The CI calculations were carried out with the Caltech Spin Eigenfunction CI program (Bobrowicz, Winter, Ladner, Moss, Harding, and Goddard).<sup>26, 27</sup>
26. F. W. Bobrowicz, Ph. D. Thesis, California Institute of Technology, 1974.
27. R. C. Ladner, Ph.D. Thesis, California Institute of Technology, 1971.
28. For states involving, for example, excitation out of the  $\pi$  orbital,  $\pi$ -correlating orbitals were taken from the ground state calculation.
29. The reader may be surprised that the ion resulting from excitation out of the oxygen n orbital has a center of charge in the CH<sub>2</sub> region. However, as a result of the polarity of the ground state wavefunction, removal of an electron in the ground state 2b<sub>2</sub> orbital (with no orbital readjustments) leads to a center of charge 0.035 Å away from the carbon (towards the oxygen). Orbital readjustments (SCF) in the ion then account for the remaining shift of 0.051 Å further away from the oxygen.
30. P. M. Guyon, W. A. Chupka, and J. Berkowitz, J. Chem. Phys., 64, 1419 (1976).

31. T. Anno and A. Sado, J. Chem. Phys., 26, 1759 (1957).
32. R. J. Buenker and S. D. Peyerimhoff, J. Chem. Phys., 53, 1368 (1970).
33. We define the effective CI  $\langle \pi^* | r^2 | \pi^* \rangle$  to be  $\langle \psi_2 | r^2 | \psi_2 \rangle - \langle \psi_1 | r^2 | \psi_1 \rangle + \langle \pi | r^2 | \pi \rangle$  where  $\psi_2$  is the  $^1(\pi - \pi^*)$  CI wavefunction,  $\psi_1$  is the ground state CI wavefunction using the orbitals of the  $^1(\pi - \pi^*)$  CI calculation and  $\pi$  is the ground state  $\pi$  orbital.
34. D. W. Turner, "Molecular Photoelectron Spectroscopy," John Wiley and Sons, Ltd., New York, New York, 1970.

### Figure Captions

Figure 1. The Rydberg IVO's (singlet state) resulting from excitation out of the  $n$  orbital. The  $3d_{xy}$  is not shown. Long dashes indicate zero amplitude; the spacing between contours is 0.01 a.u. The same conventions are used in all plots. The molecule is in the  $yz$  plane.

Figure 2. The Rydberg IVO's resulting from excitation out of the  $\pi$  orbital. The  $3d_{xy}$  is not shown. The  $\pi^*$ ,  $3p_x$ , and  $3d_{xz}$  are taken from triplet state calculations (see Figure 3 for the singlet orbitals); the remainder are singlet state orbitals.

Figure 3. The valence and Rydberg IVO's resulting from  $\pi - \pi$  singlet and triplet excitations.

EXCITED STATE ORBITALS OF  $\text{H}_2\text{CO}$   
FROM EXCITATION OUT OF THE  $n$  ORBITAL

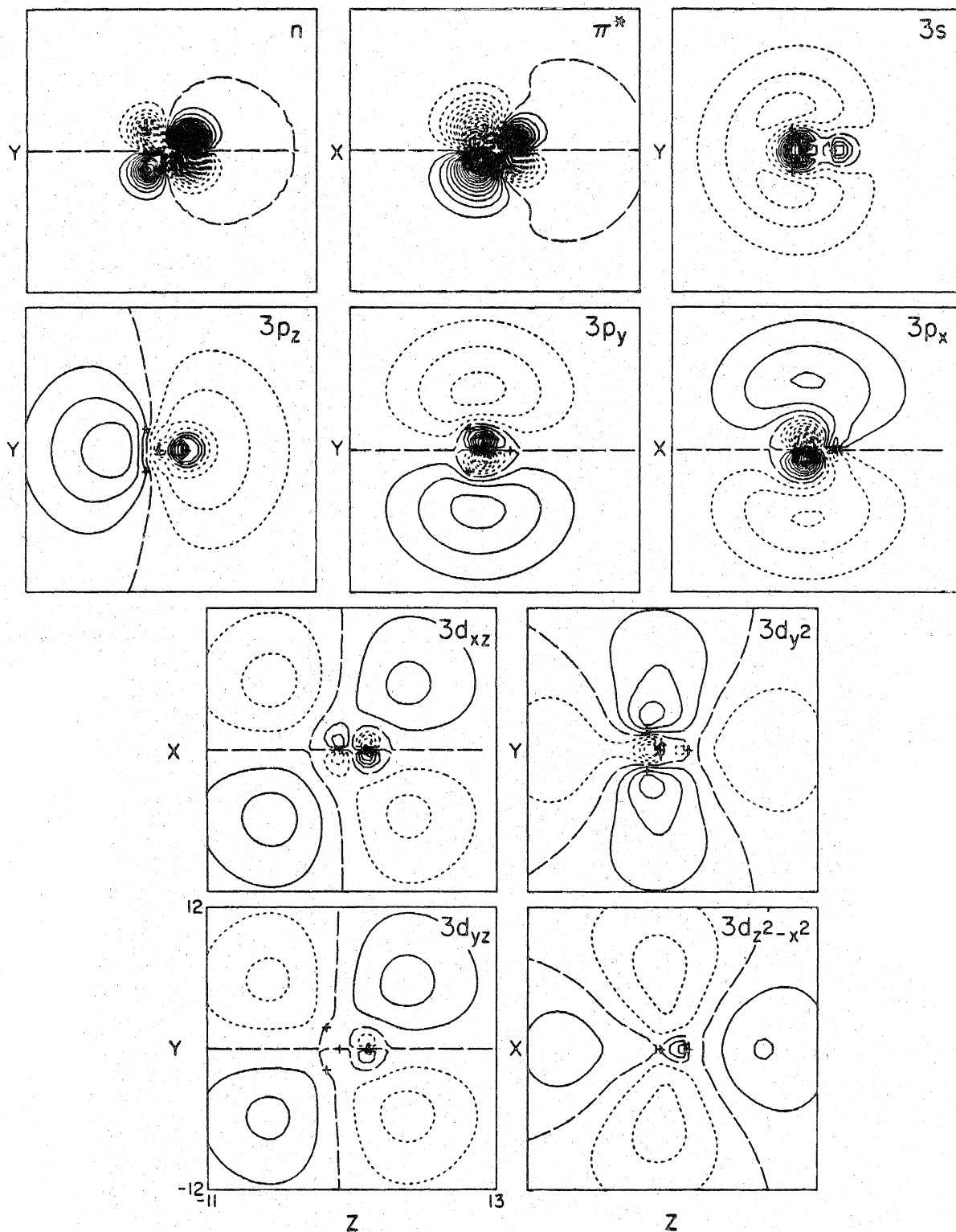


Figure 1.

EXCITED STATE ORBITALS OF  $\text{H}_2\text{CO}$   
FROM EXCITATION OUT OF THE  $\pi$  ORBITAL

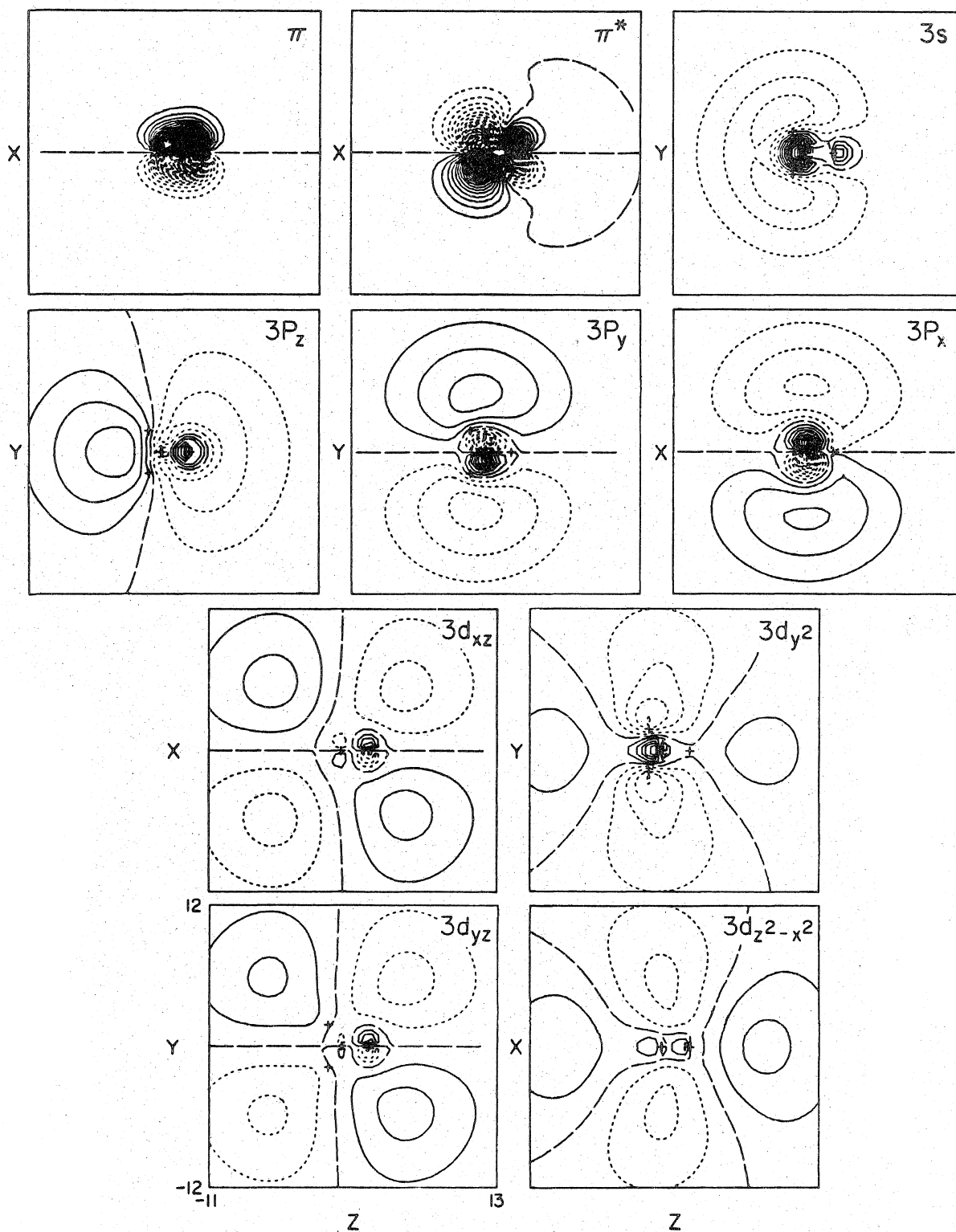


Figure 2.

EXCITED STATE ORBITALS OF CH<sub>2</sub>O  
 $\pi \rightarrow \pi^*$  STATES

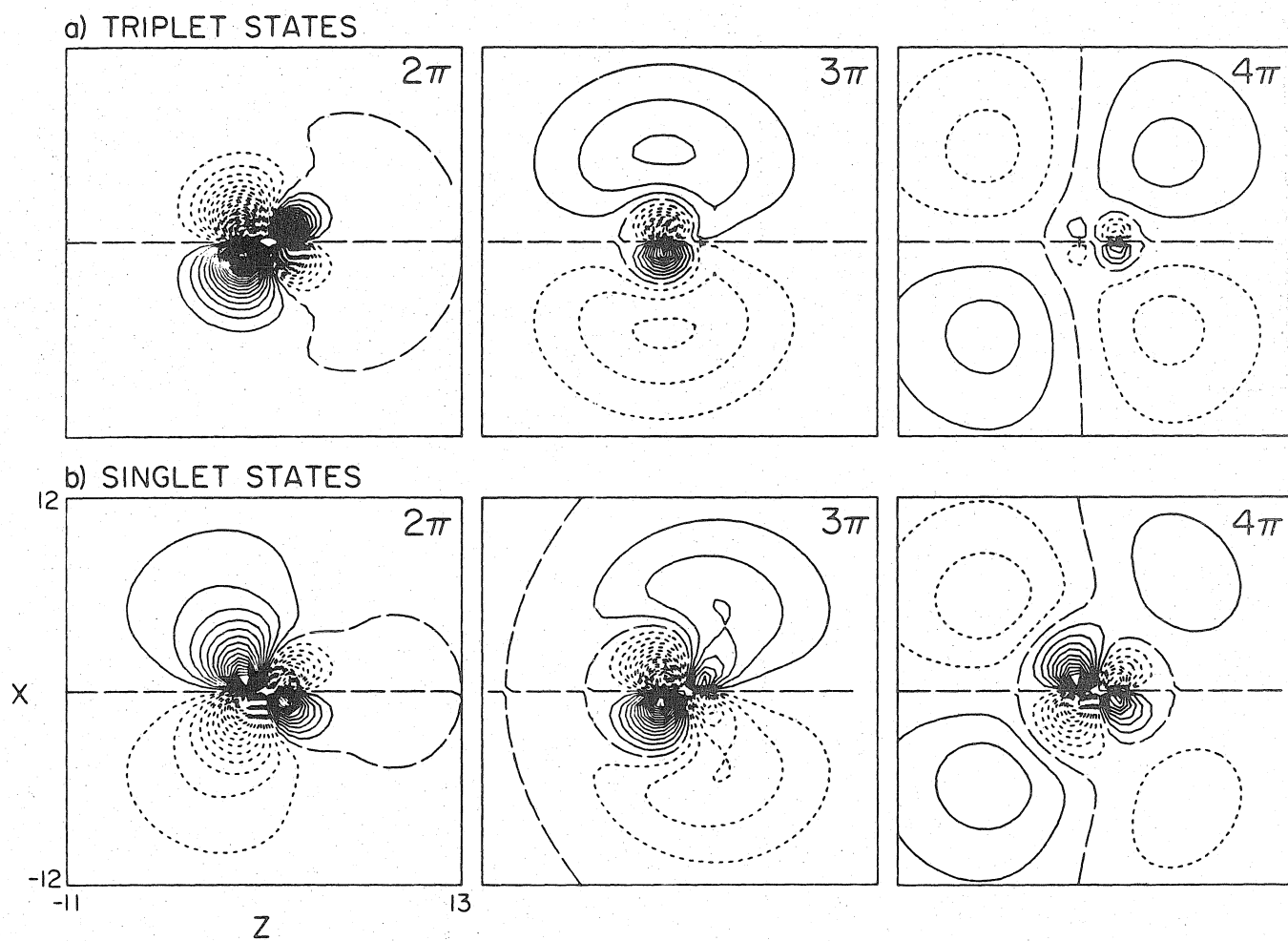


Figure 3.